

Spring 4-13-2017

Eneidyne Derived Conjugated Polymers

Keda Hu
University of New Mexico

Follow this and additional works at: https://digitalrepository.unm.edu/chem_etds

 Part of the [Materials Chemistry Commons](#), [Organic Chemistry Commons](#), and the [Polymer Chemistry Commons](#)

Recommended Citation

Hu, Keda. "Eneidyne Derived Conjugated Polymers." (2017). https://digitalrepository.unm.edu/chem_etds/69

This Dissertation is brought to you for free and open access by the Electronic Theses and Dissertations at UNM Digital Repository. It has been accepted for inclusion in Chemistry ETDs by an authorized administrator of UNM Digital Repository. For more information, please contact disc@unm.edu.

Keda Hu

Candidate

Chemistry and Chemical Biology

Department

This dissertation is approved, and it is acceptable in quality and form for publication:

Approved by the Dissertation Committee:

Prof. Yang Qin, Chairperson

Prof. Charles Melancon III

Prof. Ramesh Giri

Prof. Changjian Feng

Ene diyne Derived Conjugated Polymers

By

Keda Hu

Bachelor Chemistry, Lanzhou University, Gansu, China, 2011

DISSERTATION

Submitted in Partial Fulfillment of the

Requirements for the Degree of

Doctor of Philosophy

Chemistry

The University of New Mexico

Albuquerque, New Mexico

May, 2017

Acknowledgements

Firstly, and most importantly, I would like to express my sincere gratitude to my supervisor Prof. Yang Qin for his continuous support and guidance in the past five and half years. Prof. Qin's patience, incredible knowledge and brilliant ideas have guided and inspired me through my projects and PhD program.

Secondly, I would like to thank my committee members, Prof. Charles Melancon III, Prof. Ramesh Giri, and Prof. Changjian Feng for taking time to review the dissertation and offer their insightful comments and advice to my research proposal.

Thirdly, my thanks go to all my collaborators, whose efforts facilitate my projects. Specifically, Prof. Wei Zhang and Dr. Haishen Yang who worked with us for the synthesis of solution processable polydiacetylenes. Their input helped us achieve great results in my experiments.

Fourthly, I would like to grant my thank to my family: my parents and my wife for being so supportive throughout the years which makes my research and my life much easier.

Last but not the least, I would like to thank my host family, Jim and Priscilla Duncan and his family, as well as my friend David Hernandez for all the generous help and support in the past 5 years.

Ene diyne Derived Conjugated Polymers

By

Keda Hu

Bachelor, Chemistry, Lanzhou University, China, 2011

PhD, Chemistry, University of New Mexico, USA, 2017

Abstract

The advance of conjugated polymers (CPs) is largely relied on development of new polymerization methods, discovery of novel polymers that possess unique chemical and physical properties, and understanding of their structure-property relationship. We have employed a set of trans-enediynes (trans-EDYs) for preparation of four series of CPs, polydiacetylenes (PDAs), platinum-segmented PDAs, polytriacetylenes (PTAs) and boron doped polyacetylenes (BPAs). The resulting polymers displayed interesting optical and electrochemical properties which could be fine-tuned by the attachment of various side chains on the EDY moieties.

We have applied acyclic EDY metathesis for the synthesis of PDAs, a class of CPs that are widely studied as sensory materials and are exclusively prepared by topo chemical polymerization, a solid state polymerization. Our method represents the first example of solution processable PDAs with direct attachment of functional groups on the double bonds of PDAs which are otherwise not accessible.

PTAs are a class of nonaromatic all carbon CPs that have potential applications in nonlinear optical devices. We have prepared the first PTA bearing aromatic groups directly attached to the double bonds, allowing dramatic changes in polymer physical and electronic properties.

Several Pt containing CPs have been prepared with new structural design that is completely different than established Pt-bisacetylide polymers in that the conjugation direction of the organic chromophores is orthogonal to that of the main-chain, which could lead to better tunability and enhanced crystallinity.

Organoboron CPs have found applications in OLED and sensors due to their unique optoelectronic properties. A series of boron doped polyacetylenes (BPAs) have been obtained by hydroboration of functionalized trans-EDYs and these BPAs represent the first examples of boron main-chain conjugated polymers without aromatic units.

TABLE OF CONTENTS

LIST OF FIGURES	IX
LIST OF SCHEMES	XV
LIST OF TABLES	XVI
LIST OF ABBREVIATIONS	XVII
1 Chapter 1 Introduction	1
1.1 Motivation for Ph.D. in chemistry	1
1.2 Conjugated polymers.....	1
1.3 Initial plan: Synthesis of functionalized polyacetylenes.....	3
1.4 Development of projects	6
2 Chapter 2 Solution Processable Polydiacetylenes (PDAs) through Acyclic Ene-yne Metathesis Polymerization	9
2.1 Introduction.....	9
2.2 Experimental	11
2.3 Results and Discussion.....	17
2.4 Conclusion.....	30
2.5 NMR spectra of key compounds.....	31
3 Chapter 3 Polytriacetylenes Bearing Directly Attached Functional Groups with Tunable Physical and Electronic Properties	33
3.1 Introduction.....	33
3.2 Experimental.....	36

3.3	Results and Discussion.....	38
3.4	Conclusion.....	48
3.5	NMR spectra of key compounds.....	49
4	Chapter 4 Platinum-Segmented Polydiacetylenes.....	50
4.1	Introduction.....	50
4.2	Experimental.....	52
4.3	Results and Discussion.....	58
4.4	Conclusion.....	66
4.5	NMR spectra of key compounds.....	67
5	Chapter 5 Boron Doped Polyacetylenes	70
5.1	Introduction.....	70
5.2	Experimental.....	72
5.3	Results and Discussion.....	78
5.4	Conclusion.....	85
5.5	NMR spectra of key compounds.....	86
6	Chapter 6 Projects in Progress.....	90
6.1	Controlled Bergman Cyclization from Trans Eneidyne.....	90
6.1.1	Introduction.....	90
6.1.2	Experimental.....	91
6.1.3	Results and Discussion.....	96
6.1.4	Conclusion	112

6.1.5	NMR spectra of key compounds	113
6.2	Conjugated Zwitterion.....	117
6.2.1	Introduction	117
6.2.2	Experimental.....	117
6.2.3	NMR spectra of key compounds	120
References:	125

LIST OF FIGURES

Figure 1.1 Representative examples of CPs.....	2
Figure 1.2 Functionalized trans-EDYs	7
Figure 2.1 Size exclusion chromatograms of PDA-CH and PDA-Ph	19
Figure 2.2 ¹ H NMR of PDA-CH and PDA-Ph	20
Figure 2.3 ¹³ C NMR spectra (aromatic region) of M-a , M-b , PDA-CH and PDA-Ph	21
Figure 2.4 UV-Vis absorption (normalized) and fluorescence spectra of PDA-CH (A) and (B) and PDA-Ph (C) and (D), respectively, in chloroform solutions (2.5×10 ⁻⁴ M, r.p. units) with gradual additions of methanol	22
Figure 2.5 UV-Vis absorption spectra of chloroform (black) and mixtures of chloroform and methanol.....	23
Figure 2.6 UV-Vis absorption spectra of PDA-CH and PDA-Ph in THF at various temperatures	24
Figure 2.7 Density functional theory (DFT) calculations (B3LYP, 6-31G(d)) on polydiacetylene (PDA) model compounds having three repeating units bearing methyl (TriDA-Me) and phenyl (TriDA-Ph) substituents.....	25

Figure 2.8 Differential scanning calorimetry (DSC) histograms of PDA-CH and PDA-Ph ; 2 nd heating curves, 10 °C/min	25
Figure 2.9 Powder X-ray diffraction pattern of PDA-CH . Figure S6 Powder X-ray diffraction pattern of PDA-Ph	26
Figure 2.10 UV-Vis absorption, fluorescence and Raman spectra of thin films of PDA-CH (A) and PDA-Ph (B) drop-cast from chloroform solutions.....	27
Figure 2.11 UV-Vis absorption spectra of PDA-CH and PDA-Ph thin films drop cast from chloroform solutions at various temperatures	28
Figure 2.12 Current-voltage curves of solar cells based on 1:1 (wt:wt) PCBM blends of respective PDA-CH and PDA-Ph in dark and under simulated AM 1.5G solar irradiation (100 mW/cm ²).....	30
Figure 3.1 Size exclusion chromatograms of PDA-CH , PDA-Ph and PDA-Ph0 (CHCl ₃ w/ 0.5% NEt ₃ , 1 mL/min, RI detector) and ¹ H NMR of PDA-Ph0	39
Figure 3.2 ¹³ C NMR (CDCl ₃) spectra (sp ² and sp carbon regions) of EDY monomers and PTAs.....	40
Figure 3.3 Raman (A) and IR (B) spectra of powders of EDY-CH , EDY-Ph , PDA-CH and PDA-Ph	41
Figure 3.4 Differential scanning calorimetry (DSC) histograms of PDA-CH and PDA-Ph ; 2 nd heating curves, 10 °C/min	42

Figure 3.5 UV-Vis absorption and fluorescence emission spectra of (A) solutions (B) thin films of PDA-CH and PDA-Ph	43
Figure 3.6 Cyclic voltammograms of PDA-CH and PDA-Ph in CHCl ₃ solutions (1 mM) and thin films using Bu ₄ NPF ₆ as the supporting electrolytes (0.1 M). The voltages are referenced externally to ferrocene (Fc) redox couple. Scan rate: 100 mV/s	43
Figure 3.7 UV-vis absorption (A) and emission (B) spectra of PDA-CH in CHCl ₃ solutions (10 ⁻⁵ M repeat units) with gradual additions of methanol (percentages by volume).....	45
Figure 3.8 UV-vis absorption (A) and emission (B) spectra of PDA-Ph in CHCl ₃ solutions (10 ⁻⁵ M repeat units) with gradual additions of methanol (percentages by volume).....	45
Figure 3.9 Fluorescence spectra of poly(3-hexylthiophene) (P3HT) solutions (1.0×10 ⁻⁵ M, r.p. units, in CHCl ₃) excited at 433 nm with gradual additions of (A) PDA-CH and (B) PDA-Ph at different molar ratios (r.p. units).....	46
Figure 3.10 Stern-Volmer plots of P3HT fluorescence quenching in solutions using PDA-CH and PDA-Ph	47
Figure 4.1 Size exclusion chromatograms (SEC) of Pt-PDA-CH , Pt-PDA-Ph and Pt-PDA-Th)	60

Figure 4.2 Differential scanning calorimetry (DSC) histograms of Pt-PDA-CH , Pt-PDA-Ph and Pt-PDA-Th	61
Figure 4.3 Absorption and emission spectra of Pt-PDA-CH , Pt-PDA-Ph and Pt-PDA-Th in air-free CHCl_3 solutions (10^{-5} M repeating units, solid lines) and thin films spun cast from CHCl_3 solutions (ca. 1 mg/mL) onto commercial ITO/glass substrates (dashed lines)	62
Figure 4.4 Absorption and emission spectra of EDY-CH , EDY-Ph and EDY-Th in CHCl_3 (ca. 10^{-5} M).....	62
Figure 4.5 Cyclic Voltammograms of Pt-PDA-CH , Pt-PDA-Ph and Pt-PDA-Th (10 mM in CH_2Cl_2) externally referenced to ferrocene redox couple (0.1 M Bu_4NPF_6 as supporting electrolytes, 100 mV/s scan rate).....	64
Figure 4.6 Representative current density–voltage (I–V) curves of solar cell devices employing Pt-PDA-Ph and Pt-PDA-Th both in dark and under simulated AM1.5 G irradiation (100 mW/cm^2)	65
Figure 5.1 Size exclusion chromatograms of BPA-CH , BPA-Ph and BPA-PT (CHCl_3 w/ 0.5% NEt_3 , 1 mL/min, RI detector)	78
Figure 5.2 ^{11}B NMR of BPAs	79
Figure 5.3 Absorption and emission spectra of in THF solution (ca. 10^{-5} M) (A) and as thin film drop casted from chlorobenzene solution (B). Purple, blue and red colors are assigned to BPA-CH , BPA-Ph and BPA-PT , respectively	80

Figure 5.4 Cyclic Voltammograms of BPA-CH , BPA -Ph and BPA -PT (10 mM in CH_2Cl_2) externally referenced to ferrocene redox couple (0.1 M Bu_4NPF_6 as supporting electrolytes, 100 mV/s scan rate).....	82
Figure 5.5 Absorption spectra of BPA-CH (A), BPA-Ph (E) and BPA-PT (E) in response to F^- titration. Emission spectra of BPA-CH (B), BPA-Ph (E) and BPA-PT (F) in response to F^- titration	83
Figure 6.1 ^1H NMR spectra for isomerization of EDY-BTD T1	97
Figure 6.2 ^1H NMR spectra for EDY-BTD T1 isomers before and after heating....	98
Figure 6.3 Absorption of EDY-BTD T1 and the mixture of trans and cis isomers in chloroform. (2×10^{-5} M).....	99
Figure 6.4 Absorption of EDY-BTD T1 and isomer mixture after heating and irradiation.....	100
Figure 6.5 ^1H NMR spectra of EDY-BTD T1 isomers before and after Cu salt addition.....	101
Figure 6.6 ^1H NMR spectra of EDY-BTD T1 in presence of Cu salt treated by heat and / or light.....	102
Figure 6.7 ^1H NMR for trans EDY-Ph-OH isomerization	105
Figure 6.8 ^1H NMR of isomers of EDY-Ph-OH1 after heating at various temperature	106

Figure 6.9 ^1H NMR spectra of EDY-crown ether in presence of NaAsF_6 with heating treatment.....	108
Figure 6.10 ^1H NMR spectra of EDY-crown ether in presence of KPF_6 with heating treatment	110
Figure 6.11 ^1H NMR spectra of EDY-crown ether in presence of various equivalents of NaAsF_6	111
Figure 6.12 ^1H NMR spectra of EDY-crown ether in presence of various equivalents of KPF_6	111

LIST OF SCHEMES

Scheme 1.1 Examples of synthetic methods for PAs.....	3
Scheme 1.2 Functionalized PAs by ADMET	5
Scheme 1.3 Bergman Cyclization of EDYs.....	6
Scheme 2.1 Synthesis of Monomers and Polymers.....	18
Scheme 3.1 PTA Structures and Synthetic Methods	34
Scheme 4.1 Overview.....	51
Scheme 4.2 Synthesis of Monomers and Polymers.....	59
Scheme 5.1 Schematic drawing of main chain boron CPs	71
Scheme 5.2 Synthesis of EDY-PT	73
Scheme 6.1 Bergman cyclization controlled by the distance	91
Scheme 6.2 Transformation of nontoxic and toxic EDYs	91
Scheme 6.3 Synthesis of EDY-BTD T1	96
Scheme 6.4 Synthesis of trans EDY-Ph-OH and its BC process	104
Scheme 6.5 Synthesis of cis EDY-crown ether and its BC attempts	108
Scheme 6.6 Synthesis of the conjugated zwitterion, BF₃-ThPy-Me	117

LIST OF TABLES

Table 3.1 Summaries of electronic properties of PDA-CH and PDA-Ph	44
Table 4.1 Electronic Properties and OPV Device Parameters of Pt-PDAs.....	61
Table 5.1 Summary of the molecular weights, optical and electrochemical properties of BPAs.....	79

LIST OF ABBREVIATIONS

CP	Conjugated polymer
PA.....	Polyacetylene
PPV	Poly(p-phenylenevinylene)
P3AT	Poly(3-alkylthiophene)
PL.....	Polyfluorene
HOMO	Highest Occupied Molecular Orbital
LUMO.....	Lowest Unoccupied Molecular Orbital
ROMP.....	Ring-opening metathesis polymerization
COT.....	Cyclooctatetraenes
ADMET.....	Acyclic Diene Metathesis
BC	Bergman Cyclization
EDY	Ene diyne
EDY-CH.....	Ene diyne bearing a C ₁₁ H ₂₃ side chain
EDY-Ph	Ene diyne bearing a ^t butyl phenyl side chain
PDA.....	Polydiacetylene
DA	Diacetylene
SEC.....	Size Exclusion Chromatography

PDA-CH.....	Polydiacetylene bearing a C ₁₁ H ₂₃ side chain
PDA-Ph	Polydiacetylene bearing a 'butyl phenyl side chain
PDI	Polydispersity Index
DP	Degree of Polymerization
Mn	Number Average Molecular Weight
MALDI-TOF	Matrix-Assisted Laser Desorption–Ionization
Time-of-Flight	
UV-Vis	Ultraviolet-visible
XRD	X-ray Diffraction
DSC	Differential Scanning Calorimetry
DFT	Density Functional Theory
BHJ.....	Bulk Heterojunction
PCBM.....	Phenyl-C61-Butyric Acid Methyl Ester
J _{sc}	Short Circuit Current
V _{oc}	Open Circuit Voltage
FF	Fill Factor
PCE	Power Conversion Efficiency
ITO	Indium Tin Oxide
I-V curves	Current Density-Voltage Curves

NMR	Nuclear Magnetic Resonance
TIPS	Triisopropylsilyl
λ	Wavelength
δ	Chemical Shift
PTA	Polytriacetylene
PTA-CH	Polytriacetylene bearing a $C_{11}H_{23}$ side chain
PTA-Ph.....	Polytriacetylene bearing a ^t butyl phenyl side chain
IR.....	Infrared
T_g	Glass Transition Temperature
CV	Cyclic Voltammetry
Fc	Ferrocene
QY	Quantum Yield
P3HT	Poly(3-hexylthiophene)
OPV	Organic Photovoltaic
Pt-PDA	Pt Segmented PDA
Pt-PDA-CH	Pt Segmented PDA bearing a $C_{11}H_{23}$ side chain
Pt-PDA-Ph.....	Pt Segmented PDA bearing a ^t butyl phenyl side chain
Pt-PDA-Th.....	Pt Segmented PDA bearing an acyl thienyl side chain
EDY-Th.....	Eneidyne bearing an acyl thienyl side chain

PEDOT-PSS..... Poly(3,4-ethylenedioxythiophene) Polystyrene Sulfonate

BPA-CH..... Boron Doped Polyacetylene bearing a C₁₁H₂₃ side chain

BPA-Ph..... Boron Doped Polyacetylene bearing a 'butyl phenyl side chain

BPA-PT Boron Doped Polyacetylene bearing a phenylthiophene side chain

EDY-PT Eneidyne bearing a phenylthiophene side chain

BTD Benzothiadiazole

1 Chapter 1

Introduction

1.1 Motivation for Ph.D. in chemistry

As an undergraduate student I was fascinated by the fact that the physical and chemical properties of molecules and materials could be predicted base on the structure of the molecules and they could be changed dramatically through careful design of the structures at the molecular level. Driven by this curiosity and eager to gain deeper understanding of the structure-property relationship in organic materials, my goal in the Ph.D. program is to advance this understanding by investigating and manipulating the properties of the novel molecules and materials by engineering of molecular structures.

1.2 Conjugated polymers

Conjugated polymers (CPs) are intrinsically semiconducting organic macromolecules having alternating single and double bonds as the backbone.¹ The landmark discovery of metallic conductivity in doped polyacetylene made by Heeger, MacDiarmid, and Shirakawa in 1977^{2,3} immediately attracted research interest from both industry and academia, and tremendous efforts have been made in synthetic methodologies as well as fundamental study of structure-properties

relationship of CPs. A wide range of CPs including poly(p-phenylenevinylene)s (PPVs)⁴⁻⁷, poly(3-alkylthiophene)s^{4,8-11} (P3ATs), polyfluorene (PLs) based CPs^{4,12-14} as well as their derivatives⁴ (Figure 1.1) were prepared and studied by the research community.

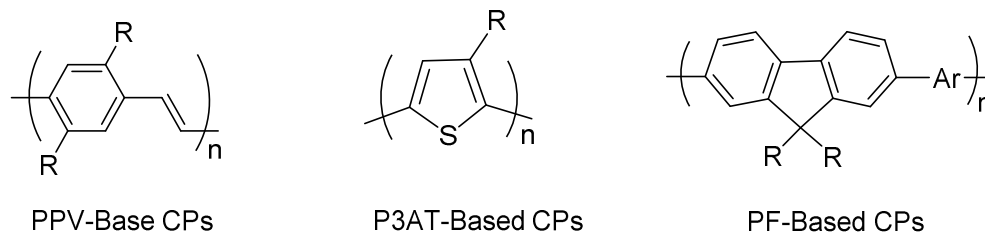


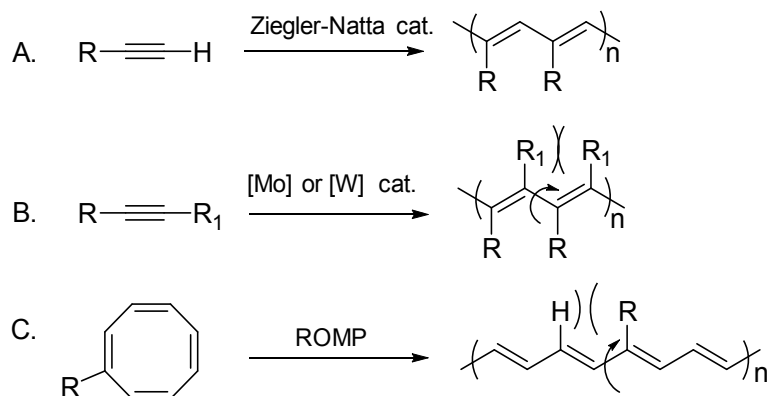
Figure 1.1. Representative examples of CPs

It is seen that the engineering of the molecular structures by attachment of different moieties either in the main chains or side chains of the CPs could efficiently manipulate properties of the resulting CPs such as solubility, luminescent efficiencies, electron and hole motilities, bandgaps, HOMO (highest occupied molecular orbital) and LUMO (lowest unoccupied molecular orbital) levels.¹⁴⁻²¹ Due to the tunable physical and chemical properties as well as good solution processability of CPs, their applications in electronic devices such as photovoltaics,^{4,22-24} sensors²⁵⁻²⁷ and OLEDs,²⁸⁻³¹ have been extensively explored and considerably advanced in the past decades. For instance, the performance of polymer solar cells has experienced a dramatic increase from the initial low power conversion efficiency of less than 0.5 %³² in 1990s to over 10 % in recent years.³³⁻
³⁵ Such improvement is not possible without careful engineering of molecular structures and fundamental understanding of the relationship between their

structures and properties. Nevertheless, overall performances of CP-based electronic devices are still not comparable with many of their inorganic counterparts, and thus continuous effort in the discovery of novel CPs with outstanding properties are critical for the further advance of material science.

1.3 Initial plan: Synthesis of functionalized polyacetylenes

Polyacetylenes, having alternating single and double carbon-carbon bonds in the backbone, represent the simplest form of a conjugated polymer and were found to be highly conductive upon doping.² This finding soon made PAs the subject of research interest and encouraged the synthesis of functionalized PAs and pursuit of its applications.



Scheme 1.1. Examples of synthetic methods for PAs

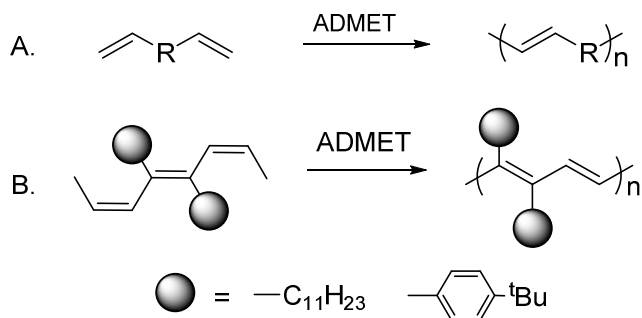
Ziegler-Natta catalysts^{36,37} were efficient for the synthesis of unsubstituted PAs and certain mono-substituted PAs from terminal alkynes with low steric hindrance (Scheme 1.1 A).^{38,39} The resulting PAs were intensely colored and had high

conductivities, however, these PAs suffered from low air-stability and low solubility, which in turn resulted in poor processability and hindered their applications.

Molybdenum- and tungsten- based compounds, on the other hand, were proved to be efficient catalysts towards polymerization of steric hindered terminal alkynes and internal alkynes to afford various mono- and di-substituted PAs (Scheme 1.1 B).⁴⁰⁻⁴⁵ Nevertheless the steric hindrance resulted from the neighboring substituents could lead to the twist of the single bonds in the main chain and reduction of the conjugation of PAs, and consequently resulted in low conductivities in the resulting PAs.^{2,44,45}

Ring-opening metathesis polymerization (ROMP),⁴⁸⁻⁵³ an olefin metathesis that is capable of polymerizing strained cyclic olefins to produce monodisperse and stereo-regular polymers, was later used as an alternative method to prepare PAs from mono-substituted cyclooctatetraenes (COTs) (Scheme 1.1 C).⁵⁴⁻⁵⁶ Various PAs derived from substituted COTs with high conjugation and solubility were synthesized and their properties were studied.⁵⁷ The fact that only one side chain is present in every four double bonds in such PAs makes choices of side chains crucial to ensure both solubility and extensive conjugation of trans-dominated PAs. Long linear alkyl chains on PAs could minimize the steric repulsion from its neighboring H (Scheme 1.1 C) to maintain planarity of the polymers, however, they are not bulky enough to solubilize PAs having high trans content ; the bulky alkyl chains that provides the solubility of trans-PAs often lead to partial loss of conjugation due to the twist the back bone of PAs induced by the repulsion between the bulky side chains.⁵⁷ As a consequence trade-off between solubility

and conjugation had to be made in such PAs, which, in fact, limits the choice of the side chains in order to keep both high conjugation and good solubility in PAs .



Scheme 1.2. Functionalized PAs by ADMET

Acyclic diene metathesis (ADMET)^{58–62} (Scheme 1.2 A) is an olefin metathesis that was first successfully adopted for polymerization of acyclic dienes by Wagener group in 1991.⁵⁸ Due to its dynamic nature, ADMET could self-correct the polymer structures during polymerization and produce the most thermodynamically stable compounds with high content of trans double bonds^{60,63,64}, and thus it has been widely used for preparation of defect-free and high-molecular-weight conjugated polymers.^{65–67}

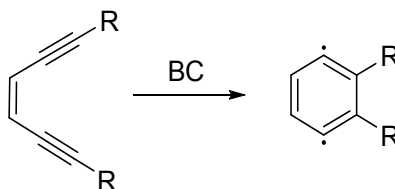
Applications of PAs in electronic devices such as solar cells have been rarely reported presumably due to the solubility and function-ability issues. Exploring applications of such intriguing materials in electronic devices would require PAs to have good solubility, feasible functionability and high planarity. Despite the viability of ADMET for the preparation of CPs, to best of our knowledge, it has never been reported for preparation of PAs.

Our proposal was to apply ADMET on (2Z,4E,6Z)-2,4,6-trienes to produce soluble and functionalized PAs with high conjugation (Scheme 1.2 B). The design

of our PAs (Scheme 1.2 B) are completely different from those reported in that two side chains are present in every other double bond of the PAs, which would potentially allow us to find a balance between the following parameters in PAs, i.e. good solubility, high planarity and effective physical and chemical tunability. Thanks to the dynamic nature of the ADMET, PAs with high trans content and effective conjugation would be expected. Theoretically, various functional groups such as phenyl, thienyl, could be pre-installed on the triene monomers to manipulate the properties of resulting PAs such as HOMO, LUMO and bandgaps for targeted applications.

A typical ADMET reaction was performed to prepare PAs bearing hexyl and phenyl side chain (Scheme 1.2 B), respectively, in the presence of different catalysts including Grubbs I,^{68,69} Grubbs II^{70,71} and Hoveyda⁷². Unfortunately, no polymerization was observed and only the monomers were recovered from the reaction mixture. The unsuccessful polymerization was postulated to be the result of high conjugation of the trienes which tend to deactivate or poison the catalyst.⁷³

1.4 Development of projects



Scheme 1.3. Bergman Cyclization of EDYs

The research on cis-enediynes, have gained long-lasting interest since the discovery of their antitumor activity in the naturally occurring EDYs in 1980s.⁷⁴⁻⁷⁷

Bergman cyclization (BC)⁷⁸⁻⁸², a cyclization process produces aromatic 1,4-diradical in cis-EDYs (Scheme 1.3), was founded to be one of the mechanisms responsible for the antitumor activity of naturally occurring EDYs including calicheamicins⁸³⁻⁸⁵. With an ultimate goal of applying cis-EDYs as antitumor drugs, significant research effort has been made to the modification of EDY molecules and kinetic study of their BC reactivity in search for a general structural design of EDYs that allows the trigger of BC process under ambient conditions.⁸⁶⁻⁹¹

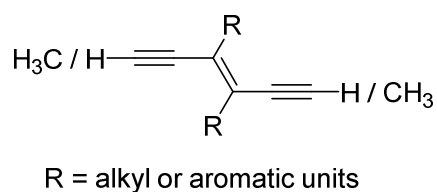


Figure 1.2. Functionalized trans-EDYs

In sharp contrast to the extensive research on cis-EDYs, studies on trans-EDYs are much less explored by the community. Regardless of the disappointing results of the ADMET reactions for PA synthesis, we were delighted to find that the precursors of trans-trienes, trans-EDYs (Figure 1.2), were capable of various reactions such as metathesis and coupling reactions, to yield several unique classes of conjugated polymers that were otherwise not easily accessible.

Our research on the EDY derived conjugated polymers⁹²⁻⁹⁴ have expanded the scope of chemistry that EDYs are capable of, and have advanced our understanding towards the chemistry of EDYs including coupling reactions, metathesis and addition reactions as well as the optoelectronic and physical properties of conjugated polymers as a function of the side chains on EDYs. Future work based on EDYs may include the incorporation of new side chains on EDYs,

the exploration of novel polymers by application of other new reactions such as click reactions, and study of Bergman cyclization on the cis-EDYs that could be potentially photo-converted from trans-EDYs.

2 Chapter 2

Solution Processable Polydiacetylenes (PDAs) through Acyclic Ene-alkyne Metathesis Polymerization

(Reproduced from *Chemical Science* **2013**,4, 3649-3653. with permission from the Royal Society of Chemistry)

2.1 Introduction

Since the first report on the solid-state preparation of polydiacetylene (PDA) in 1969,⁹⁵ extensive research efforts have been devoted to this classic type of conjugated polymers.^{96,97} PDAs are considered quasi one-dimensional semiconductors having macroscopic long-range coherence and anisotropy.^{98,99} These materials undergo intriguing optical changes among blue, red and yellow phases upon exposure to external stimuli including temperature,¹⁰⁰⁻¹⁰² solvents,¹⁰³ pressure,^{104,105} light exposure¹⁰⁶ and specific biological analytes.^{107,108} PDAs have found widespread applications in non-linear optics,^{109,110} organic conductors^{111,112} and sensory materials.¹¹³⁻¹¹⁵ Despite a large number of examples, PDAs reported to date have been synthesized exclusively from a single type of reaction, i.e. irradiation induced topochemical polymerization of diacetylene (DA) monomers in crystals, films, gels and micellar structures.⁹⁶ Such reactions occur efficiently only

if the DA monomers are able to pack into periodic structures within very strict geometrical boundaries.¹¹⁶ Flexibility around diacetylene moieties is required to accommodate spatial rearrangement when two sp hybridized carbon atoms in every DA monomer change to sp² hybridization in resulting PDA chains.¹¹⁷ As a result, few types of DA monomers, typically having alkyl spacers between DA cores and functional side-groups, can be successfully polymerized.^{96,97} Electronic properties of resulting PDAs are thus difficult to modify by substituent variation.^{118–120} Moreover, the obtained PDAs usually have limited solubility, making integration of these materials into solution-fabricated electronic devices challenging.

Notably, there have been efforts in building short-chain PDA analogs having a few eneyne repeating units through iterative condensation reactions and the resulting oligomers serve as discrete models for studying corresponding long-chain polymer properties.^{121–132} Although these synthetic methods have led to well-defined oligomers with precise structural control, high molecular weight polymers are difficult to achieve using these step-by-step approaches. We report here the synthesis of solution processable PDAs through acyclic enediyne metathesis polymerization^{133–140} of methyl terminated trans-enediyne^{141–144} monomers bearing different substituents. Physical and electronic properties of the resulting PDAs are shown both experimentally and theoretically to depend on the nature of the side-groups. To the best of our knowledge, our method represents the first example of PDA synthesis by solution polymerization and of alkyne metathesis on enediyne substrates.

2.2 Experimental

Materials and General Methods

All reagents and solvents were used as received from Sigma-Aldrich or VWR unless otherwise noted. Phenyl-C61-butyric acid methyl ester (PCBM, >99.5%) was purchased from American Dye Source. Triisopropyl((trimethylsilyl)ethynyl)silane was synthesized as described previously.¹⁴⁵ THF was distilled from Na/benzophenone prior to use. Anhydrous dichloromethane was obtained by distillation over CaH₂ and degassed through several freeze-pump-thaw cycles. The 300.13 MHz ¹H and 75.48 MHz ¹³C NMR spectra were recorded on a Bruker Avance III Solution 300 spectrometer. All solution ¹H and ¹³C NMR spectra were referenced internally to the solvent peaks. Size exclusion chromatography (SEC) analyses were performed in chloroform with 0.5% (v/v) triethylamine (1 mL/min) using a Waters Breeze system equipped with a 2707 autosampler, a 1515 isocratic HPLC pump and a 2414 refractive index detector. Two styragel columns (Polymer Laboratories; 5 m Mix-C), which were kept in a column heater at 35 °C, were used for separation. The columns were calibrated with polystyrene standards (Varian). Ultraviolet-Visible (UV-Vis) absorption spectra were recorded on a Shimadzu UV-2401 PC spectrometer over a wavelength range of 250-800 nm. Fluorescence emission spectra were obtained using a Varian Cary Eclipse Fluorometer. Raman spectra were obtained on a DXR SmartRaman spectrometer over a frequency range of 50.5–3350 cm⁻¹. Differential scanning calorimetry (DSC) measurements were performed on a Mettler Toledo

DSC STAR[®] system with ca. 5 mg sample and at a scan rate of 10 °C / min. The results reported are from the second heating cycle.

Solar Cell Fabrication and Testing

ITO-coated glass substrates (China Shenzhen Southern Glass Display. Ltd, 8 Ω/□) were cleaned by ultrasonication sequentially in detergent, DI water, acetone and isopropyl alcohol, each for 15 min followed by UV-ozone treatment (PSD Series, Novascan) for 45 min. MoO₃ (10 nm) was deposited inside a glovebox integrated Angstrom Engineering Åmod deposition system at a base vacuum level < 7 × 10⁻⁸ Torr. Polymer/PCBM blend solutions were then spun-cast at predetermined speeds using a glovebox integrated spin coater (Special Coating Systems, SCS-G3). Al (100 nm) was lastly thermally evaporated through patterned shadow masks. Current–voltage (I–V) characteristics were measured by a Keithley 2400 source-measuring unit under simulated AM1.5G irradiation (100 mW/cm⁻²) generated by a Xe arc-lamp based Newport 67005 150-W solar simulator equipped with an AM1.5G filter (Newport). The light intensity was calibrated using a Newport thermopile detector (model 818P-010-12) equipped with a Newport 1916-C Optical Power Meter.

1-(Triisopropylsilyl)tetradec-1-yn-3-one (2a). To a suspension of 6.96 g AlCl₃ (52.20 mmol) in 150 mL dry CH₂Cl₂ was added 11.0 g triisopropyl(trimethylsilyl)ethynylsilane (43.21mmol) and 10.0 g dodecanoyl chloride 1a (45.71mmol) at 0 °C. After stirring for 45 min at 0 °C and then 1 h at

room temperature, the reaction was quenched with ice water. The reaction mixture was extracted with hexanes twice. The organic layer was combined, washed sequentially with saturated NaHCO₃ solution and brine, and dried over anhydrous Na₂SO₄. Compound 2a was purified by column chromatography (hexanes as eluent) as a light yellow oil (13.49 g, 85.6%). ¹H NMR (300.13 MHz, CDCl₃): δ (ppm) = 0.87 (t, 3H, J³_{HH} = 6.9Hz), 1.09–1.11 (m, 21H), 1.25 (m, 16H), 1.69 (m, 2H), 2.54 (t, 2H, J³_{HH} = 7.2 Hz). ¹³C NMR (75.48 MHz, CDCl₃), δ (ppm) = 10.9, 14.0, 18.4, 22.6, 24.2, 28.9, 29.3, 29.4, 29.5, 45.5, 95.0, 104.2, 187.7.

(E)-(3,4-Diundecylhexa-3-en-1,5-diyne-1,6-diyl)bis(triisopropylsilane) (3a).

To a suspension of 4.84 g zinc powder (74.04 mmol) in 100 mL dry THF was added 4.05 mL TiCl₄ (36.94 mmol) dropwise at 0 °C under nitrogen. The mixture was heated to reflux for 45 min until a dark solution was obtained, and then cooled down to 0 °C. Compound 2a (8.20 g, 22.49 mmol) was added through a degassed syringe and the reaction mixture was refluxed for an additional 24 h. The reaction was quenched with NaHCO₃, extracted with ethyl ether twice. The combined organic phase was washed with saturated brine and dried over anhydrous Na₂SO₄. Compound 3a was purified by column chromatography (hexanes as eluent) as a clear oil (5.78 g, 73.7%). ¹H NMR (300.13 MHz, CDCl₃): δ (ppm) = 0.88 (t, 6H, J³_{HH} = 6.9Hz), 1.08–1.12 (m, 42H), 1.25 (m, 32H), 1.56 (m, 4H), 2.45 (t, 4H, J³_{HH} = 7.2Hz). ¹³C NMR (75.48 MHz, CDCl₃), δ (ppm) = 11.4, 14.1, 18.7, 22.8, 28.4, 29.1, 29.5, 29.6, 29.8, 32.0, 35.2, 100.4, 106.4, 130.6.

(E)-12,13-Diethynyltetracos-12-ene (4a). To a solution of 3a (5.78 g, 8.29 mmol) in 50 mL THF was added 34.42 ml tetrabutylammonium fluoride (1M in THF, 34.42 mmol). The reaction mixture was stirred overnight at room temperature and was extracted with hexanes twice. The combined organic phase was washed with brine solution and dried over Na₂SO₄. After removal of solvent, the crude product was purified by column chromatography (hexanes as eluent) to afford 4a as a white solid (2.89 g, 90.6%). ¹H NMR (300.13 MHz, CDCl₃): δ (ppm) = 0.88 (t, 6H, J³_{HH} = 6.9 Hz), 1.26 (m, 32H), 1.54 (m, 4H), 2.42 (t, 4H, J³_{HH} = 7.2 Hz), 3.40 (s, 2H). ¹³C NMR (75.48 MHz, CDCl₃), δ (ppm) = 14.1, 22.7, 28.1, 29.0, 29.4, 29.5, 29.6, 29.7, 31.9, 34.8, 82.5, 86.1, 130.3.

(E)-12,13-Di(prop-1-ynyl)tetracos-12-ene (M-a). To a solution of 4a (2.50 g, 6.50 mmol) in 20 mL dry THF was added 6.17 mL ⁿBuLi (2.5M in hexanes, 15.42 mmol) dropwise at -78 °C under nitrogen atmosphere. The mixture was stirred for 15 min and allowed to warm up to room temperature and stirred for additional 15 min. The reaction mixture was then cooled down to -78 °C and 1.2 mL CH₃I (19.28 mmol) was added through a syringe. The solution was slowly warmed up to room temperature and stirred for another 2 h. The reaction mixture was quenched with water after, extracted with hexanes twice. The combined organic phase was washed with brine solution and dried over Na₂SO₄. After removal of solvent the crude product was purified by column chromatography (hexanes as eluent) and recrystallized from hexanes to give **M-a** as a white solid (2.4 g, 89.5%). ¹H NMR (300.13 MHz, CDCl₃): δ (ppm) = 0.88 (t, 6H, J³_{HH} = 6.9 Hz), 1.26 (m, 32H), 1.50 (m,

4H), 2.02 (s, 6H), 2.34 (t, 4H, $J_{\text{HH}}^3 = 7.2\text{Hz}$). ^{13}C NMR (75.48 MHz, CDCl_3), δ (ppm)=4.7, 14.1, 22.7, 28.4, 29.0, 29.4, 29.5, 29.6, 29.7, 31.9, 34.9, 79.2, 93.6, 128.6.

PDA-CH. The ligand L (15 mg, 0.036 mmol) and the catalyst precursor Mo (24 mg, 0.036 mmol) were premixed in dry CCl_4 (4 mL) for 10 minutes at r.t. to generate the active catalyst in situ. Subsequently, the monomer (**M-a**) (200 mg, 0.48 mmol) was added together with 5 Å molecular sieves (1.8 g, powder) with the aid of CCl_4 (8 mL). The resultant suspension was stirred at 60 °C for 3 d. Then the solids in the reaction mixture were separated by centrifugation, followed by washing with CHCl_3 (4 × 12 mL). The combined solution was filtered through a pad of celite. The filtrate was concentrated to ca. 10 mL, and methanol (ca. 60 mL) was added. The red precipitates were collected by filtration, washed with methanol (ca. 15 mL) and dried under high vacuum (155 mg, 90%). ^1H NMR (300.13 MHz, CDCl_3): δ (ppm) = 0.84-0.90, 1.26, 1.54-1.59, 2.48. ^{13}C NMR (75.48 MHz, CDCl_3), δ (ppm) = 14.1, 21.5, 22.7, 27.7, 28.8, 29.8, 31.9, 35.4, 45.2, 99.3, 129.8. SEC (CHCl_3 , 1 mL/min): $M_n = 15,600$, $M_w = 29,640$, $PDI = 1.9$.

1-(4-Tert-butylphenyl)-3-(triisopropylsilyl)prop-2-yn-1-one (2b). The compound 2b was prepared from 1b according to the procedures described for the synthesis of 2a. (84.3%).

^1H NMR (300.13 MHz, CDCl_3): δ (ppm) = 1.15–1.19 (m, 21H), 1.35 (s, 9H), 7.51 (d, 2H, $J^3_{\text{HH}} = 8.4\text{Hz}$), 8.11 (d, 2H, $J^3_{\text{HH}} = 8.4\text{Hz}$). ^{13}C NMR (75.48 MHz, CDCl_3), δ (ppm) = 11.1, 18.6, 31.0, 35.2, 97.2, 103.2, 125.6, 129.5, 134.3, 158.0, 177.1.

(E)-(3,4-bis(4-tert-butylphenyl)hexa-3-en-1,5-diyne-1,6-diyl)

bis(triisopropylsilane) (3b). The compound 3b was prepared from 2b according to the procedures described for the synthesis of 3a. (73.1%). ^1H NMR (300.13 MHz, CDCl_3): δ (ppm) = 0.99–1.11 (m, 42H), 1.32 (s, 18H), 7.33 (d, 4H, $J^3_{\text{HH}} = 8.7\text{Hz}$), 7.80 (d, 4H, $J^3_{\text{HH}} = 8.7\text{Hz}$). ^{13}C NMR (75.48 MHz, CDCl_3), δ (ppm) = 11.3, 18.6, 31.3, 34.6, 101.2, 107.5, 124.6, 129.0, 129.2, 136.1, 150.9.

((E)-4,4'-(hexa-3-en-1,5-diyne-3,4-diyl)bis(tert-butylbenzene) (4b). The compound 4b was prepared from 3b according to the procedures described for the synthesis of 4a. (Yield 75.5%). ^1H NMR (300.13 MHz, CDCl_3): δ (ppm) = 1.34 (s, 18H), 3.40 (s, 2H), 7.41 (d, 4H, $J^3_{\text{HH}} = 8.7\text{Hz}$), 7.79 (d, 4H, $J^3_{\text{HH}} = 8.7\text{Hz}$). ^{13}C NMR (75.48 MHz, CDCl_3), δ (ppm) = 31.3, 34.7, 84.0, 86.7, 124.8, 128.4, 128.7, 135.4, 151.5.

(E)-4,4'-(octa-4-en-2,6-diyne-4,5-diyl)bis(tert-butylbenzene) (M-b). The monomer M-b was prepared from 4b according to the procedures described for the synthesis of M-a as a slightly yellow solid. (88.2%). ^1H NMR (300.13 MHz, CDCl_3): δ (ppm) = 1.34 (s, 18H), 1.96 (s, 6H), 7.38 (d, 4H, $J^3_{\text{HH}} = 8.7\text{Hz}$), 7.79 (d,

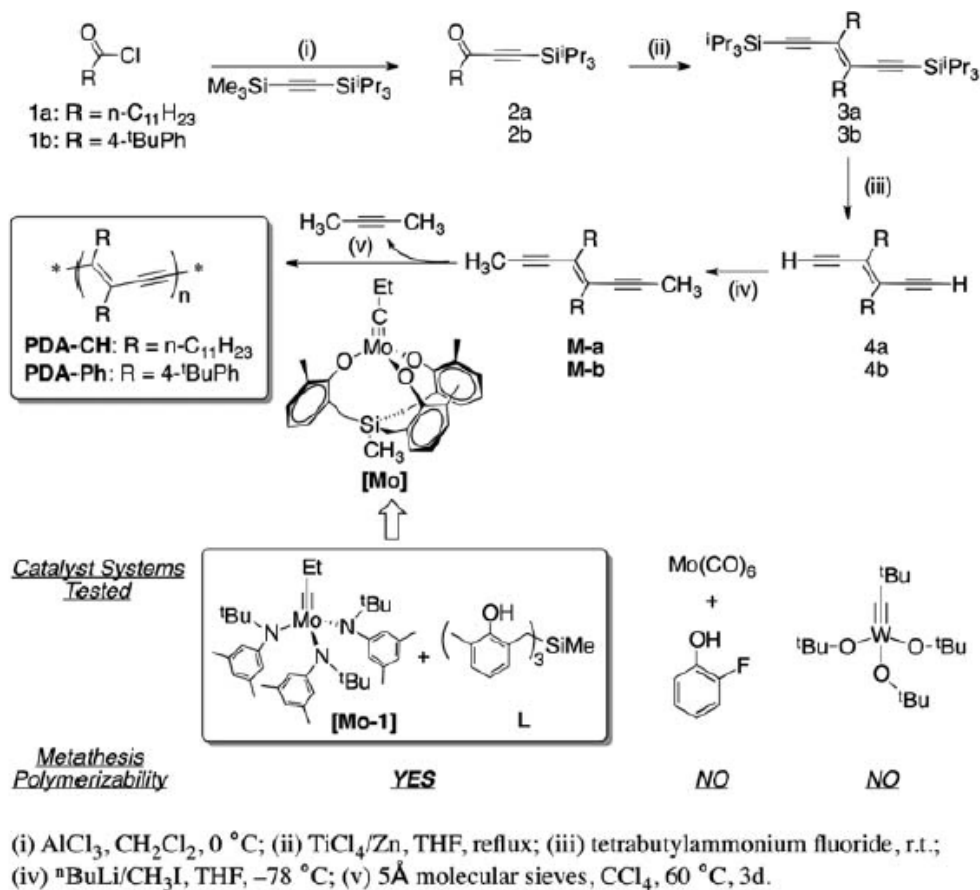
4H, $J_{\text{HH}}^3 = 8.7\text{Hz}$). ^{13}C NMR (75.48 MHz, CDCl_3), δ (ppm) = 5.0, 31.3, 34.6, 81.0, 94.5, 124.6, 127.1, 128.6, 136.9, 150.6

PDA-Ph. The ligand L (11 mg, 0.026 mmol) and the catalyst precursor Mo (17 mg, 0.026 mmol) were premixed in dry CCl_4 (3 mL) for 10 minutes at r.t. to generate the active catalyst *in situ*. Subsequently, the monomer M-b (127 mg, 0.34 mmol) was added together with 5 Å molecular sieves (1.3 g, powder) with the aid of CCl_4 (5 mL). The resultant suspension was stirred at 60 °C for 3 d. Then the molecular sieves were removed by filtration and the filtrate was concentrated under vacuum. The obtained residue was dissolved in ethyl ether (ca. 20 mL), followed by the addition of of methanol (ca. 20 mL). The red precipitate was collected and dried under high vacuum overnight (87 mg, 80%). ^1H NMR (300.13 MHz, CDCl_3): δ (ppm) = 1.23-1.28, 7.09-7.11, 7.36-7.38. ^{13}C NMR (75.48 MHz, CDCl_3), δ (ppm) = 31.4, 34.6, 99.9, 124.5, 128.3, 128.9, 135.4, 150.8. SEC (CHCl_3 , 1 mL/min): $M_n = 10,200$, $M_w = 11220$, $PDI = 1.4$.

2.3 Results and Discussion

The synthesis of enediyne monomers bearing n-undecyl and 4-tert-butylphenyl substituents, and their metathesis polymerization are summarized in scheme 2.1; detailed experimental procedures and characterization data are included in the experimental section. Notably, compounds **3a** and **3b**, obtained, respectively, from McMurry coupling reactions of **2a** and **2b**, have trans configurations in the central double bonds due to the bulky triisopropylsilyl moieties.¹⁴⁶ Solution polymerization

of **M-a** and **M-b** was initially attempted using $\text{Mo}(\text{CO})_6$ and various phenolic ligands,¹⁴⁷⁻¹⁵⁰ as well as the well-defined Schrock alkylidyne complex $(\text{tBuO})_3\text{WCCMe}_3$,^{151,152} as catalysts under conditions that have been successfully



Scheme 2.1. Synthesis of Monomers and Polymers

applied in alkyne metathesis and preparation of poly(aryleneethynylene)s. No polymerization was detected, however, as no color change was observed and only starting materials were recovered after prolonged reaction times. This lack of reactivity may be attributed to enhanced conjugation and thus higher stability of triple bonds in these trans-enediynes relative to those in isolated and aromatic alkynes.

We have recently developed a well-defined and highly active alkyne metathesis catalyst **[Mo]** obtained by treating the pre-catalyst **[Mo-1]** with triphenolsilane ligand **L** in situ, as shown in scheme 2.1.¹⁵³ By using such podand ligand design,^{154–157} one of the two open substrate-binding sites is blocked and small alkyne polymerization side reactions are completely suppressed. Both **M-a** and **M-b** were successfully polymerized in CCl₄ using ca. 7–8 mol% in situ generated **[Mo]** in the

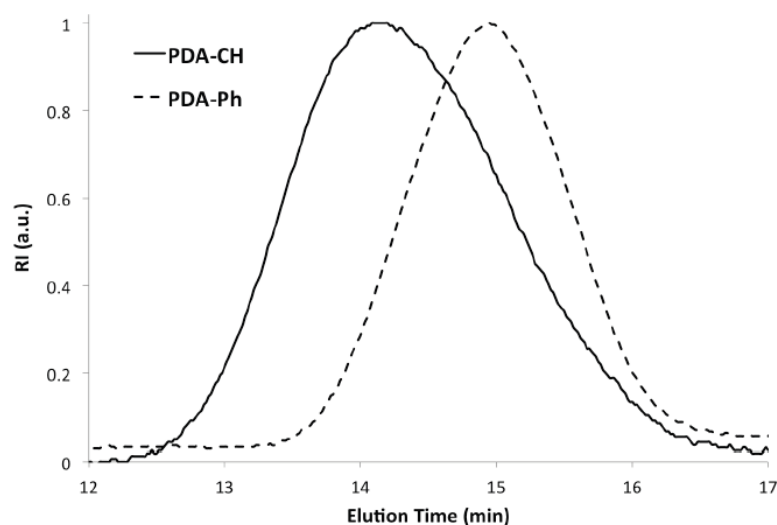


Figure 2.1. Size exclusion chromatograms of **PDA-CH** and **PDA-Ph** (CHCl₃ w/0.5% NEt₃, 1 mL/min, RI detector).

presence of 5 Å molecular sieve powders (scavenger for the 2-butyne by-product)¹⁵⁸ to give respective **PDA-CH** and **PDA-Ph** in high yields as red solids. Molecular weights of these polymers were estimated against polystyrene standards from size exclusion chromatography (SEC, Figure 2.1) to be $M_n=15,600$, $PDI=1.9$ and DP (degree of polymerization) = 47 for **PDA-CH**; and $M_n=10,200$, $PDI=1.4$ and $DP = 32$ for **PDA-Ph**. Chemical structures of both polymers were confirmed by ¹H and ¹³CNMR spectroscopy^{159,160} as shown in figure 2.2 and figure

2.3. As shown in figure 2.3, two acetylenic ^{13}C signals are observed at 79.2 and 93.6 ppm for **M-a** and 81.0 and 94.5 ppm for **M-b**. Upon polymerization, each set of signals downfield shifts and merges into a single signal at 99.3 ppm for **PDA-CH** and 99.9 ppm for **PDA-Ph**, respectively. Such observation confirms the successful polymerization leading to symmetrically substituted triple bonds along

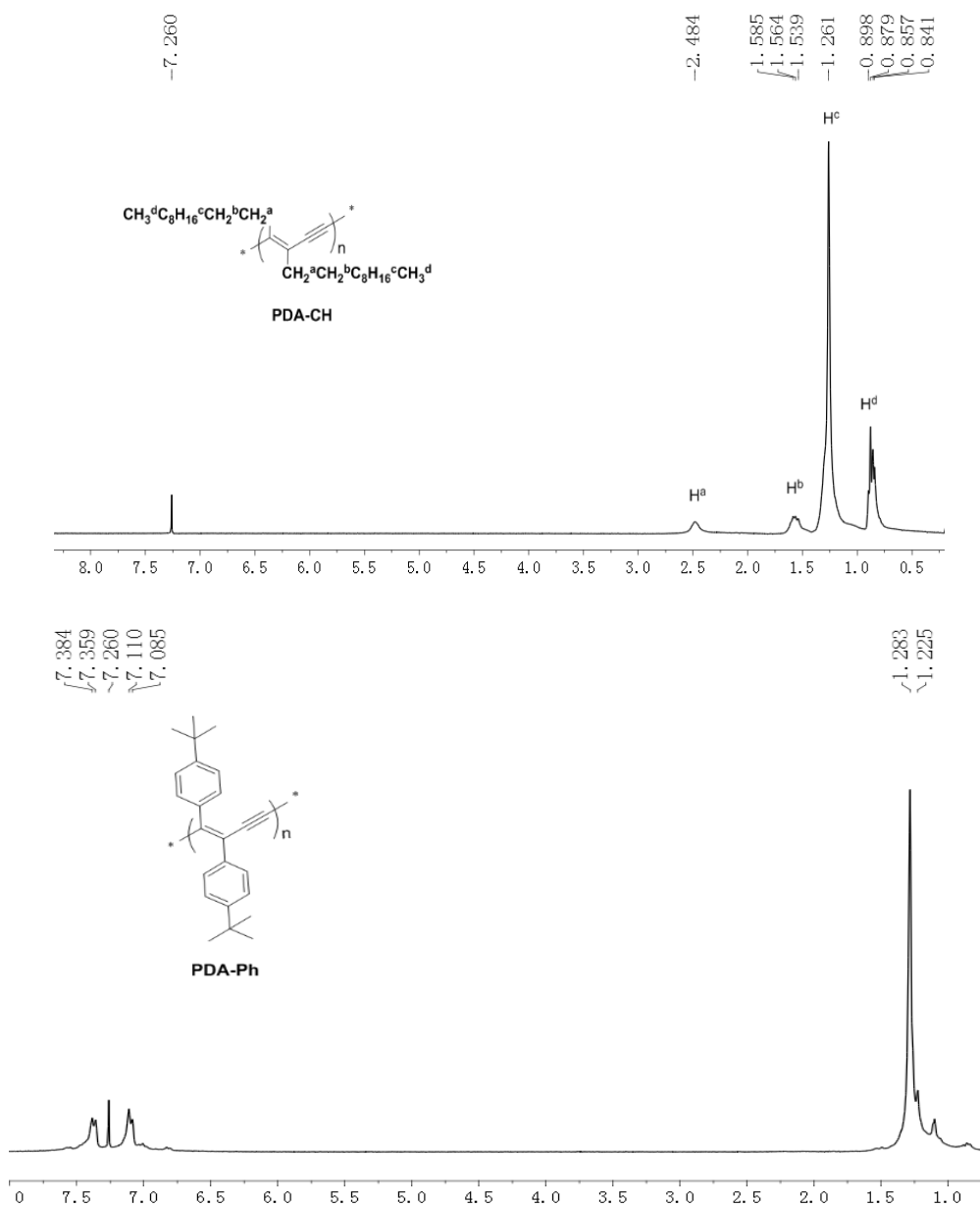


Figure 2.2. ^1H NMR of **PDA-CH** and **PDA-Ph**.

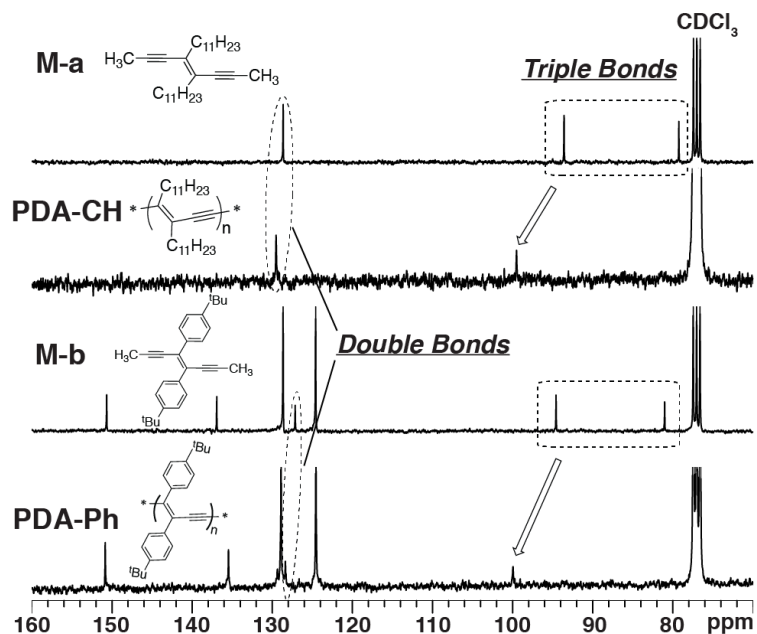


Figure 2.3. ^{13}C NMR spectra (aromatic region) of **M-a**, **M-b**, **PDA-CH** and **PDA-Ph**

polymer backbones. The fact that the acetylenic chemical shift values for both polymers are close to 100 ppm, a value previously predicted by extrapolating oligomer data toward infinite chain length,¹²⁴ confirms highmolecular weights for both polymers. ^{13}C signals of double bonds in both polymers are also slightly down field shifted from those in corresponding monomers due to enhanced conjugation. Additionally, in the ^1H NMR spectra of both polymers (Figure 2.2), signals corresponding to terminal methyl groups as observed in the spectra of respective monomers disappear, suggesting relatively high molecular weights for the polymers. We have also performed matrix-assisted laser desorption–ionization time-of-flight (MALDI-TOF) massspectrometry analysis in order to probe the possibilities of ring-formation during the polymer synthesis. However, no polymeric ions could be observed presumably due to the non-polar nature of these polymers. UV-Vis absorption and fluorescence measurements are performed on dilute

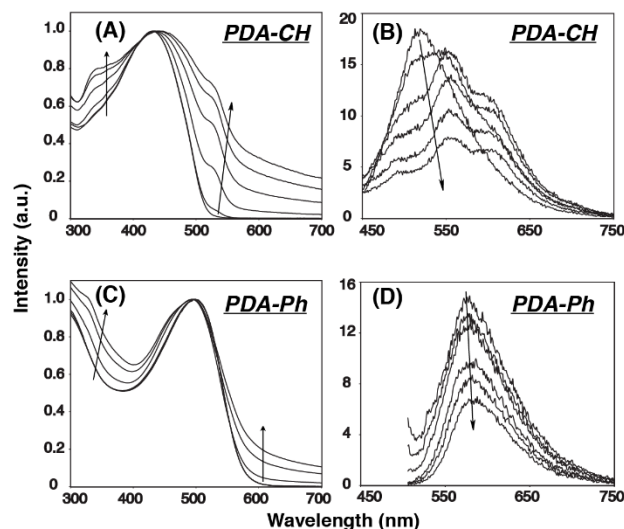


Figure 2.4. UV-Vis absorption (normalized) and fluorescence spectra of **PDA-CH** (A) and (B) and **PDA-Ph** (C) and (D), respectively, in chloroform solutions (2.5×10^{-4} M, r.p. units) with gradual additions of methanol. Black arrows indicate increasing methanol volume fractions at 0%, 17%, 29%, 40%, 49% and 58%.

chloroform solutions of the polymers (2.5×10^{-4} M, r.p. units) with gradual additions of methanol up to 58% by volume, beyond which both polymers start to precipitate. As shown in figure 2.4, PDA-CH has a λ_{max} of 430 nm in chloroform, blue-shifted by ca. 30 nm from typical values for solutions of yellow-chain PDAs bearing side-chains capable of non-covalent interactions, which have been shown to adopt “Porod–Kratky” worm-like conformations in solution.^{161,162} The blue-shifted absorption of PDA-CH thus suggests a more flexible backbone and shorter persistence and effective conjugation lengths, presumably due to the absence of intramolecular non-covalent interactions. Peaks at ca. 350 nm arising with methanol additions are likely due to mixed-solvent effects not associated with polymer aggregation, as indicated by control experiments in the absence of polymers shown in Fig 2.5. Such peaks are also absent in thermochromism studies

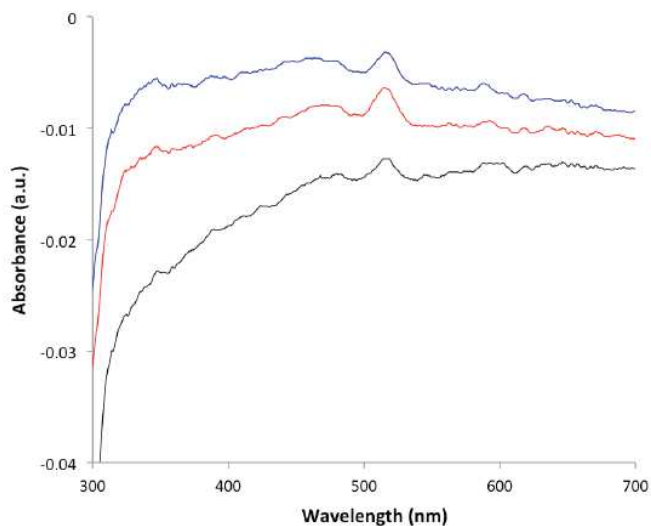


Figure 2.5. UV-Vis absorption spectra of chloroform (black) and mixtures of chloroform and methanol (red: 17% methanol; blue: 29% methanol; by volume).

as shown in Fig. 2.6. On the other hand, **PDA-Ph** shows a λ_{max} at 500 nm, a value close to those of red-chain PDAs. Upon gradual additions of methanol, λ_{max} 's of **PDA-CH** slightly red shift and a shoulder at ca. 525 nm becomes apparent, indicating the formation of red-chain species.¹⁰¹ Fluorescence signals (ex. 430 nm, $\lambda_{\text{em}} = 515$ nm, chloroform) also red shift and become more structured ($\lambda_{\text{em}} = 495$, 555 and 605 nm, 58% methanol). This yellow to red transition in **PDA-CH** is attributed to aggregation and planarization of the polymer main-chain, leading to enhanced delocalization and longer conjugation lengths.

On the other hand, only a slight blue shift of λ_{max} up to 10 nm and no apparent change in fluorescence ($\lambda_{\text{em}} = 580$ nm) are observed for **PDA-Ph** (Figure 2.4 C and D). This is presumably caused by the presence of bulky tert-butylphenyl substituents that prevent close packing and planarization of PDA chains. Aggregation may even force the main-chain to be more twisted, leading to the

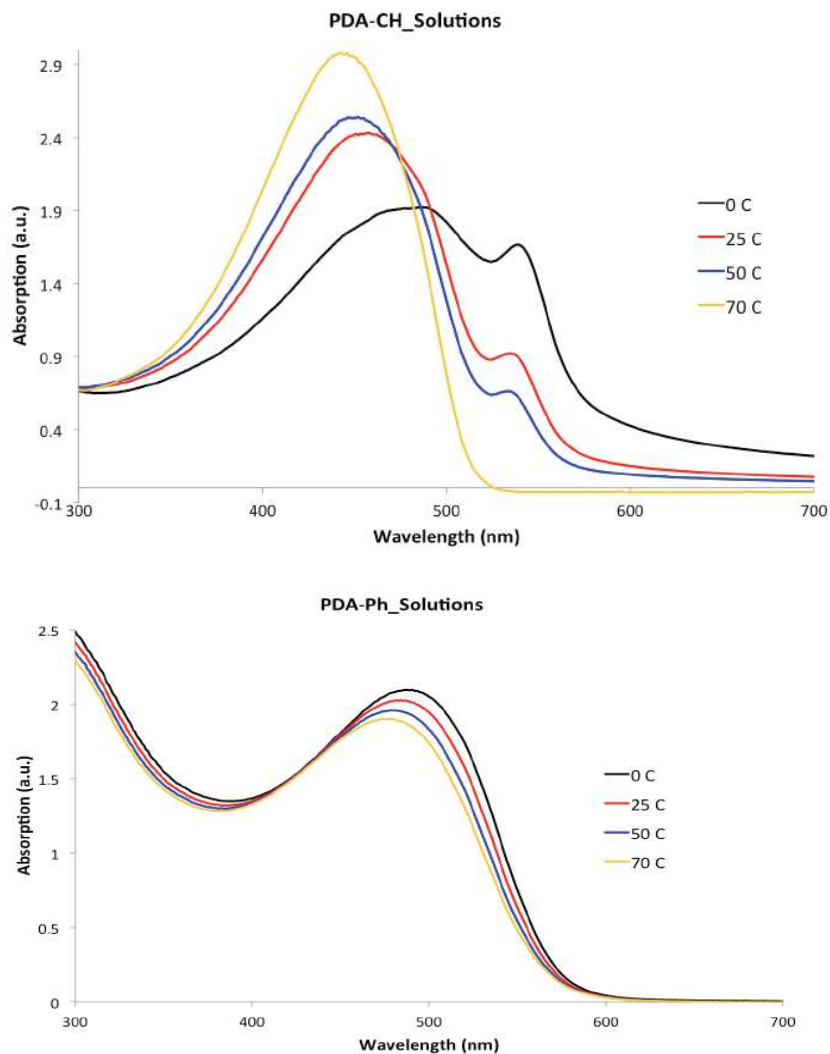


Figure 2.6. UV-Vis absorption spectra of **PDA-CH** and **PDA-Ph** in THF at various temperature

observed blueshift in absorption. Such aggregation behavior is also observed in thermochromism studies as shown in Fig. 2.6. While the THF solution of **PDA-CH** shows red-shifted λ_{max} 's and pronounced absorption shoulders at ca. 530 nm at low temperatures, blue-shifted and completely featureless absorption profile is observed at 70 °C. On the contrary, only a slight red-shift in λ_{max} (ca. 10 nm) is observed for **PDA-Ph** in THF by going from 70 to 0 °C, and no shoulder peaks can be observed. Thus, the red appearance of **PDA-Ph** is most likely due to

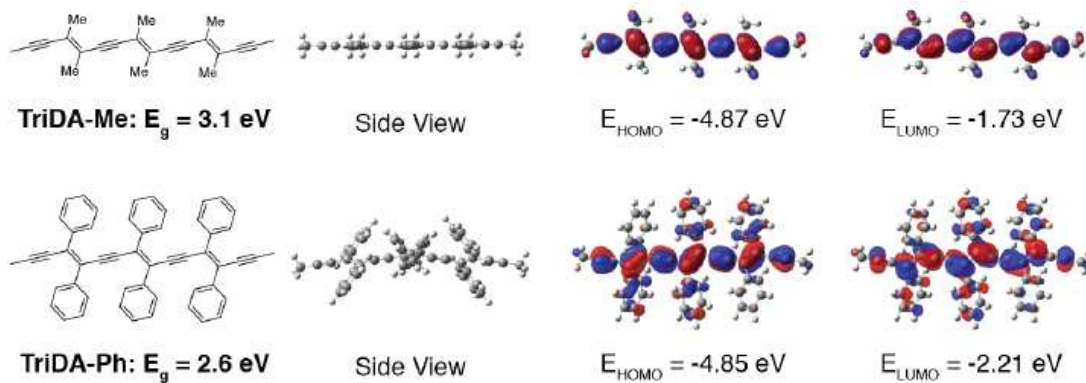


Figure 2.7. Density functional theory (DFT) calculations (B3LYP, 6-31G(d)) on polydiacetylene (PDA) model compounds having three repeating units bearing methyl (TriDA-Me) and phenyl (TriDA-Ph) substituents

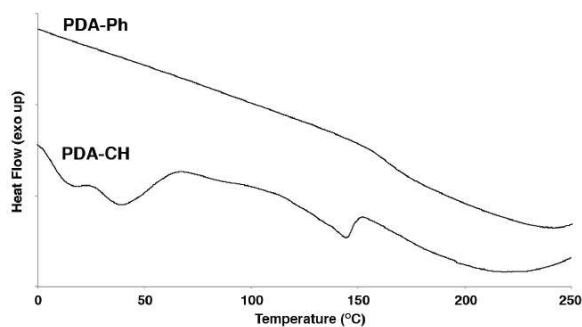


Figure 2.8. Differential scanning calorimetry (DSC) histograms of **PDA-CH** and **PDA-Ph**; 2nd heating curves, 10 °C/min.

modification of the main-chain electronic states through direct conjugation of the aromatic substituents, even though the main-chain conformation may still be in a “yellow form”. Fluorescence quantum yields in dilute chloroform solutions are estimated to be 0.1% for **PDA-CH** and 0.09% for **PDA-Ph** using quinine bisulfate (in 0.1M H₂SO₄) as a standard.¹³¹ Such low quantum efficiencies are consistent with literature reported values for yellow-chain PDAs.¹⁶³

The observed side-group effects are elucidated by density functional theory (DFT)¹⁶⁴ calculations (B3LYP, 6-31G(d)) performed on trimeric model compounds bearing methyl (TriDA-Me) and phenyl (TriDA-Ph) groups (Fig. 2.7). TriDA-Ph has a bandgap of 2.6 eV, 0.5 eV smaller than that of TriDA-Me, consistent with the longer wavelength absorptions by **PDA-Ph**. TriDA-Me shows a completely planar optimized geometry while TriDA-Ph has a slightly bent backbone with twisted phenyl substituents, indicating difficulties in close packing of polymer chains in the case of **PDA-Ph**. Indeed, differential scanning calorimetry (DSC) measurements on both polymers show distinct thermal behaviors (Fig. 2.8).

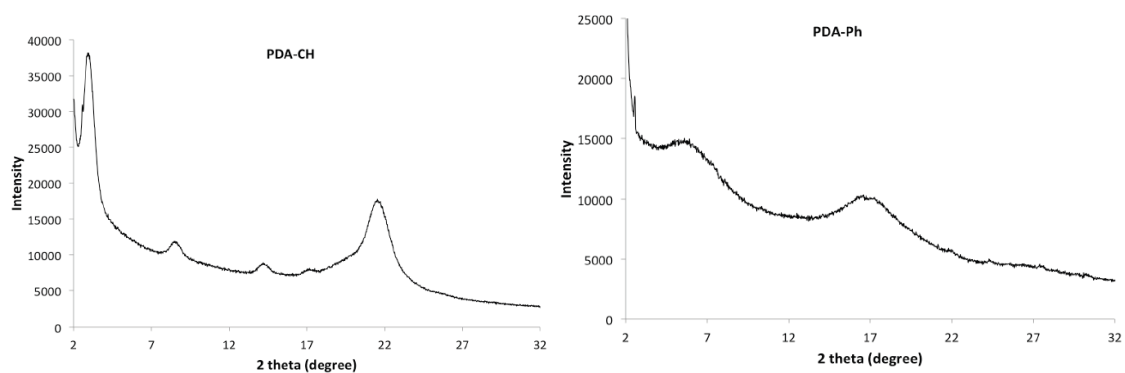


Figure 2.9. Powder X-ray diffraction pattern of **PDA-CH** and **PDA-Ph**.

Multiple melting transitions are observed for **PDA-CH**, indicating high crystallinity in the solid state. The transitions at ca. 15 °C and 40 °C are assigned to side group melting and that at ca. 140 °C to main-chain melting. On the contrary, **PDA-Ph** shows no melting behavior up to 250 °C with only a glass transition observed at ca. 155 °C (onset), indicating its amorphous nature. The crystalline nature of **PDA-CH** is further confirmed by powder X-ray diffraction (XRD) as multiple sharp scattering peaks are observed (Fig. 2.9). The lamellar distance is calculated to be

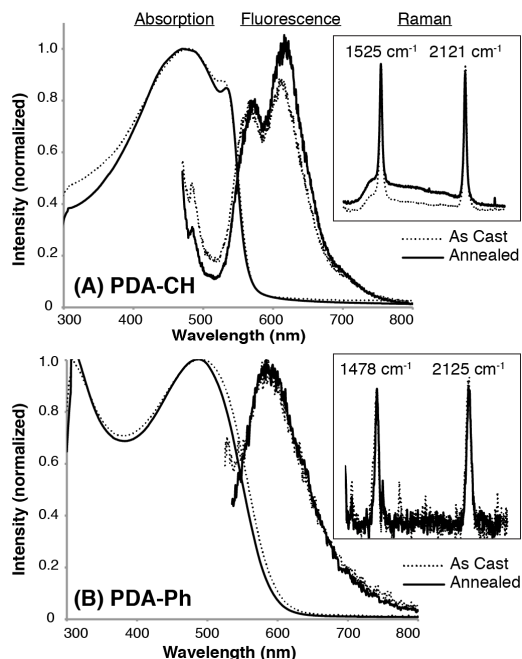


Figure 2.10. UV-Vis absorption, fluorescence and Raman spectra of thin films of **PDA-CH** (A) and **PDA-Ph** (B) drop-cast from chloroform solutions. Data for both as-cast films and the same films annealed at 155 °C for 10 min are presented.

30.6 Å ($2\theta=2.84^\circ$), corresponding to stacking of fully stretched C₁₁H₂₃ side-chains without interdigitation. On the other hand, only two broad peaks are observed in the XRD profile of **PDA-Ph** (Fig. 2.9), giving a lamellar packing distance of ca. 16 Å.

Similar trends are observed in thin films of **PDA-CH** and **PDA-Ph** as shown in Fig. 2.10. In situ thermochromic absorption studies on thin films of both **PDA-CH** and **PDA-Ph**, respectively, show very similar profiles in the temperature range of 0 to 70 °C (Fig. 2.11). Compared with solution data, λ_{\max} of as-cast **PDA-CH** thin film red shifts to ca. 475 nm and the shoulder peak at 525 nm becomes more pronounced. Three emission peaks ($\lambda_{\text{exc}} = 460$ nm) are observed at 482, 568 and

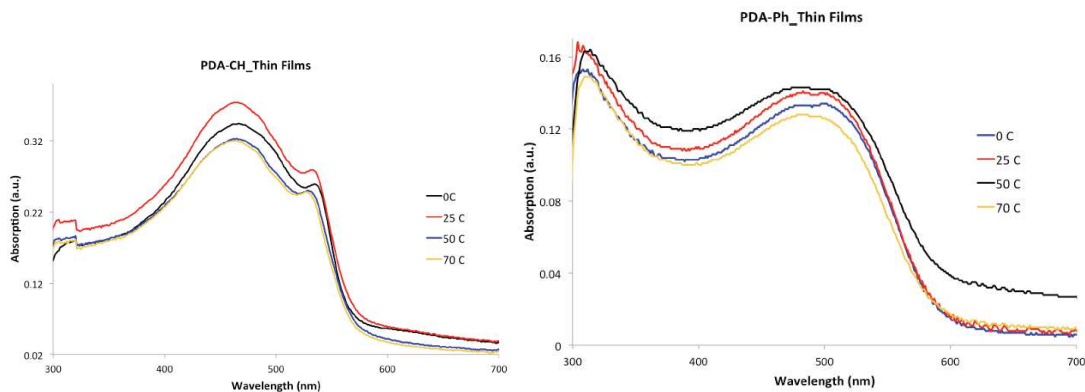


Figure 2.11. UV-Vis absorption spectra of **PDA-CH** and **PDA-Ph** thin films drop cast from chloroform solutions at various temperatures.

610nm. The 482 nm peak blue shifts and decreases in relative intensity, when compared with solution emission profiles, and the other two both red shift and increase in intensities. After annealing the same film at 155 °C for 10 min, the 525 nm absorption shoulder peak becomes more resolved, accompanied by a decrease in relative intensity of the 482 nm peak as well as slight red shift and increase in relative intensities of the peaks at 570 and 615 nm. Raman scattering measurements show identical signals at 1525 and 2121 cm^{-1} for as-cast and annealed films. These frequencies are due to respective double and triple bond stretches and correspond to red–yellow-chain PDA species.¹⁶⁵ Thus, the red-shift in emission spectra of annealed film is likely due to conformational change and ordering of the side-groups without perturbing significantly the main-chain structures and bond orders.^{166–168} Exact nature of the yellow- and red-chain species requires further investigation.

As expected, thin films of **PDA-Ph** show almost identical photophysical properties as in solutions (Fig. 2.10 B). λ_{\max} blue shifts slightly to 485 nm in as-cast film and further to 480 nm in thermal annealed film. Fluorescence profiles in both as-cast and annealed films show no difference with those in solutions and identical Raman scattering is observed for both films. The observed blue shift in absorption is likely due to ordering of the bulky side-groups that leads to conformations favoring slightly more twisted main-chain geometries. The double bond stretch of **PDA-Ph** at 1478 cm^{-1} is surprisingly in the range of typical “blue-chain” PDAs.¹⁶⁵ This is likely due to electron delocalization from double bonds to the phenyl side-groups, thus reducing electron density and bond strengths, causing reduction in vibrational frequencies.

There have been increasing interests in using conjugated polymers for organic electronic devices through low-cost high-throughput solution processes.^{4,169–171} Existing PDAs have rarely been applied in electronic devices due to limited solubility and tunability in electronic properties. Our methodology provides a facile way to produce soluble PDAs having different side-groups directly attached to the main-chains. For a proof of concept, we have fabricated bulk heterojunction (BHJ) organic solar cells using **PDA-CH** and **PDA-Ph**, respectively, blended with equal weight of phenyl-C61-butyric acid methyl ester (PCBM) as active layers. A conventional device structure of ITO/MoO₃/active layer/Al is applied and device performances are summarized in Fig. 2.12. The best devices are made from **PDA-CH**, giving on average a short circuit current (J_{sc}) of 0.44 mA cm^{-2} , an open circuit voltage (V_{oc}) of 0.6 V, a fill factor (FF) of 35% and a power conversion efficiency

(PCE) of 0.09%. Devices made from **PDA-Ph** showed reduced J_{sc} , thus lower PCEs, likely caused by the polymer's amorphous nature. Both polymers out-

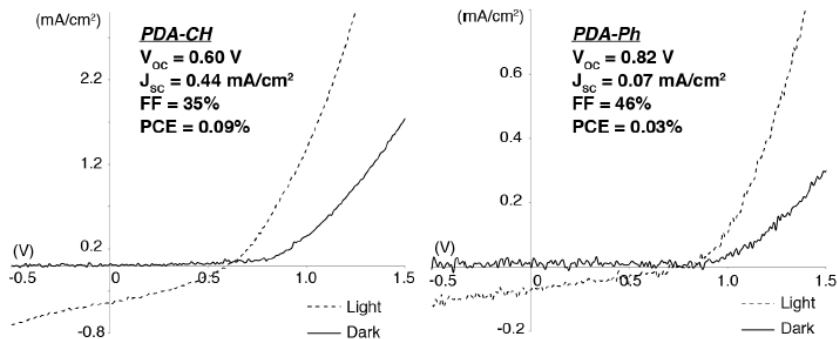


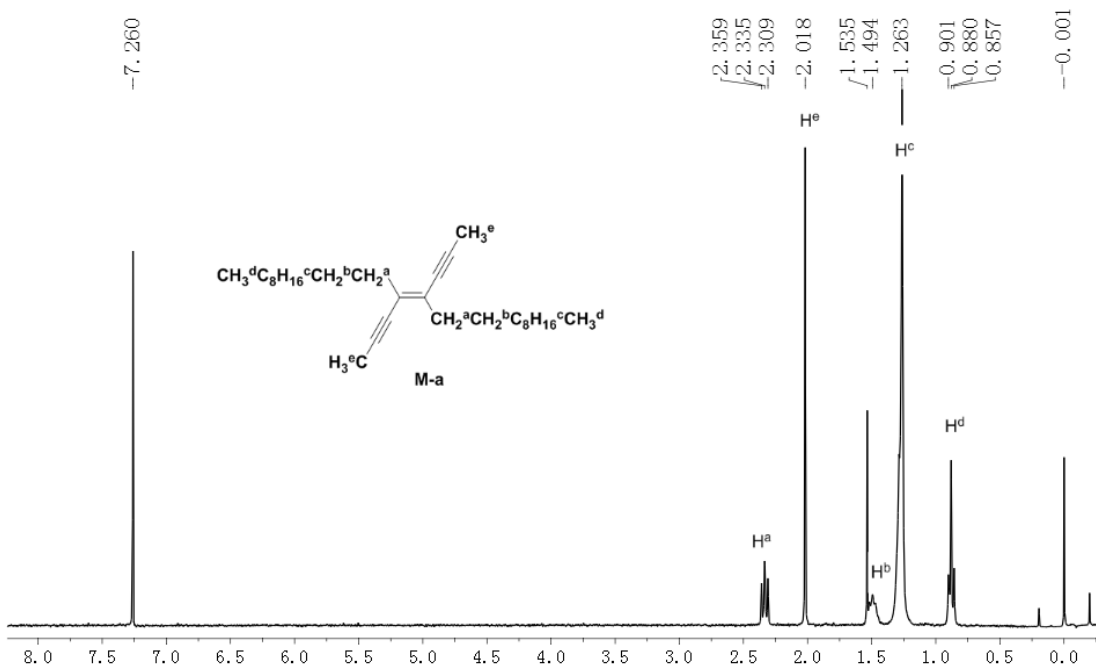
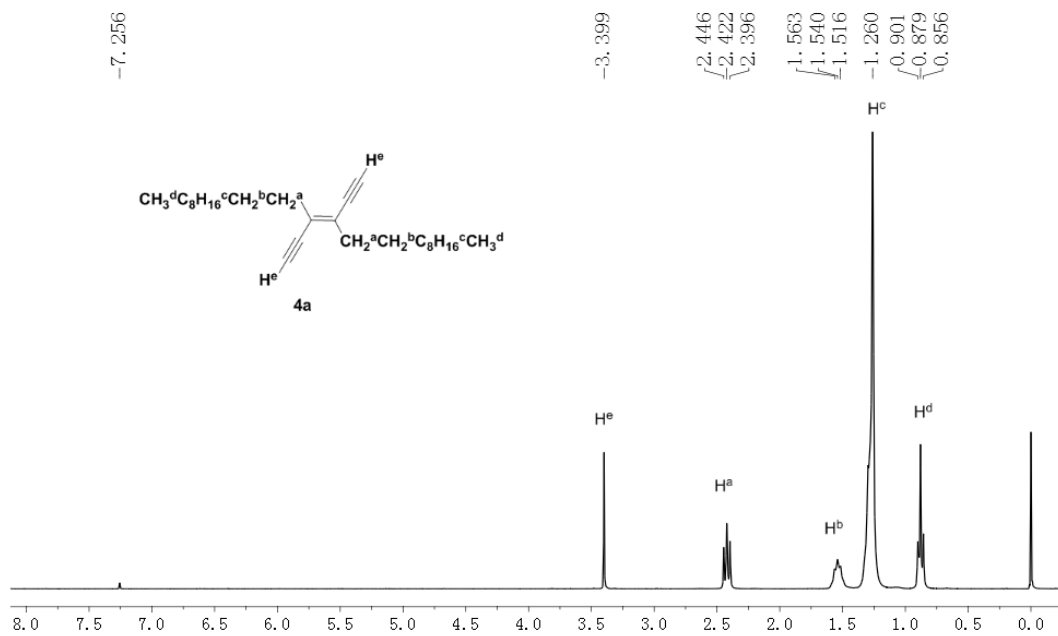
Figure 2.12. Current-voltage curves of solar cells based on 1:1 (wt:wt) PCBM blends of respective **PDA-CH** and **PDA-Ph** in dark and under simulated AM 1.5G solar irradiation (100 mW/cm²).

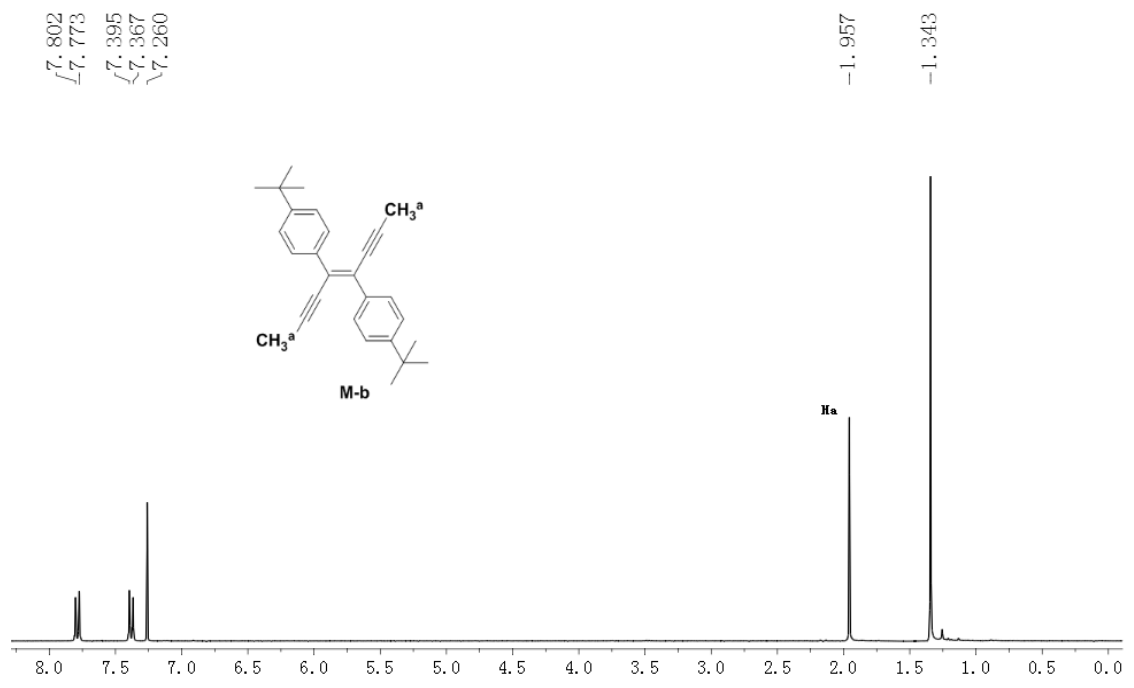
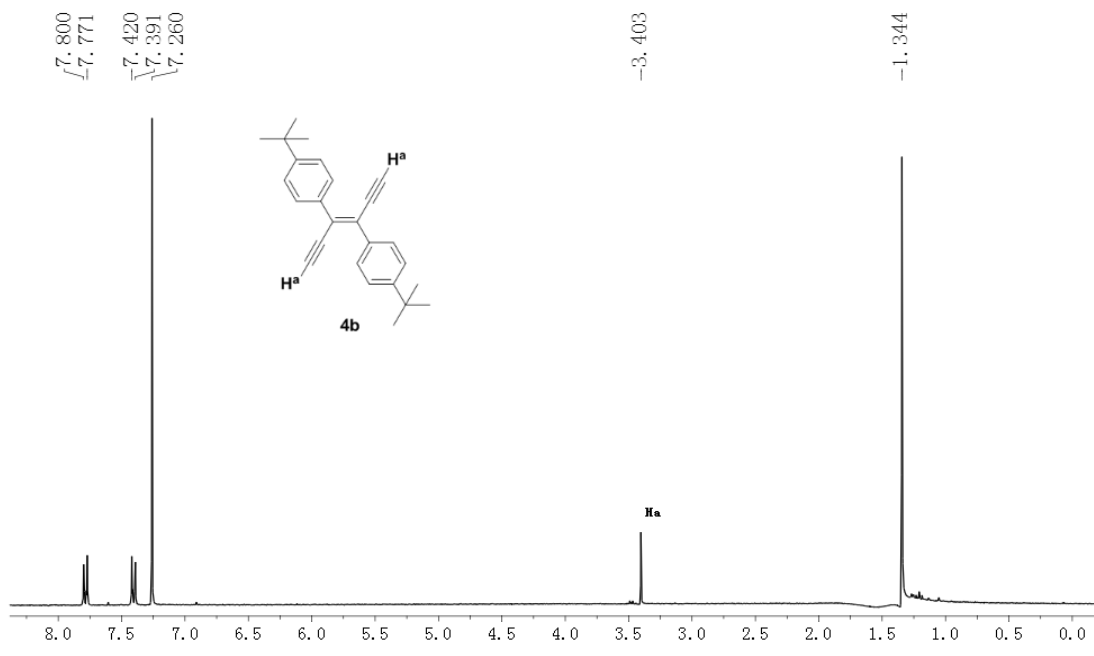
performed, by more than 100-fold, the only previous example of solar cells employing PDAs from solid-state polymerization.¹⁷² We are currently optimizing cell performance and studying charge generation mechanisms in these PDA devices in more detail.

2.4 Conclusion

In summary, we have developed a versatile methodology for the synthesis of soluble and functional PDAs. Physical and electronic properties of the resulting polymers can be tuned by careful selection of different side-groups. We are currently optimizing the reaction conditions in order to achieve higher molecular weight polymers and to gain deeper insights in their structure–property relationship. Our findings open up doors for PDAs towards previously less explored areas in solution-processed electronic device applications.

2.5 NMR spectra of key compounds





3 Chapter 3

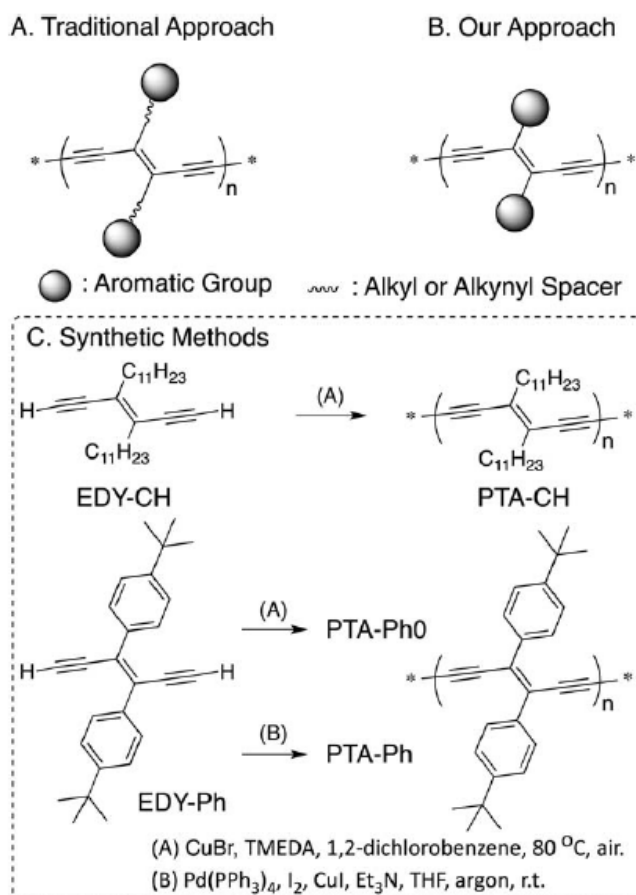
Polytriacetylenes Bearing Directly Attached Functional Groups with Tunable Physical and Electronic Properties

(Reproduced from *Journal of Polymer Science Part A: Polymer Chemistry* **2016**, 54,1391–1395, with permission from Wiley-VCH Verlag GmbH & Co. KGaA)

3.1 Introduction

Conjugated polymers (CPs) have attracted tremendous research interests due to tunable physical and electronic properties as well as increasing applications inorganic electronic devices including photovoltaics, light emitting diodes and sensors.¹⁷³ Among a plethora of examples, polytriacetylenes (PTAs) are a unique class of CPs that possess non-aromatic all-carbon backbones and were first reported by Diederich and coworkers.^{174,175} PTAs have exhibited good stability and non-linear optical properties, but it is the unusual electronic properties that generate the most curiosity. PTAs are considered an intermediate molecular-wire-like structure transitioning from polyacetylenes (PAs) and polydiacetylene (PDAs) towards the still elusive carbon allotrope, carbynes.^{176,177} Unlike PAs and PDAs, p-

electrons on the backbones of PTAs are cylindrical in shape so that PTAs are able to maintain similar extents of electronic conjugation even when the main chain is



Scheme 3.1. PTA Structures and Synthetic Methods

severely distorted by rotation due to the steric repulsion of bulky substituents.^{178,179}

Traditionally, PTAs are prepared through Glaser-Hay type coupling reactions on alkylated trans-enediyne (EDY) or doubly substituted tetraalkynylethene monomers.^{141,180–182} Various functional groups, including alkyl, silyl, aromatic and dendritic moieties, have been installed as side-chains of PTAs. However, due to the nature of monomers used, these functional groups are exclusively attached to the PTA main-chains through alkyl or alkynyl spacers, as illustrated in scheme 3.1

(A). Electronic communication between these functional groups, especially aromatic ones, and the PTA main-chains is thus expectedly weak due to the non-conjugated alkyl spacers and reduced conjugation in alkyne spacers. In order to more effectively fine-tune the electronic properties of PTAs, including bandgaps and HOMO/LUMO energy levels, direct attachment of different aromatic functional groups to the double bonds along PTA main-chains, as shown in scheme 3.1(B), is highly desirable. Noticeably, Fowler and Lauher et al. have developed solid state topological polymerization methods for the synthesis of PTAs from triacetylene (TA) monomers,^{176,183,184} similar to those applied in PDA synthesis.^{96,97} Due to the stringent requirements on crystal packing geometries, only a few TA monomers bearing substituents containing alkyl spacers and hydrogen bonding units have been successfully polymerized. To the best of our knowledge, there have been no examples of PTAs having aromatic substituents directly attached to the mainchains and a general strategy leading to such desirable structures is lacking.

We have recently developed a facile methodology for the preparation of a series of substituted EDY monomers containing various aromatic substituents directly attached to the double bonds, which have been utilized for the preparation of soluble PDAs and metal-segmented PDAs.^{92,93} Herein, we report the synthesis and characterization of PTAs containing directly attached aromatic substituents from our EDY monomers and show that physical and electronic properties of the resulting polymers can indeed be modified through the more enhanced main-chain/side-chain conjugation. For a proof of concept, we started out by preparing

PTAs having simple alkyl and phenyl substituents, and the synthetic procedures are outlined in scheme 3.1(C).

3.2 Experimental

Materials and General Methods

All reagents and solvents were used as received from Sigma-Aldrich or VWR unless otherwise noted. THF was distilled from Na/benzophenone prior to use. Anhydrous dichloromethane was obtained by distillation over CaH_2 and degassed through several freeze-pump-thaw cycles. The 300.13 MHz ^1H and 75.48 MHz ^{13}C NMR spectra were recorded on a Bruker Avance III Solution 300 spectrometer. All solution ^1H and ^{13}C NMR spectra were referenced internally to the solvent peaks. Size exclusion chromatography (SEC) analyses were performed in chloroform with 0.5% (v/v) triethylamine (1 mL/min) using a Waters Breeze system equipped with a 2707 autosampler, a 1515 isocratic HPLC pump and a 2414 refractive index detector. Two styragel columns (Polymer Laboratories; 5 m Mix-C), which were kept in a column heater at 35 °C, were used for separation. The columns were calibrated with polystyrene standards (Varian). Ultraviolet-Visible (UV-Vis) absorption spectra were recorded on a Shimadzu UV-2401 PC spectrometer over a wavelength range of 250-900 nm. Fluorescence emission spectra were obtained using a Varian Cary Eclipse Fluorometer. Differential scanning calorimetry (DSC) measurements were performed on a Mettler Toledo DSC STARe system with ca. 5 mg sample and at a scan rate of 10 °C / min. The results reported are from the second heating cycle. Infrared (IR) spectra were recorded on a Bruker Alpha-P

instrument, where powders were used in ATR mode. Raman spectra were obtained from a DXR SmartRaman spectrometer over a frequency range of 50.0–3350 cm^{-1} .

Synthesis of PDA-CH: To a mixture of **EDY-CH** (50 mg, 0.13 mmol) and CuBr (24 mg, 0.17 mmol) were added 2 mL of 1,2-dichlorobenzene (kept over 4Å molecular sieves), phenylacetylene (0.1 mg, 0.001 mmol) and tetramethylethylenediamine (0.03 mL, 0.2 mmol). The reaction mixture was stirred in air at 80 °C overnight. The resulting viscous solution was precipitated in methanol, filtrated and dried under high vacuum to afford 37 mg (74.6%) red waxy solid.

^1H NMR (300.13 MHz, CDCl_3): δ (ppm) = 0.90, 1.28, 1.58, 2.48. ^{13}C NMR (75.48 MHz, CDCl_3): δ (ppm) = 14.1, 22.7, 28.5, 28.9, 29.4, 29.7, 32.0, 35.1, 84.7, 132.6. SEC (CHCl_3 , 1 mL/min): M_n = 24.4 kDa, M_w = 50.0 kDa, PDI = 2.1.

Synthesis of PDA-Ph0: To a mixture of **EDY-Ph** (30 mg, 0.088 mmol) and CuBr (20 mg, 0.14 mmol) was added 2 mL of 1,2-dichlorobenzene (kept over 4Å molecular sieves), phenylacetylene (0.09 mg, 0.0009 mmol) and tetramethylethylenediamine (0.03 ml, 0.2 mmol). The reaction mixture was stirred in air at 80 °C overnight. The reaction mixture was precipitated in methanol, filtrated and dried under high vacuum to 8 mg red fine powder (26.7%).

^1H NMR (300.13 MHz, CDCl_3): δ (ppm) = 1.26, 1.32, 7.18, 7.36, 7.61. SEC (CHCl_3 , 1 mL/min): M_n = 2.9 kDa, M_w = 9.5 kDa, PDI = 3.3.

Synthesis of PDA-Ph: To a mixture of **EDY-Ph** (20 mg, 0.059 mmol), Pd(PPh₃)₄ (3 mg, 0.0026 mmol), I₂ (32 mg, 0.13 mmol) and CuI (28 mg, 0.15 mmol) was added 1 mL of Et₃N and 5 mL of THF in a glovebox under argon. The mixture was stirred at r. t. for 12h, and then phenylacetylene (7 mg, 0.069 mmol) was added to the reaction mixture, and the reaction was stirred for another 4.5 h. The reaction mixture was precipitated in methanol, filtrated and dried under high vacuum to afford 15 mg (75.4%) dark purple solid.

¹H NMR (300.13 MHz, CDCl₃): δ (ppm) = 1.33, 7.37, 7.66. ¹³C NMR (75.48 MHz, CDCl₃): δ (ppm) = 31.3, 34.8, 85.5, 87.2, 125.0, 128.6, 129.9, 134.8, 152.1. SEC (CHCl₃, 1 mL/min): *M*_n = 35.2 kDa, *M*_w = 98.7 kDa, *PDI* = 2.8.

3.3 Results and Discussion

Synthesis of both monomers, **EDY-CH** and **EDY-Ph** have been reported previously.⁹² The conventional Glaser-Hay type oxidative acetylenic coupling reactions [condition A, Scheme 3.1(C)] were first applied for the synthesis of **PDA-CH**. High molecular weight polymers (*M*_n = 24.4 kDa, *PDI* = 2.1) were smoothly obtained as a red solid by precipitation into methanol. On the other hand, the Glaser-Hay coupling did not satisfactorily lead to well-defined polymers using the tert-butylphenyl substituted monomer **EDY-Ph**. Under such conditions, the resulting **PDA-Ph0** displays relatively small molecular weight (*M*_n = 2.9 kDa, *PDI* = 3.3) and in the ¹H NMR spectrum (Figure 3.1) extra peaks with high intensities can be observed, the origin of which is currently unknown. Similar results were

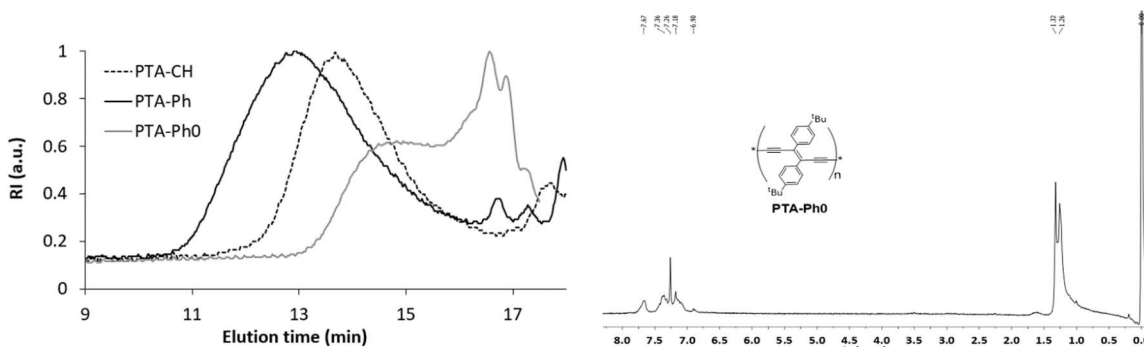


Figure 3.1. Size exclusion chromatograms of **PDA-CH**, **PDA-Ph** and **PDA-Ph0** (CHCl_3 w/ 0.5% NEt_3 , 1 mL/min, RI detector) and ^1H NMR of **PDA-Ph0**.

obtained even by extensively optimizing the reaction conditions including temperature, catalyst loading and concentration. We do not fully understand the causes of such reactivity differences and it is possible that the direct attachment of phenyl substituents changes the reactivity/stability of the EDY intermediates containing acetylenic radicals, leading to undesired side reactions. We thus turned into the palladium catalyzed oxidative coupling reactions [condition B, Scheme 3.1(C)].¹⁸⁵ In the presence of catalytic amount of $\text{Pd}(\text{PPh}_3)_4$ and excess of CuI and I_2 in mixture solvents of THF and triethylamine, **PDA-Ph** was obtained with high molecular weight ($M_n = 35.2$ kDa, PDI = 2.8) in high yields as a dark purple solid. Size exclusion chromatograms (SEC) of both **PDA-CH** and **PDA-Ph** show single broad peaks (Fig. 3.1), which is typical for step-growth polymerizations. Structures of both polymers were first analyzed by NMR spectroscopy and the results are summarized in Figure 3.2. Upon polymerization, ^1H NMR signals become broad in both cases, which is commonly observed in polymers. The ^{13}C signals of **EDY-CH** at 128.6 ppm for the double bond carbons and 93.6/79.2 ppm for the triple bond carbons shift to 132.6 ppm and merge into one broad peak at 84.7 ppm,

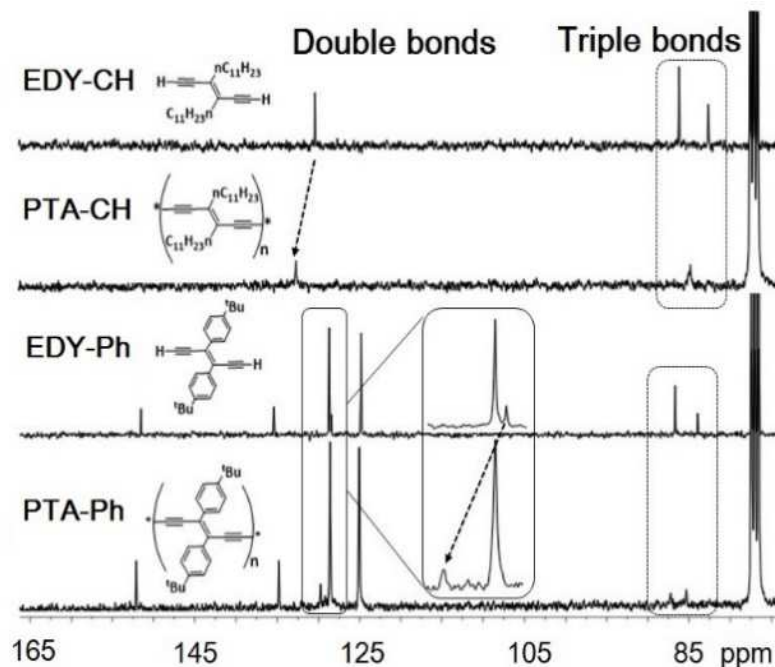


Figure 3.2. ^{13}C NMR (CDCl_3) spectra (sp^2 and sp carbon regions) of EDY monomers and PTAs.

respectively, in **PDA-CH**. As for **PDA-Ph**, while signals from the phenyl substituents do not show significant changes from monomer to polymer, the double bond signal experiences a large downfield shift from 127.1 to 129.7 ppm and the two triple bond carbon signals at 94.5 and 81.0 ppm become much closer at 86.8 and 85.4 ppm. These observations strongly suggest the formation of PTA polymers having symmetrically substituted double bonds as expected. Raman and IR spectroscopies were used as complementary methods for the confirmation of the proposed PTA structures. As illustrated in Figure 3.3A, both EDY monomers and PTAs display two major groups of signals in the Raman spectra, with peaks between 1400 cm^{-1} and 1600 cm^{-1} assigned to double bond stretching modes and those between 2000 cm^{-1} and 2200 cm^{-1} assigned to triple bond stretching modes, respectively. These values are consistent with reported double bond and triple

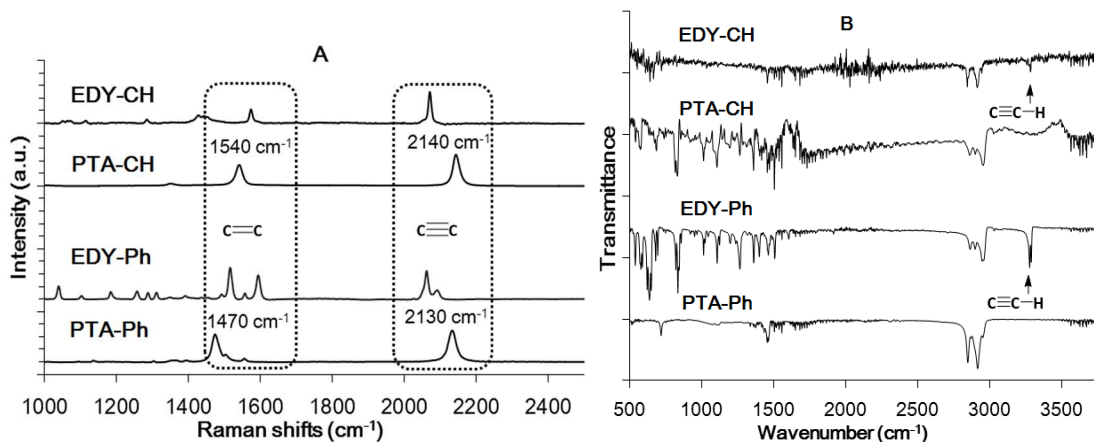


Figure 3.3. Raman (A) and IR (B) spectra of powders of **EDY-CH**, **EDY-Ph**, **PDA-CH** and **PDA-Ph**.

bond stretches of conjugated eneyne small molecules and polymers.^{92,165} A general trend is that upon polymerization, signals from the double bond stretching modes are redshifted while those from the triple bond stretching modes are blue-shifted. This observation indicates that the electron densities on the double bonds are smaller in the PTAs than in the monomers due to enhanced conjugation and delocalization along the polymer main-chains and correspondingly, the electron densities on the triple bonds become relatively increased. It is also noticeable that these stretching frequencies are smaller in **PDA-Ph** than those in **PDA-CH**, which can be explained by reduced electron densities on the polymer main-chains of **PDA-Ph** due to delocalization to the directly attached phenyl substituents. Also clearly observed in the IR spectra (Fig. 3.3 B), the peaks around 3300 cm⁻¹, belonging to the terminal acetylenic C-H stretching modes from both EDY monomers, completely disappeared upon polymerization, strongly suggesting the consumption of the monomers and successful polymerization into PTAs.

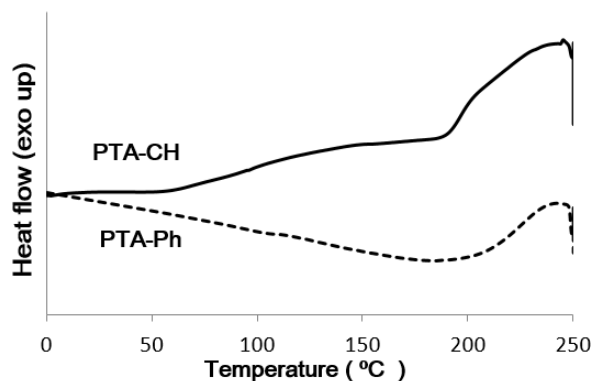


Figure 3.4. Differential scanning calorimetry (DSC) histograms of **PDA-CH** and **PDA-Ph**; 2nd heating curves, 10 °C/min.

We expect different physical properties between **PDA-CH** and **PDA-Ph** due to the size and rigidity differences between the linear flexible n-undecyl side-chains and bulky rigid 4-tertbutylphenyl substituents, respectively. Indeed, **PDA-CH** is soluble in a variety of organic solvents including THF, chlorobenzene, chloroform and even partially soluble in hexanes. On the other hand, **PDA-Ph** can only be solubilized in chloroform and chlorobenzene. DSC measurements (Fig. 3.4) shows a glass transition temperature (T_g) at ca. 50 °C and a melting transition peaking at ca. 190 °C for **PDA-CH**, suggesting certain degrees of crystallinity of this polymer. On the contrary, no obvious thermal transitions can be found for **PDA-Ph**, indicating its amorphous nature that is likely caused by inefficient packing from the bulky and rigid 4-tert-butylphenyl side-chains.

Electronic properties of these polymers were studied by UV-vis absorption and fluorescence spectroscopy (Fig. 3.5), as well as by cyclic voltammetry (CV, Fig 3.6), and the results are summarized in Table 3.1. In dilute CHCl_3 solutions, **PDA-CH** displays a λ_{max} at 440 nm and an emission peak λ_{em} at 494 nm while **PDA-Ph**

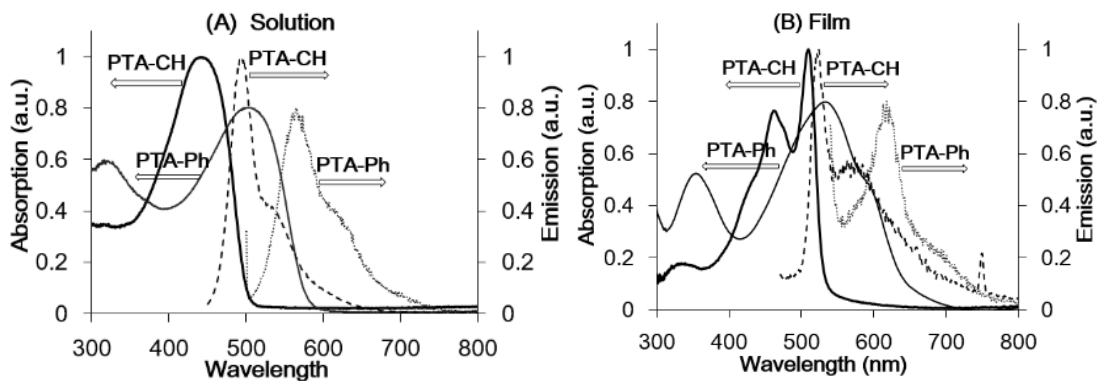


Figure 3.5. UV-Vis absorption and fluorescence emission spectra of (A) solutions (2.0×10^{-5} M, r.p. units, in CHCl_3) and (B) thin films of **PDA-CH** and **PDA-Ph**.

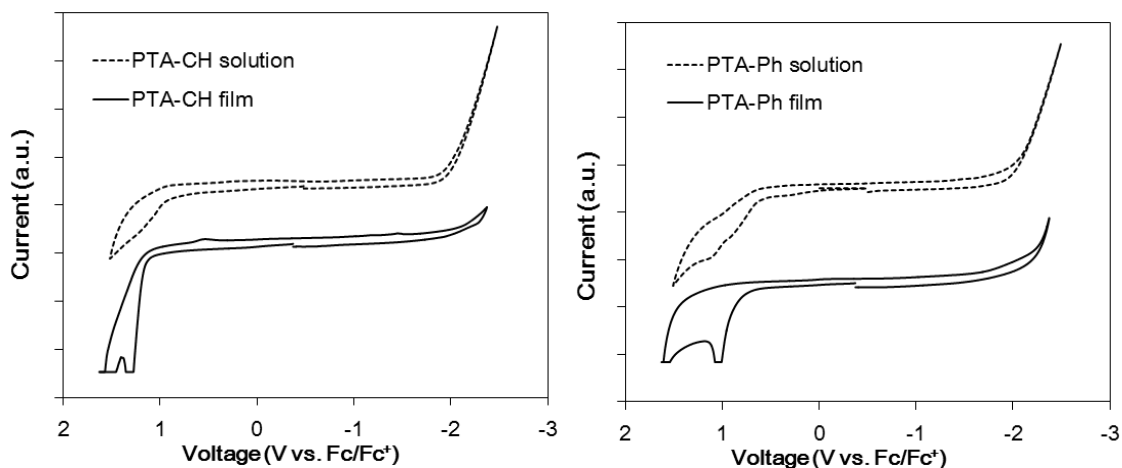


Figure 3.6. Cyclic voltammograms of **PDA-CH** and **PDA-Ph** in CHCl_3 solutions (1 mM) and thin films using Bu_4NPF_6 as the supporting electrolytes (0.1 M). The voltages are referenced externally to ferrocene (Fc) redox couple. Scan rate: 100 mV/s

has a λ_{max} at 493 nm and λ_{em} at 565 nm. From the absorption onsets, optical bandgaps are calculated to be 2.3 and 2.1 eV for **PDA-CH** and **PDA-Ph**, respectively. The smaller bandgap and red-shifted absorption and emission observed in **PDA-Ph** can be explained by the electronic contribution from the

directly attached phenyl substituents, as confirmed by CV for **PDA-CH** and **PDA-Ph**, the difference between which matches well with the difference between the

	λ_{\max} (nm) ^a	λ_{onset} (nm) ^b	λ^{em} (nm) ^c	Quantum yield ^d	Bandgap (eV) ^e	HOMO (eV) ^f	LUMO (eV) ^g
PTA-CH	440 (510)	533 (542)	494 (524)	1.40%	2.33 (2.28)	-5.72 (-6.00)	-3.39 (-3.72)
PTA-Ph	493 (535)	590 (655)	565 (618)	0.07%	2.10 (1.89)	-5.54 (-5.67)	-3.44 (-3.78)

Table 3.1. Summaries of electronic properties of **PDA-CH** and **PDA-Ph**.

a. Absorption maximum in CHCl₃ solution (ca. 10⁻⁵ M), thin film date in parentheses. b. Absorption edge in CHCl₃ solution (ca. 10⁻⁵ M), thin film date in parentheses. c. Emission maximum in CHCl₃ solution (ca. 10⁻⁵ M), thin film date in parentheses. d. Emission quantum yield in CHCl₃ solution. e. Estimated from the onset of the absorption, thin film date in parentheses. f. Obtained from the electrochemical oxidation onset in CHCl₃ solution, thin film date in parentheses. g. Obtained from the difference of the optical bandgap and HOMO, thin film date in parentheses.

optical bandgaps. Thus, the direct attachment of phenyl groups mostly raises the HOMO energy levels without perturbing the LUMO levels of the PTA polymers, which is understandable since the LUMO level is expected to reside mainly on the more electron deficient triple bonds along the main-chains. Fluorescence quantum yields of **PDA-CH** and **PDA-Ph** were determined to be 1.4% and 0.1% in chloroform solution, respectively, using quinine bisulfate as the standard. The quantum yields of these PTAs are significantly higher than identically substituted PDAs,⁹² while the phenyl substituted polymers consistently have lower quantum yields than the alkylated ones. Upon casting into thin films, both **PDA-CH** and **PDA-Ph** experienced large red-shifts in both absorption and emission spectra as shown in Figure 3.5B. The absorption profile of **PDA-CH** is significantly more structured than that of **PDA-Ph**, which indicates more crystalline structures in **PDA-CH** and is consistent with the DSC results.

PDAs with proper side-chain substitutions are well-known to undergo thermochromic and solvatochromic transitions. We did not observe significant thermochromisms in our newly prepared PTAs in both powder and thin film forms, but did observe apparent solvatochromism as shown in Figures 3.7 and 3.8. By

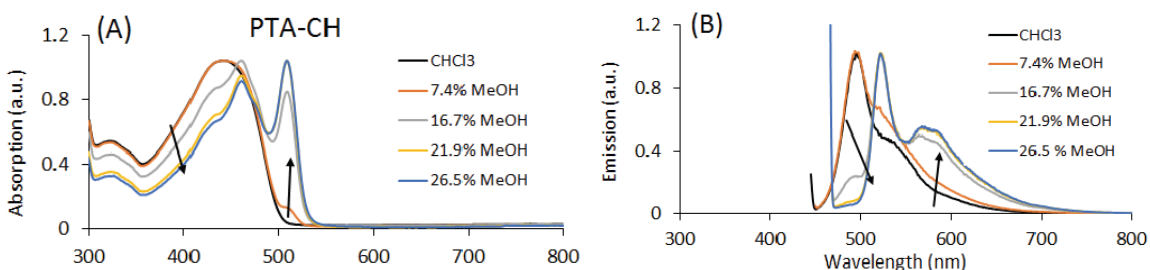


Figure 3.7. UV-vis absorption (A) and emission (B) spectra of **PDA-CH** in CHCl_3 solutions (10^{-5}M repeat units) with gradual additions of methanol (percentages by volume).

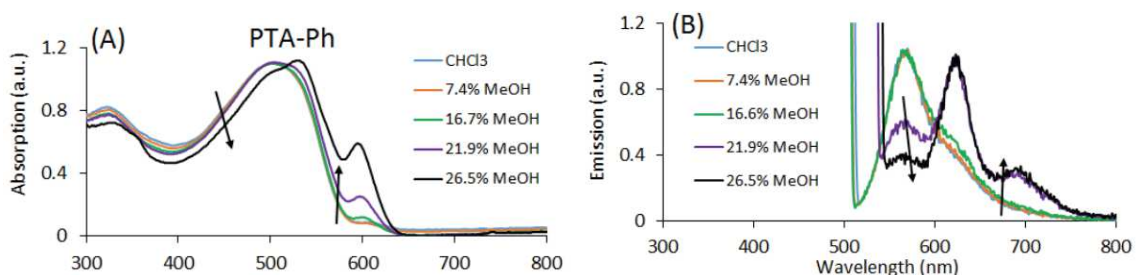


Figure 3.8. UV-vis absorption (A) and emission (B) spectra of **PDA-Ph** in CHCl_3 solutions (10^{-5}M repeat units) with gradual additions of methanol (percentages by volume).

gradual additions of methanol, a poor solvent for both PTAs, new vibronic features at 508 nm for **PDA-CH** and 585 nm for **PDA-Ph** become increasingly apparent until the volume fractions of methanol reach ca. 30% when the polymers start to precipitate. Noticeably, the feature at 585 nm for **PDA-Ph** (Fig. 3.8A) induced by methanol addition is more pronounced than that from the thin films (Fig. 3.5 B), indicating more ordered aggregation of **PDA-Ph** by slow additions of a poor solvent.

Meanwhile, with the additions of methanol, emission spectra of both PTAs become more structured and red-shifted, similar to those observed in the transitions from solutions to thin films.

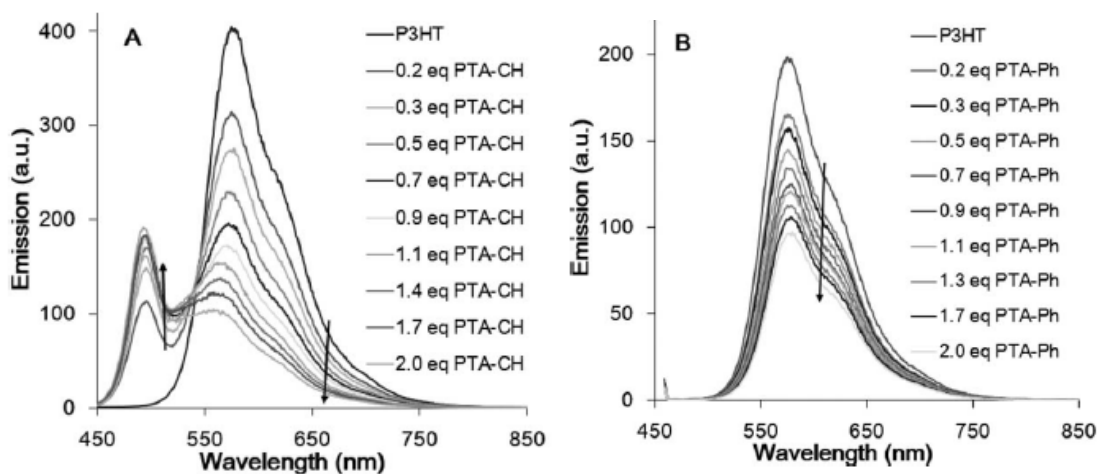


Figure 3.9. Fluorescence spectra of poly(3-hexylthiophene) (P3HT) solutions (1.0×10^{-5} M, r.p. units, in CHCl_3) excited at 433 nm with gradual additions of (A) **PDA-CH** and (B) **PDA-Ph** at different molar ratios (r.p. units).

We next explored the possibilities of applying the PTAs in organic electronic devices by performing fluorescence quenching experiments on poly(3-hexylthiophene) (P3HT) using PTACH and **PDA-Ph**. P3HT is the most studied CP in organic photovoltaic (OPV) devices that have been considered promising candidates as portable, light weight and low cost alternative energy sources.^{186,187} The most efficient CP based OPVs involve blending of a CP and a fullerene derivative, as the electron acceptor, to form the so-called bulk heterojunction (BHJ).¹⁸⁸ However, fullerenes are generally expensive and do not absorb light strongly. Thus, alternative electron acceptors are greatly sought after,

among which polymers capable of accepting and conducting electrons are promising due to their better film forming ability than small molecules.¹⁸⁹

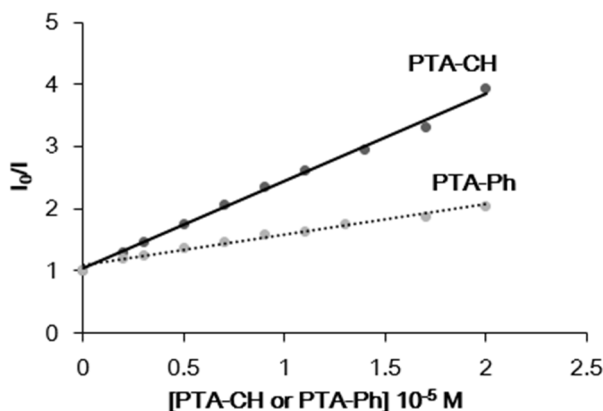


Figure 3.10. Stern-Volmer plots of P3HT fluorescence quenching in solutions using **PDA-CH** and **PDA-Ph** and their linear fits for quenching constants calculation.

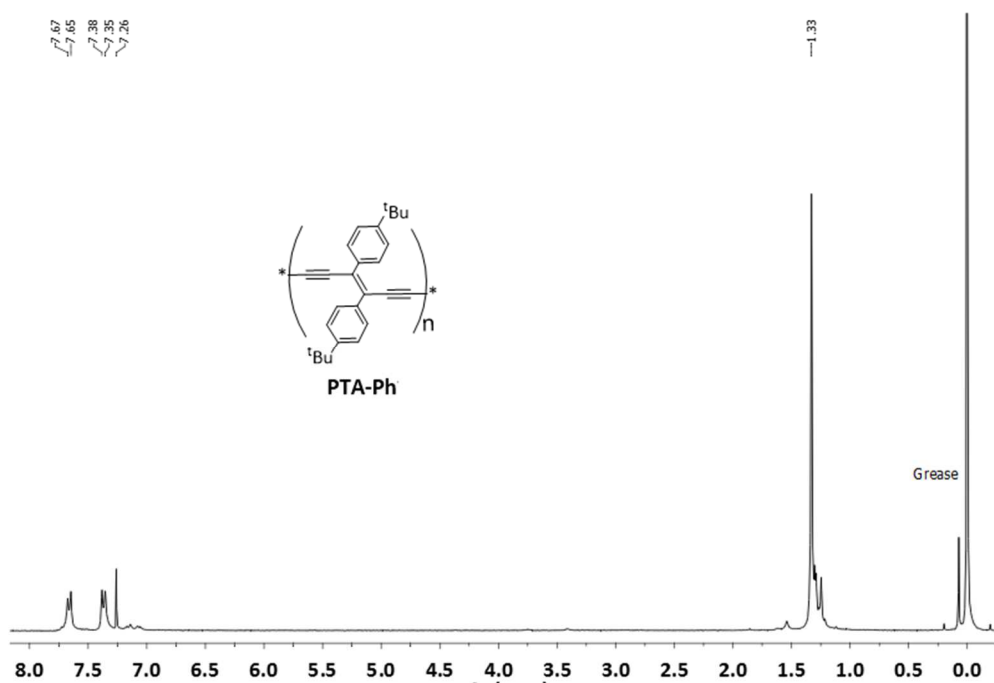
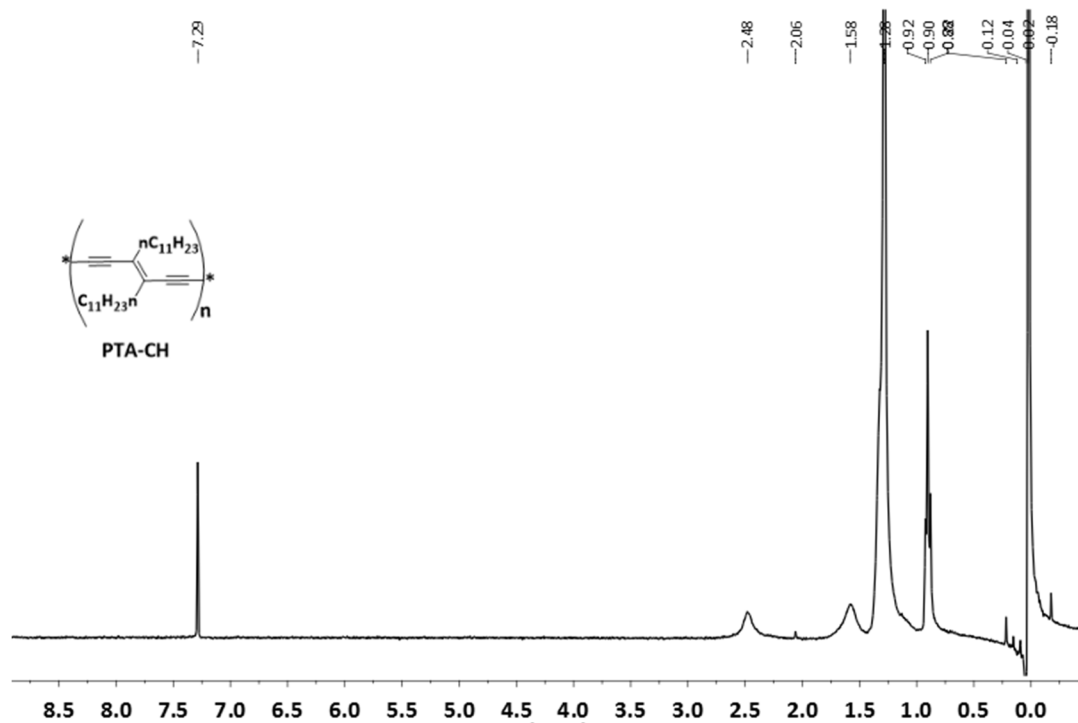
PTAs possess electron deficient triple bonds along the polymer backbone and the cylindrical orbital shapes can promote enhanced electron delocalization and conduction. As a first step, we studied P3HT fluorescence quenching behaviors using PTAs in dilute solutions to assess the feasibility of electron transfer reactions between the polymers and the results are shown in Fig. 3.9. The concentrations of P3HT are kept low (1×10^{-5} M) so that the maximum absorbance is less than 0.1 and aliquots of concentrated PTA solutions (1×10^{-5} M) were added gradually. This ensures that any fluorescence changes observed are not caused by concentration changes or competing absorption between the polymers. Both **PDA-CH** and **PDA-Ph** quench the fluorescence of P3HT significantly. A 4-fold decrease in P3HT emission intensity was observed when 2 eq. of **PDA-CH** was added, accompanied by increased intensities of **PDA-CH** emission at ca. 500 nm. In the case of **PDA-**

Ph, ca. 50% of emission intensity was quenched when 2 eq. of the quencher was added, while due to the very weak emission of **PDA-Ph** that is overlapped with the emission of P3HT, fluorescence of **PDA-Ph** was not detected. We assign such quenching behaviors to electron transfer since the emission of P3HT has little overlaps with the absorption of both PTAs in dilute solutions, which excludes the possibility of resonance energy transfer. From the Stern-Volmer plots (Fig. 3.10), the quenching constants for **PDA-CH** and **PDA-Ph** are respectively $1.4 \times 10^5 \text{ M}^{-1}$ and $4.9 \times 10^4 \text{ M}^{-1}$. Based on the similar LUMO levels for both PTAs, the smaller quenching constant for **PDA-Ph** is likely caused by the bulky phenyl side-chains that increase contact distances between the two polymers and make short-ranged electron transfer reaction more difficult.

3.4 Conclusion

In summary, we have successfully prepared PTA polymers having directly attached aromatic substituents. Our methodology allows facile tuning of physical and electronic properties of PTAs by installing electronically distinct moieties directly onto the main-chains, which has been hardly achievable using previously established methods. Emission quenching of a prototypical CP used in OPV devices, P3HT, has been observed by these PTAs, most likely through electron transfer reactions. These observations suggest possible applications of functional PTAs in organic electronic devices, which is currently under investigation.

3.5 NMR spectra of key compounds



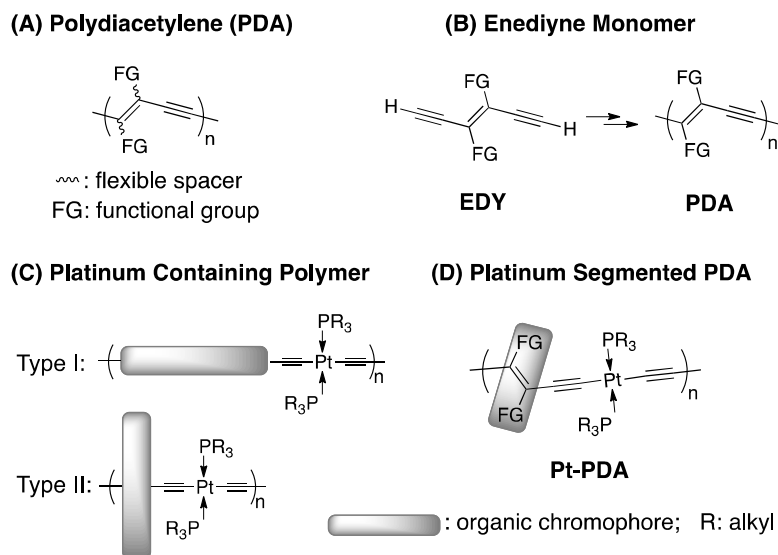
4 Chapter 4

Platinum-Segmented Polydiacetylenes

(Reproduced from *Journal of Polymer Science Part A: Polymer Chemistry* **2014**, 52, 2662–2668, with permission from Wiley-VCH Verlag GmbH & Co. KGaA)

4.1 Introduction

Among an overwhelmingly large amount of examples, polydiacetylenes (PDAs, Scheme 4.1 A) represent one of the prototypical and unique classes of CPs since the initial discovery in 1969.⁹⁵ PDAs are considered quasi one-dimensional semiconductors having macroscopic long-range coherence and anisotropy, which undergo intriguing optical changes among blue, red and yellow phases upon exposure to external stimuli.^{96,97,100,101,104–108} PDAs have found applications in non-linear optics,^{109,110,190–192} organic conductors^{111,112} and most widely, as sensory materials.^{113–115} However, PDAs have rarely been applied in solution processed organic electronic devices. Stringent geometrical requirements during the commonly applied topochemical solid-state synthesis severely limit structural variations of substituents directly attached the polymer backbone.^{96,116,117} Electronic properties of resulting PDAs are thus difficult to modify through substituent variation and the polymers usually have limited solubility, making integration of these materials into solution-fabricated electronic devices challenging. We have



Scheme 4.1. Overview

recently developed a facile synthetic route towards functionalized eneiyne (EDY, Scheme 4.1 B) molecules.⁹² Following methylation of the terminal alkynes, PDAs having directly attached aromatic groups and tunable electronic properties were obtained via a novel acyclic eneiyne metathesis polymerization technique. Incorporation of transition metals into CP frameworks is another intriguing strategy to adjust polymer electronic features and result in properties characteristic to metals.^{193–200} Platinum containing CPs are a commonly encountered class of such metal incorporated polymers, which have been applied frequently in organic photovoltaics (OPVs).^{201–214} Typical Pt containing polymers have the Type I structures shown in Scheme 4.1C, in which the organic chromophores feature several electron-rich and -poor aromatic moieties connected in series along the main chain direction.^{215–221} In such donor-acceptor design, chromophores typically contain several aromatic rings side-by-side and are relatively long. The increased chromophore length can potentially dilute Pt induced spin-orbit coupling effects

and lower triplet generation yields that have been considered beneficial for OPV operations.^{222–227} For this regard, the Type II structure shown in Scheme 4.1 can be especially interesting, in which chromophores are connected through the short axis and the distance between chromophore and Pt centers is greatly reduced. Such structural motif has yet to be studied in detail for Pt containing CPs.

We report herein the synthesis and characterization of a series of Pt segmented PDAs (Pt-PDAs) as shown in Scheme 4.1D. These structures can be considered PDAs having every other double bond replaced with a Pt center. The remaining double bonds bear two functional groups that are fully conjugated with each other and with the main-chain, leading to the Type II structure discussed above. Impacts on polymer properties and OPV device performance with such structural design, *i.e.* Pt incorporation and chromophore conjugation perpendicular to polymer main-chain, are studied in detail.

4.2 Experimental

Materials and General Methods

All reagents and solvents were used as received from Sigma- Aldrich or VWR unless otherwise noted. Phenyl-C61-butyric acid methyl ester (PCBM, >99.5%) was purchased from American Dye Source. Triisopropyl((trimethylsilyl)ethynyl)silane (M1) was synthesized as described previously.¹⁴⁵ THF was distilled from Na/benzophenone before use. Anhydrous dichloromethane was obtained by distillation over CaH₂ and degassed through several freeze-pump-thaw cycles. The 300.13 MHz ¹H, 75.48 MHz ¹³C NMR, and

121.5 MHz ^{31}P NMR spectra were recorded on a Bruker Avance III Solution 300 spectrometer. All solution ^1H and ^{13}C NMR spectra were referenced internally to the tetramethylsilane peaks. Size exclusion chromatography (SEC) analyses were performed in chloroform with 0.5% (v/v) triethylamine (1 mL/min) using a Waters Breeze system equipped with a 2707 autosampler, a 1515 isocratic HPLC pump, and a 2414 refractive index detector. Two styragel columns (Polymer Laboratories; 5 μm Mix-C), which were kept in a column heater at 35 $^{\circ}\text{C}$, were used for separation. The columns were calibrated with polystyrene standards (Varian). Ultraviolet–visible (UV–vis) absorption spectra were recorded on a Shimadzu UV-2401 PC spectrometer over a wavelength range of 250–800 nm. Fluorescence emission spectra were obtained using a Varian Cary Eclipse Fluorometer. Differential scanning calorimetry (DSC) measurements were performed on a Mettler Toledo DSC STARe system with about 5–10 mg sample and at a scan rate of 10 $^{\circ}\text{C}/\text{min}$. The results reported are from the second heating cycle. Cyclic Voltammetry was performed at 25 $^{\circ}\text{C}$ on a CH Instrument CHI604xD electrochemical analyzer using a glassy carbon working electrode, a platinum wire counter electrode and a Ag/AgCl reference electrode calibrated using ferrocene redox couple (4.8 eV below vacuum).

Solar Cell Fabrication and Testing

ITO-coated glass substrates (China Shenzhen Southern Glass Display. Ltd, 8 Ω/\square) were cleaned by ultrasonication sequentially in detergent, DI water, acetone and isopropyl alcohol, each for 15 min followed by UV-ozone treatment (PSD Series,

Novascan) for 45 min. MoO₃ (10 nm) was deposited inside a glovebox integrated Angstrom Engineering Åmod deposition system at a base vacuum level < 7 × 10⁻⁸ Torr. Polymer/PCBM blend solutions were then spun-cast at predetermined speeds using a glovebox integrated spin coater (Special Coating Systems, SCS-G3). Al (100 nm) was lastly thermally evaporated through patterned shadow masks. Current–voltage (I–V) characteristics were measured by a Keithley 2400 source-measuring unit under simulated AM1.5G irradiation (100 mW/cm⁻²) generated by a Xe arc-lamp based Newport 67005 150-W solar simulator equipped with an AM1.5G filter (Newport). The light intensity was calibrated using a Newport thermopile detector (model 818P-010-12) equipped with a Newport 1916-C Optical Power Meter.

1-(thiophen-2-yl)-3-(triisopropylsilyl)prop-2-yn-1-one (M2): To a suspension of AlCl₃ (7.36 g, 55.2 mmol) in 200 mL hexanes was added triisopropyl(trimethylsilyl)ethynylsilane (11.72 g, 46.0 mmol) and thiophene-2-carbonyl chloride (6.95 g, 47.4 mmol) at 0 °C. After stirring for 45 min at 0 °C and 3 h at room temperature, the reaction was quenched with water and ice mixture. The reaction mixture was extracted with hexanes twice. The organic phase was combined, washed with saturated NaHCO₃ solution and saturated brine, dried with anhydrous Na₂SO₄. After removal of solvents, the crude product was recrystallized in methanol at –20 °C to afford **M2** as a light yellow solid (12.2 g, 90.1%).

¹H NMR (300.13 MHz, CDCl₃): δ (ppm) = 1.12-1.34 (m, 21H), 7.16 (dd, 1H, J_{HH}³ = 4.8 and 3.6 Hz), 7.70 (d, 1H, J_{HH}³ = 4.8 Hz), 7.94 (d, 1H, J_{HH}³ = 3.6 Hz). ¹³C NMR

(75.48 MHz, CDCl₃): δ (ppm) = 10.1, 18.4, 96.3, 102.5, 128.3, 134.8, 135.1, 144.8, 169.0.

(E)-(3,4-di(thiophen-2-yl)hexa-3-en-1,5-diyne-1,6-diyl) bis(triisopropylsilane)

(M3): To a suspension of zinc powder (5.10 g, 78.0 mmol) in 300 mL dry THF was added TiCl₄ (4.22 mL, 38.9 mmol) drop wise at 0 °C under nitrogen. The mixture was heated to reflux for 5 h till a dark solution was obtained, and then cooled down to 0 °C. Compound **M2** (7.50 g, 25.7 mmol) and pyridine (2.50 mL, 28.3 mmol) was added through a degassed syringe and the reaction mixture was refluxed for another 24 h. The reaction was quenched with saturated sodium bicarbonate, extracted with ethyl ether twice. The combined organic phase was washed with saturated brine and dried with anhydrous Na₂SO₄. Compound **M3** was recrystallized in hexane and ethanol at -20 °C as a light brown solid (3.50 g, 49.3%).

¹H NMR (300.13 MHz, CDCl₃): δ (ppm) = 1.11-1.23 (m, 42H), 7.00 (dd, 2H, $J_{\text{HH}}^3 =$ and 3.9 Hz), 7.31 (d, 2H, $J_{\text{HH}}^3 = 5.1$ Hz), 8.00 (d, 2H, $J_{\text{HH}}^3 = 3.9$ Hz). ¹³C NMR (75.48 MHz, CDCl₃): δ (ppm) = 11.4, 18.7, 106.2, 106.4, 118.8, 126.5, 126.8, 129.3, 142.2.

(E)-1,1'-(5,5'-(1,6-bis(triisopropylsilyl)hexa-3-en-1,5-diyne-3,4-

diyl)bis(thiophene-5,2-diyl))bis(dodecan-1-one) (M4): To a suspension of AlCl₃ (0.600 g, 4.50 mmol) in 20 mL dry dichloromethane was added dodecanoyl chloride (1.29 mL, 5.40 mmol) and compound **M3** (1.01 g, 1.81 mmol) at 0 °C. After stirring for 45 min at 0 °C and 12 h at room temperature, the reaction was quenched

with water and ice mixture, extracted with hexanes twice. The organic layer was combined, washed with saturated NaHCO₃ solution, saturated brine and dried with anhydrous Na₂SO₄. Compound **M4** was passed through a silica gel column (eluent CH₂Cl₂) and then recrystallized in hexane at -20 °C as a red solid (0.83 g, 50.0%).
¹H NMR (300.13 MHz, CDCl₃): δ (ppm) = 0.88 (t, 6H, $J_{\text{HH}}^{\beta} = 6.6$ Hz), 1.11-1.24 (m, 42H), 1.26-1.33 (m, 32H), 1.72 (m, 4H), 2.86 (t, 4H, $J_{\text{HH}}^{\beta} = 7.5$ Hz), 7.62 (d, 2H, $J_{\text{HH}}^{\beta} = 3.9$ Hz), 7.96 (d, 2H, $J_{\text{HH}}^{\beta} = 3.9$ Hz). ¹³C NMR (75.48 MHz, CDCl₃): δ (ppm) = 11.3, 14.1, 18.7, 22.7, 24.8, 29.3, 29.4, 29.5, 29.6, 31.9, 39.6, 104.7, 110.5, 120.4, 130.6, 130.9, 144.0, 148.6, 193.5.

(E)-1,1'-(5,5'-(hexa-3-en-1,5-diyne-3,4-diyl)bis(thiophene-5,2-

diyl))bis(dodecan-1-one) (EDY-Th). To a solution of **M4** (2.00 g, 2.20 mmol) in 40 mL THF was added tetrabutylammonium fluoride (1M in THF, 8.80 mL, 8.80 mmol) and 1 mL water. The mixture was stirred overnight at room temperature. The reaction mixture was then extracted with ethyl ether twice, washed with saturated brine and dried over anhydrous Na₂SO₄. After removal of solvent, the crude product was passed through a silica gel column (eluent CH₂Cl₂) and then recrystallized in hexane and chloroform at -20 °C to afford **EDY-Th** as a yellow powder (1.10 g, 83.3%).

¹H NMR (300.13 MHz, CDCl₃): δ (ppm) = 0.88 (t, 6H, $J_{\text{HH}}^{\beta} = 6.6$ Hz), 1.26-1.33 (m, 32H), 1.72 (m, 4H), 2.89 (t, 4H, $J_{\text{HH}}^{\beta} = 7.5$ Hz), 4.07 (s, 2H), 7.62 (d, 2H, $J_{\text{HH}}^{\beta} = 4.2$ Hz), 7.88 (d, 2H, $J_{\text{HH}}^{\beta} = 4.2$ Hz). ¹³C NMR (75.48 MHz, CDCl₃): δ (ppm) = 14.1, 22.7,

24.8, 29.3, 29.4, 29.5, 29.6, 31.9, 39.4, 81.8, 93.7, 120.5, 130.7, 131.6, 144.7, 147.4, 193.9.

General procedure for the synthesis of Pt-PDAs using Pt-PDA-CH as a representative.

The reaction was set up in a glovebox under Argon. To a solution of 0.20 mmol **EDY-CH** monomer and 0.20 mmol *trans*-Pt(PEt₃)₂Cl₂ was added 19 mg CuI (0.10 mmol), 10 mL dry CH₂Cl₂ and 3 mL dry triethylamine. After stirring at room temperature for 24 h under argon, the reaction was quenched by exposing to air. The reaction mixture was concentrated to ca. 0.7 mL, and then added dropwise to 30 mL methanol for precipitation. The polymers were collected by filtration, washed with methanol and dried under high vacuum.

Pt-PDA-CH was isolated as a yellow waxy solid (80 mg, 82.9 %).

¹H NMR (300.13 MHz, CDCl₃): δ (ppm) = 0.88, 1.09-1.17, 1.25, 1.51, 2.07, 2.38. ¹³C NMR (75.48 MHz, CDCl₃): δ (ppm) = 8.26, 14.1, 15.9, 16.1, 16.3, 22.7, 29.4, 29.7, 29.8, 29.9, 30.1, 31.9, 36.7, 127.1. ³¹P NMR (121.5 MHz, CDCl₃): δ (ppm) = 12.20 (J_{P-Pt} = 2425 Hz). SEC (CHCl₃, 1 mL/min): M_n = 11.9 kDa, M_w = 23.8 kDa, PDI = 2.0.

Pt-PDA-Ph was isolated as a yellow powder (20 mg, 88.5 %).

¹H NMR (300.13 MHz, CDCl₃): δ (ppm) = 0.74, 0.92, 1.25, 1.44, 1.72-1.83. ¹³C NMR (75.48 MHz, CDCl₃): δ (ppm) = 8.2, 15.7, 31.4, 34.4, 123.7, 128.9. ³¹P NMR (121.5

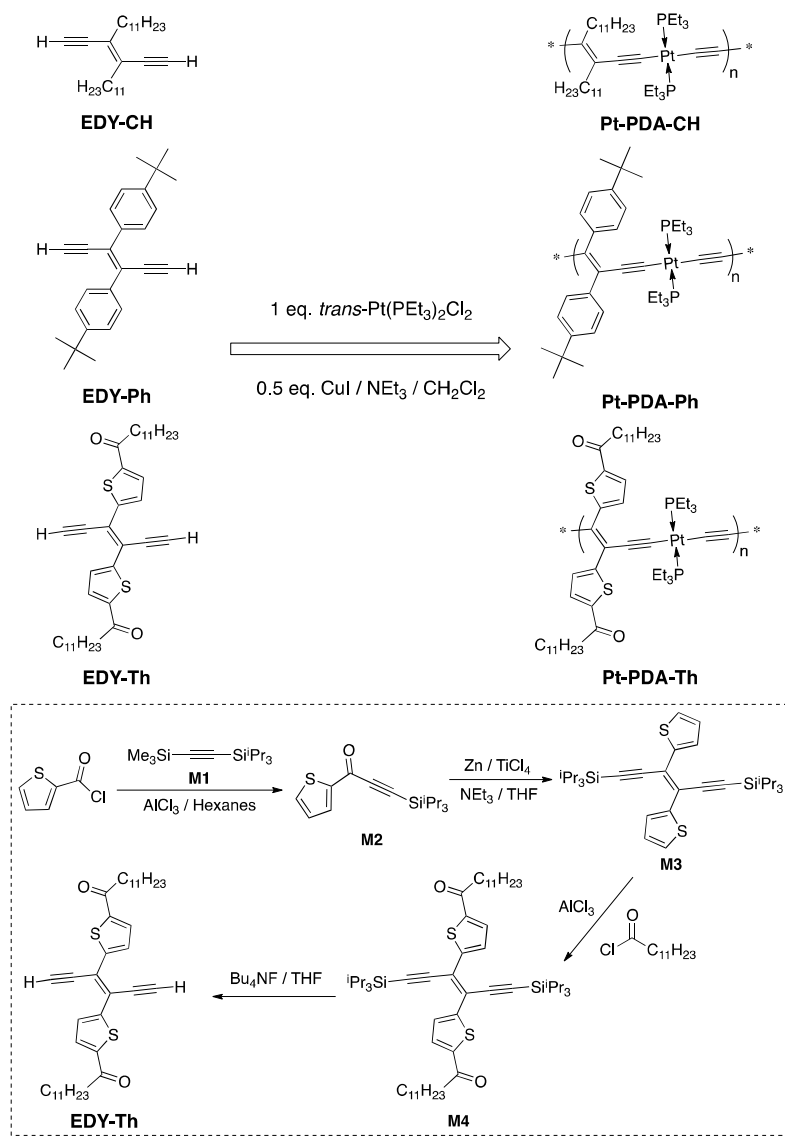
MHz, CDCl₃): δ (ppm) = 11.96 ($J_{\text{P-Pt}} = 2349$ Hz). SEC (CHCl₃, 1 mL/min): $M_n = 12.3$ kDa, $M_w = 22.1$ kDa, $PDI = 1.8$.

Pt-PDA-Th was isolated as a red powder (34 mg, 95.0 %).

¹H NMR (300.13 MHz, CDCl₃): δ (ppm) = 0.87, 1.19-1.26, 1.78, 2.12, 2.91, 7.68, 8.43. ¹³C NMR (75.48 MHz, CDCl₃): δ (ppm) = 8.5, 14.1, 16.1, 16.3, 16.6, 22.7, 25.2, 29.4, 29.6, 29.7, 31.9, 39.4, 131.4, 141.6, 154.7, 193.8. ³¹P NMR (121.5 MHz, CDCl₃): δ (ppm) = 12.56 ($J_{\text{P-Pt}} = 2341$ Hz). SEC (CHCl₃, 1 mL/min): $M_n = 13.1$ kDa, $M_w = 27.6$ kDa, $PDI = 2.1$.

4.3 Results and Discussion

Synthesis of EDY monomers and Pt-PDA polymers are summarized in Scheme 4.2. Preparation of **EDY-CH** and **EDY-Ph** was described previously⁹² and **EDY-Th** was synthesized similarly from commercially available thiophene-2-carbonyl chloride. In order to impart good solubility to resulting polymers, long alkyl side chains are the most commonly applied strategy. Attempts to install linear alkyl substituents at the 5-thienyl positions of **M3**, including lithiation followed by SN2 reaction with alkyl halides and halogenation followed by cross-coupling with alkyl Grignard reagents, failed to generate the desired products. Instead, acylation under Friedel–Crafts conditions led smoothly to **M4** that was easily converted to **EDY-Th** via desilylation. Polymerization was conducted by combining these EDY monomers with equimolar trans-Pt(PEt₃)₂Cl₂, respectively, in the presence of CuI and NEt₃ in CH₂Cl₂, which led to corresponding Pt-PDAs in high yields.



Scheme 4.2. Synthesis of Monomers and Polymers.

The polymers were purified by precipitation into and extraction with methanol, and were extensively dried under high vacuum. New reaction intermediates and resulting polymers were fully characterized by NMR spectroscopy, which supports proposed structures and matches those of related compounds reported previously.^{228,92} Molecular weights of the Pt-PDA polymers were estimated by SEC against polystyrene standards. All three polymers showed mono-modal profiles

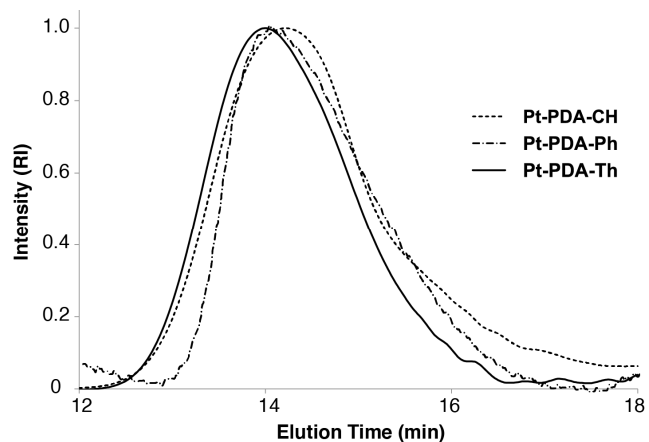


Figure 4.1. Size exclusion chromatograms (SEC) of **Pt-PDA-CH**, **Pt-PDA-Ph** and **Pt-PDA-Th** (CHCl_3 w/ 0.5% NEt_3 as eluent, 35 °C, 1 mL/min, RI detector).

(Fig. 4.1) and similar M_n 's of 11.9, 12.3 and 13.1 kDa were obtained for **Pt-PDA-CH**, **Pt-PDA-Ph**, and **Pt-PDA-Th**, respectively. Similar polydispersity indexes (PDIs) of about 2 were obtained for the polymers, which is typical of stepwise polymerization processes. These Pt-PDAs are readily soluble in various organic solvents including CHCl_3 , toluene, chlorobenzene and THF, and so forth. **Pt-PDA-CH** appears as a yellow wax and is even soluble in hexanes, likely due to the long undecyl side chains and the absence of any rigid aromatic groups. Both **Pt-PDA-Ph** and **Pt-PDA-Th** exist as solids, the former being yellow while the latter being red. Such apparently different solid state properties were probed in more detail by DSC measurements (Fig. 4.2). A melting transition ranging from 20 to 40 °C was observed for **Pt-PDA-CH**, which is likely due to side chain melting when considering the melting point of docosane ($n\text{-C}_{22}\text{H}_{46}$) at about 40 °C. No endotherms could be observed for **Pt-PDA-Ph** from 230 to 250 °C and large, irreversible exothermic transitions appeared above about 170 °C, possibly due to

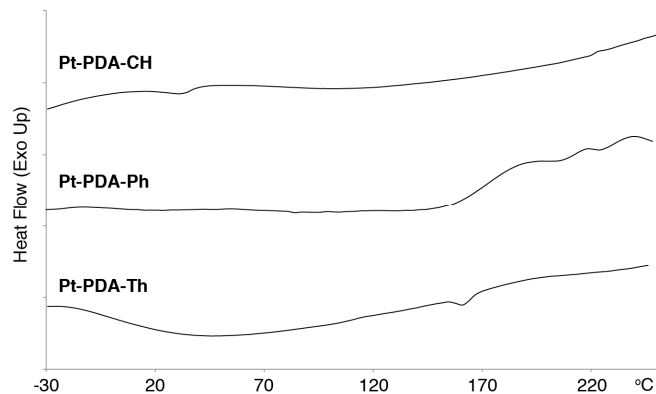


Figure 4.2. Differential scanning calorimetry (DSC) histograms of **Pt-PDA-CH**, **Pt-PDA-Ph** and **Pt-PDA-Th** (5–10 mg, 10 °C/min, 2nd heating curve, exotherm up).

	λ_{\max} (nm) ^a	λ_{em} (nm) ^b	Bandgap ^c (eV)	HOMO ^d (eV)	LUMO ^e (eV)	V_{OC} (V) ^f	J_{SC} (mA/cm ²) ^f	FF ^f	PCE (%) ^f
Pt-PDA-CH	388 (380)	417 (419)	2.9 (2.9)	−4.8	−1.9	— ^g	— ^g	— ^g	— ^g
Pt-PDA-Ph	422 (433)	454 (457)	2.7 (2.5)	−4.8	−2.1	0.65	0.61	0.38	0.15
Pt-PDA-Th	490 (497)	548 (552)	2.4 (2.3)	−5.2	−2.8	0.79	0.69	0.47	0.26

Table 4.1. Electronic Properties and OPV Device Parameters of Pt-PDAs.

^a CHCl₃ solutions (ca. 10^{−5} M), thin film data in parentheses; ^b excited at λ_{\max} , CHCl₃ solutions (ca. 10^{−5} M), thin film data in parentheses; ^c optical bandgap estimated from absorption edge, thin film data in parentheses; ^d estimated from oxidation onset in CH₂Cl₂ solution; ^e obtained from the difference between HOMO and optical bandgap in solution; ^f average of five devices; ^g not tested, see text.

polymer decomposition. Significant steric hindrance originated from bulky tert-butylphenyl and triethylphosphine substituents likely explains the amorphous nature and poor stability of the polymer. On the other hand, **Pt-PDA-Th**, bearing smaller and more planar acyl thienyl side groups, has a melting transition at 154–169 °C, indicating enhanced crystallinity. Optical properties of the Pt-PDAs are evaluated by absorption and emission spectroscopy in both dilute CHCl₃ solutions and as thin films. The results are summarized in Table 4.1 and Figure 4.3, and absorption and emission spectra of corresponding EDY monomers are shown in

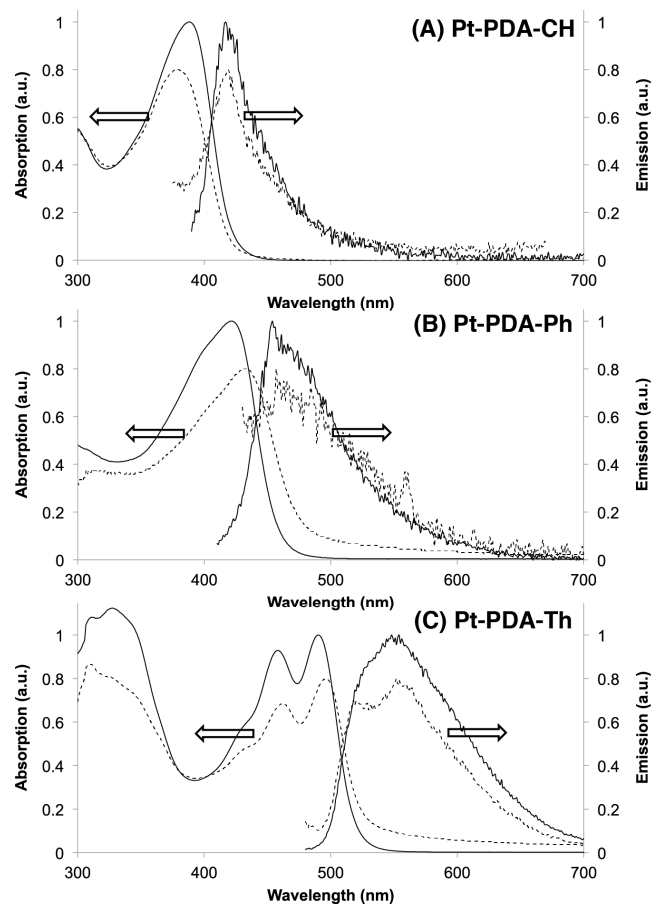


Figure 4.3. Absorption and emission spectra of **Pt-PDA-CH**, **Pt-PDA-Ph** and **Pt-PDA-Th** in air-free CHCl_3 solutions (10^{-5} M repeating units, solid lines) and thin films spun cast from CHCl_3 solutions (ca. 1 mg/mL) onto commercial ITO/glass substrates (dashed lines).

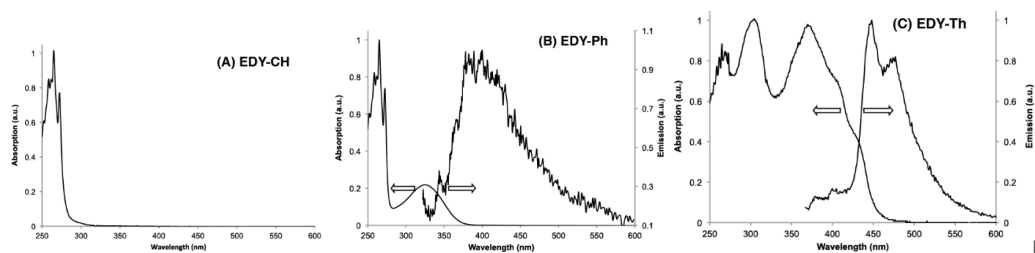


Figure 4.4. Absorption and emission spectra of **EDY-CH**, **EDY-Ph** and **EDY-Th** in CHCl_3 (ca. 10^{-5} M).

Figure 4.4. As seen in Figure 4.3, optical properties of Pt-PDAs are clearly tunable by variation of functional groups directly attached to the main chain double bonds. Both absorption and emission maxima red shift to longer wavelengths through replacing alkyl substituents with aromatic groups. The red-shift is more pronounced in **Pt-PDA-Th** due to the less aromatic, and thus more delocalized, thiophene moieties and electron withdrawing carbonyl groups. Such effect is further confirmed by cyclic voltammetry as shown in Figure 4.5. All three polymers showed multiple irreversible oxidation events and two common oxidation peaks having onsets at about 1.05 and 1.34 V (against Ag/AgCl reference electrode) are observed for all polymers. These are ascribed to stepwise two-electron oxidations at the platinum centers, consistent with previous literature reports.²²⁹ As expected, the first oxidation potentials are different due to the various extent of side chain conjugation in these polymers, which can be conveniently used to estimate the polymers' HOMO energy levels. While both **Pt-PDA-CH** and **Pt-PDA-Ph** have similar HOMO energy levels at about -4.8 eV, **Pt-PDA-Th** has a deeper lying HOMO level at about -5.2 eV. No reduction events could be observed for all three polymers within the experimental electrochemical window and the LUMO levels were thus estimated from the optical bandgaps (Table 4.1). **Pt-PDA-CH** exhibits structureless absorption and emission profiles while clear vibronic structures could be observed in the case of **Pt-PDA-Th**. Only slight red-shift can be observed in both absorption and emission profiles of **Pt-PDA-Ph** and **Pt-PDA-Th** compared with corresponding solution spectra, indicating an overall amorphous nature that has been observed in most other Pt-containing polymers. Interestingly, an 8-nm

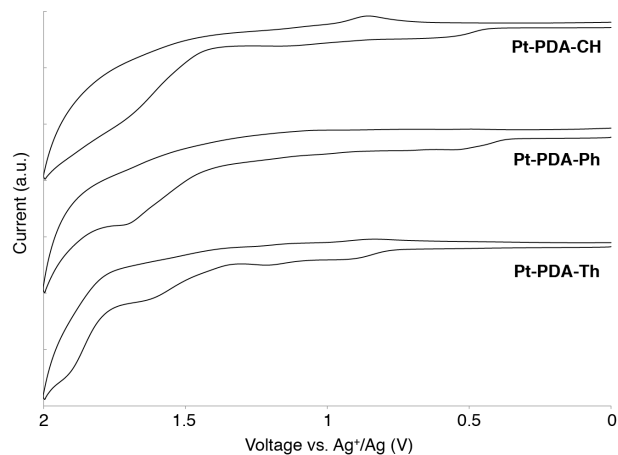


Figure 4.5. Cyclic Voltammograms of **Pt-PDA-CH**, **Pt-PDA-Ph** and **Pt-PDA-Th** (10 mM in CH_2Cl_2) externally referenced to ferrocene redox couple (0.1 M Bu_4NPF_6 as supporting electrolytes, 100 mV/s scan rate).

blue-shift is observed in the thin film absorption of **Pt-PDA-CH**, which is possibly due to side chain entanglement leading to main chain twist and reduction in conjugation lengths. Emissions of all three polymers are likely fluorescence in nature since relatively small Stoke's shifts and no emission intensity difference could be observed both in degassed and aerated solutions. Fluorescence quantum efficiencies are estimated against anthracene standards to be about 0.02, 0.2, and 0.03% for **Pt-PDA-CH**, **Pt-PDA-Ph**, and **Pt-PDA-Th**, respectively. Similarly, no fluorescence could be observed for **EDY-CH** while both **EDY-Ph** (0.13%) and **EDY-Th** (0.15%) have very low quantum efficiencies. There is thus likely an intrinsic ultra-fast excited state deactivation pathway other than Pt induced intersystem crossing in these EDY monomers and corresponding Pt-PDA polymers, which could be similar in nature as the dark states in blue-phase PDAs.⁹⁷

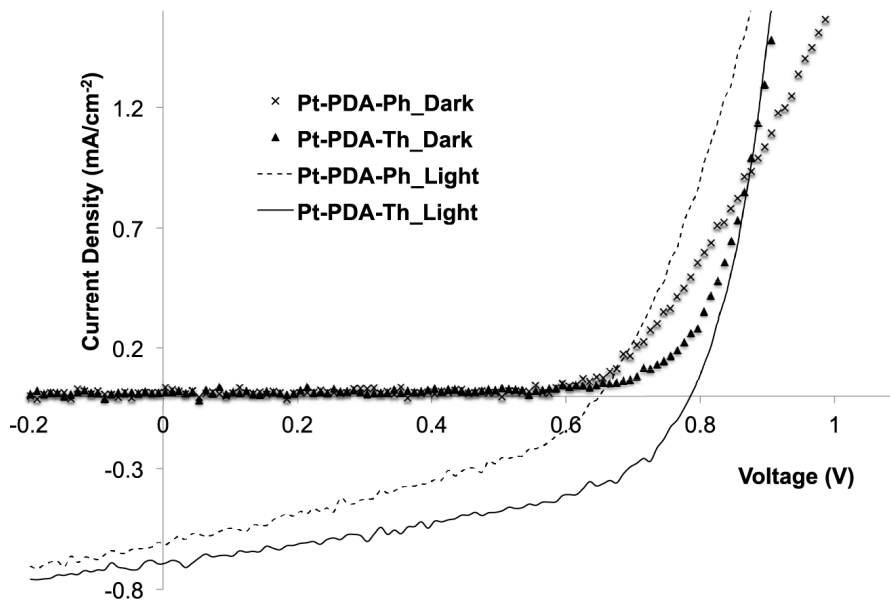


Figure 4.6. Representative current density–voltage (I – V) curves of solar cell devices employing **Pt-PDA-Ph** and **Pt-PDA-Th** both in dark and under simulated AM1.5 G irradiation (100 mW/cm^2).

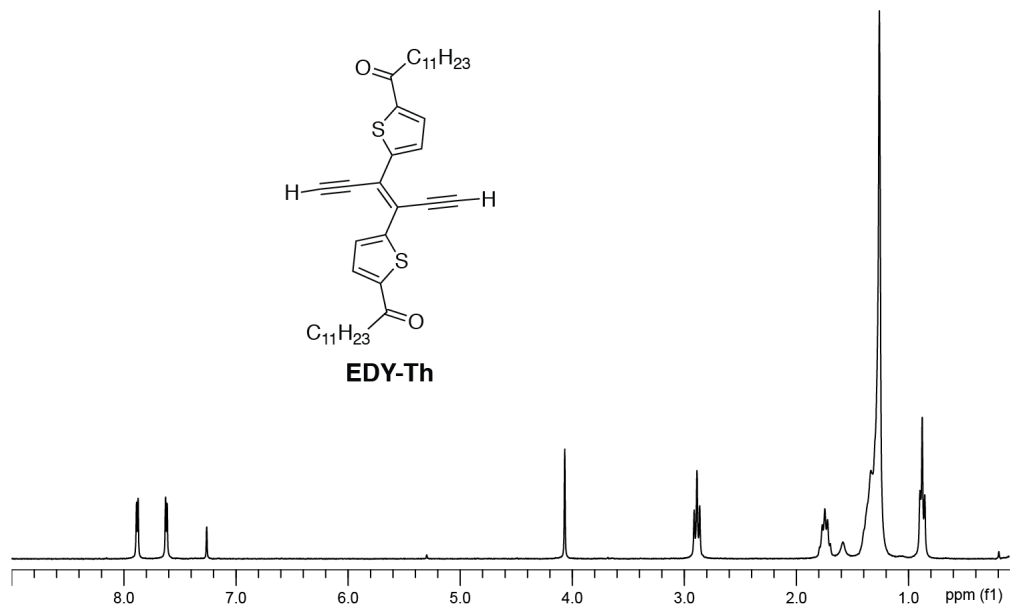
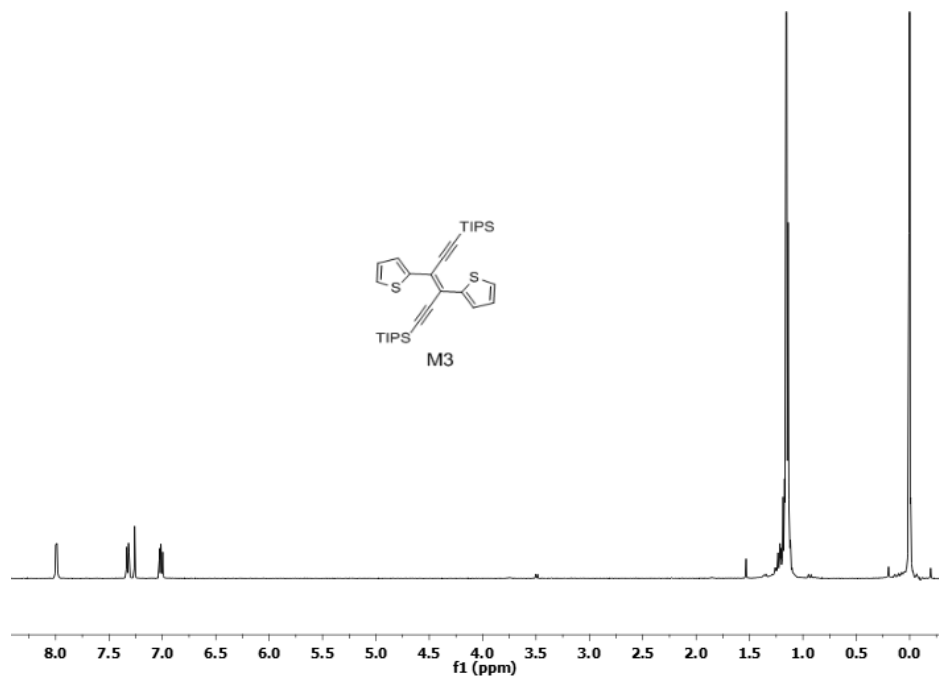
To further explore the possibility of applying these Pt-PDAs in solution processed electronic devices, bulk heterojunction (BHJ) OPVs were fabricated using these polymers and phenyl-C61-butyric acid methyl ester (PCBM) as the electron acceptor. All devices adopt the basic structure ITO/MoO₃ (10 nm)/active layer (100 nm)/Al (100 nm) and the active layer contains Pt-PDA and PCBM in a 1/2 ratio by weight. We have also experimented using the commonly applied PEDOT: PSS as the anode interfacial layer while keeping other fabrication parameters constant. All devices under test showed very low efficiencies that are strongly limited by reduced open circuit voltage (V_{oc}) values at 0.4 V for **Pt-PDA-Ph** and 0.14 V for **Pt-PDA-Th**, respectively. Such low V_{oc} values indicate non-Ohmic contacts between the anode and the active layer, as well as possible current leakage by using PEDOT: PSS, which is consistent with our previous

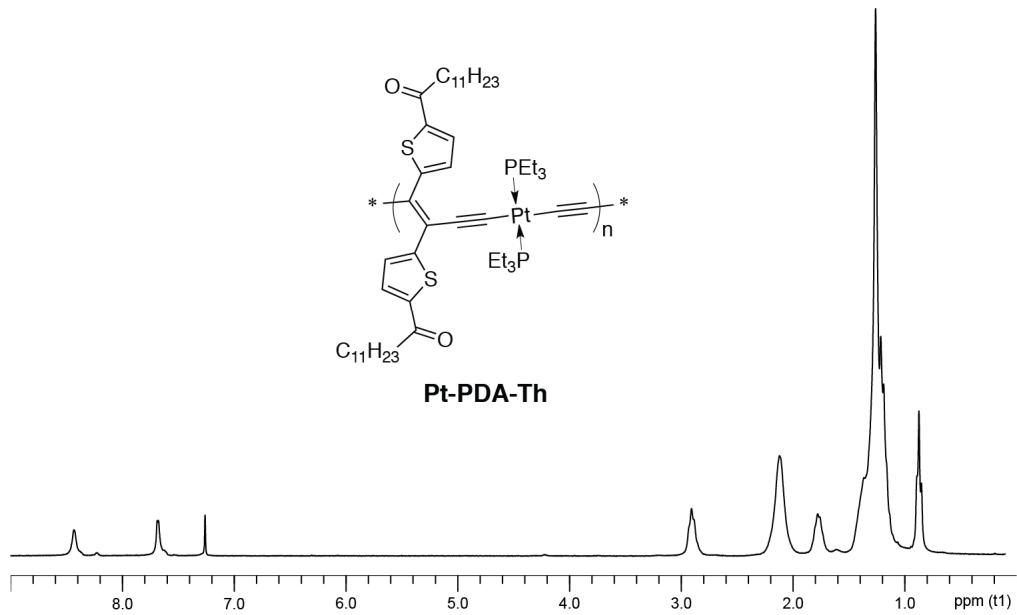
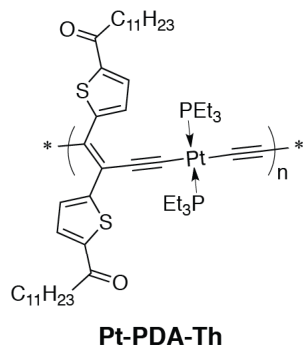
observations in OPVs employing similar Pt-containing polymers.²²⁸ 14 Devices were tested under as-cast conditions since thermal annealing was found to degrade performance significantly. Due to the low melting point and waxy nature of **Pt-PDA-CH**, no satisfactory blend films could be obtained and photovoltaic effects could not be observed. On the other hand, devices made from **Pt-PDA-Ph** and **Pt-PDA-Th** gave average power conversion efficiencies (PCEs) of 0.15% and 0.26% (Table 4.1, Figure 4.6), respectively. The latter showed a 0.14 V higher open circuit voltage (V_{oc}), which correlates well with the deeper lying HOMO level of **Pt-PDA-Th**. OPVs of both polymers suffer greatly from low short circuit currents (J_{sc}) and fill factors (FFs), which can be resulted from large bandgaps, amorphous nature and short-lived excitons. We are currently optimizing these devices and studying the charge generation mechanisms in more detail.

4.4 Conclusion

In summary, we have successfully prepared a novel series of platinum segmented polydiacetylenes that bear conjugated side groups directly attached to the polymer main chains. Physical and electronic properties of resulting polymers can be systematically tuned through variation of the side groups and substituents. With proper selection of conjugated side chains, such Pt-PDA structural design can lead to polymers having interesting optical and electronic properties, and potentially finding applications in organic electronic devices including OPVs.

4.5 NMR spectra of key compounds





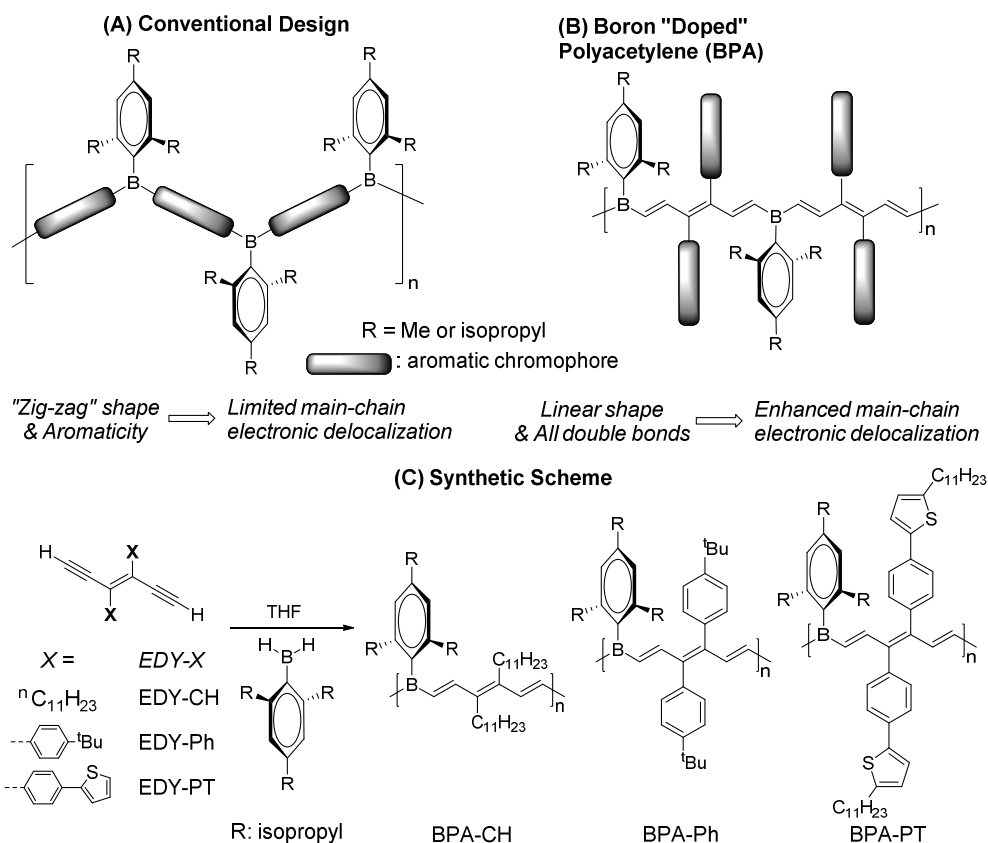
5 Chapter 5

Boron Doped Polyacetylenes

(Manuscript in preparation)

5.1 Introduction

Among a large library of CPs, main-chain organoboron CPs^{230–232} are a class of materials that incorporate tricoordinate borane into the main chain of CPs and display intriguing optical and electronic properties result from the interplay of empty p-orbital and π conjugated moieties. In particular, these conjugated materials are highly emissive with high quantum yields and possess nonlinear optical behavior, enabling their applications as optoelectronics such as OLEDs and nonlinear optical devices.^{29,31,233,234} The empty p-orbital of boron centers in the CPs can bind with certain Lewis base such as F^- , CN^- and certain amines, and therefore makes them attractive candidates for detection of toxic chemicals.^{234–238} The first examples of stable main chain boron containing CPs were prepared by Chujo and his coworker through hydroboration reaction in which steric protected arylboranes^{239–241} were reacted with aromatic dialkyne species to afford poly(vinylenearylenevinylene borane)s.²³² Later, organometallic condensation reactions^{242,237} tin-boron exchange protocols^{243–245} and transition metal catalyzed coupling reactions^{236,246} were developed and widely applied to embed boron in the main chain of conjugated polymers that were not accessible by hydroboration.



Scheme 5.1. Schematic drawing of main chain boron CPs (A) conventional design and (B) Boron doped polyacetylenes. (C) Synthesis of by hydroboration of EDYs.

Nevertheless, all the main-chain functionalized boron containing CPs reported so far bear aromatic units in the π conjugated moieties Scheme 5.1 A and due to the rigidity of aromatic rings the main chain of such polymer tend to adopt a zig-zag geometry. It is the aromaticity and zig-zag geometry resulted from the aromatic rings that often lead to less effective conjugation and large bandgaps in the main-chain functionalized boron containing CPs. On the other hand, aromatic unit-free boron main-chain CPs such as polyboracetylene only bears carbon-carbon double bonds as π conjugation, were theoretically predicted to have more effective conjugation and a zero bandgap.²⁴⁷ Despite the intriguing properties of such

organoboron polymers, polyboracetylene or its analogies have not been synthesized and reported presumably because of the synthetic challenge.

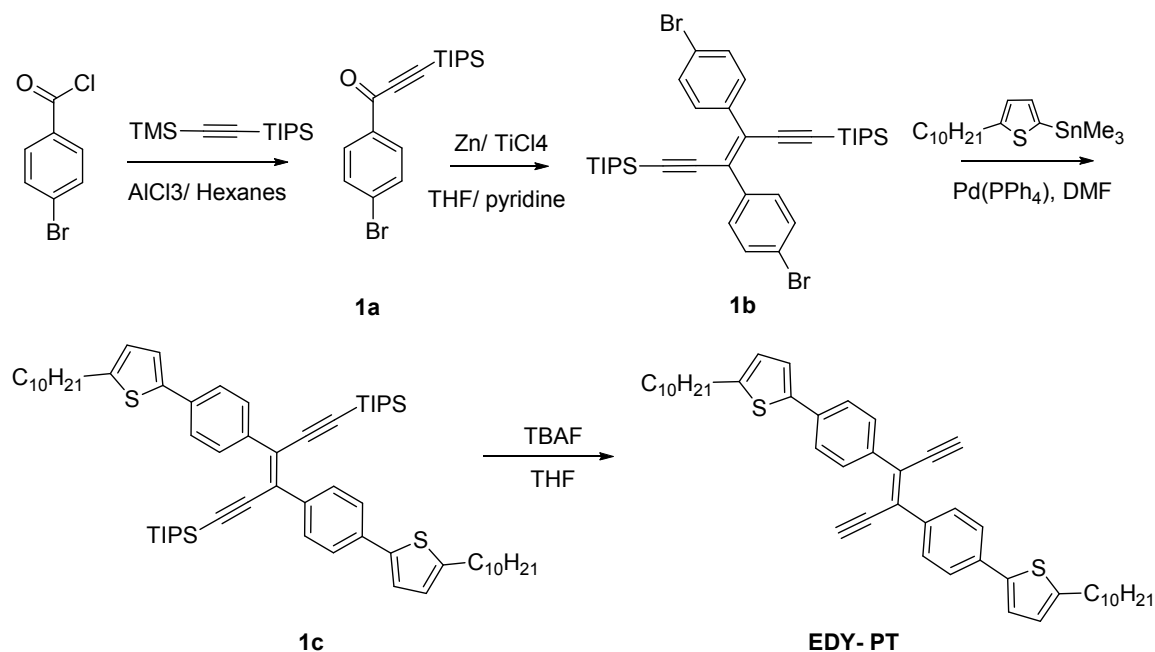
Our recent work on the trans-enediyne derived CPs⁹²⁻⁹⁴ have showed that the physical and chemical properties of these aromatic unit-free materials are tunable by the side chains of the polymers, and inspired us the synthesis of BPAs (Scheme 5.1 B) through hydroboration of functionalized trans-EDYs.

5.2 Experimental

Materials and General Methods

All reagents and solvents were used as received from Sigma-Aldrich or VWR unless otherwise noted. Triisopropyl(trimethylsilyl)ethynylsilane¹⁴⁵ was synthesized as described previously. THF was distilled from Na/benzophenone prior to use. Anhydrous dichloromethane was obtained by distillation over CaH₂ and degassed through several freeze-pump-thaw cycles. The 300.13 MHz ¹H and 75.48 MHz ¹³C NMR spectra were recorded on a Bruker Avance III Solution 300 spectrometer. All solution ¹H and ¹³C NMR spectra were referenced internally to the solvent peaks. Size exclusion chromatography (SEC) analyses were performed in chloroform with 0.5% (v/v) triethylamine (1 mL/min) using a Waters Breeze system equipped with a 2707 autosampler, a 1515 isocratic HPLC pump and a 2414 refractive index detector. Two styragel columns (Polymer Laboratories; 5 m Mix-C), which were kept in a column heater at 35 °C, were used for separation. The columns were calibrated with polystyrene standards (Varian). Ultraviolet-Visible (UV-Vis) absorption spectra were recorded on a Shimadzu UV-2401 PC

spectrometer over a wavelength range of 250-800 nm. Fluorescence emission spectra were obtained using a Varian Cary Eclipse Fluorometer.



Scheme 5.2. Synthesis of **EDY-PT**

1-(4-bromophenyl)-3-(triisopropylsilyl)prop-2-yn-1-one (1a): To a suspension of AlCl₃ (5.84 g, 43.80 mmol) in 100 mL hexanes was added triisopropyl((trimethylsilyl)ethynyl)silane (8.96 g, 35.20 mmol) and 4-bromobenzoyl chloride (8.0 g, 36.45 mmol) at 0 °C. After stirring for 45 min at 0 °C and then 1 h at room temperature, the reaction was quenched with ice water. The reaction mixture was extracted with hexanes twice. The organic layer was combined, washed sequentially with saturated NaHCO₃ solution and brine, and dried over anhydrous Na₂SO₄. Compound **1a** was purified by recrystallization in hexanes as a light yellow solid (10.1 g, 87.7 %).

^1H NMR (300.13 MHz, CDCl_3): δ (ppm) = 1.09–1.24 (m, 21H), 7.64 (d, 2H, $J_{\text{HH}}^3 = 8.4$ Hz), 8.04 (d, 2H, $J_{\text{HH}}^3 = 8.7$ Hz). ^{13}C NMR (75.48 MHz, CDCl_3), δ (ppm)=11.1, 18.5, 98.8, 102.6, 129.5, 130.8, 131.9, 135.5, 176.3.

(E)-3,4-bis(4-bromophenyl)-1,6-bis(triisopropylsilyl)hexa-3-en-1,5-diyne (1b):

To a suspension of 4.86 g zinc powder (74.35 mmol) in 100 mL dry THF was added 4.05 mL TiCl_4 (36.94 mmol) dropwise at 0 °C under nitrogen. The mixture was heated to reflux for 45 min until a dark solution was obtained, and then cooled down to 0 °C. Compound **1a** (9.0 g, 24.63 mmol) and 2.2 mL pyridine was added through a degassed syringe and the reaction mixture was refluxed for an additional 24 h. The reaction was quenched with NaHCO_3 , extracted with ethyl ether twice. The combined organic phase was washed with saturated brine and dried over anhydrous Na_2SO_4 . Compound **1b** was purified by recrystallization in THF/Ethanol as a light yellow solid (2.8 g, 57.1%).

^1H NMR (300.13 MHz, CDCl_3): δ (ppm) = 0.98- 0.99 (m, 42H), 7.46 (d, 4H, $J_{\text{HH}}^3 = 8.7$ Hz), 7.74 (d, 4H, $J_{\text{HH}}^3 = 8.4$ Hz). ^{13}C NMR (75.48 MHz, CDCl_3), δ (ppm)=11.2, 18.5, 103.7, 106.1, 122.3, 128.5, 130.8, 130.9, 137.7.

(E)-2-decyl-5-(4-(4-(4-(5-decylthiophen-2-yl)phenyl)-1,6-

bis(triisopropylsilyl)hexa-3-en-1,5-diyn-3-yl)phenyl)thiophene (1c): To a suspension of **1b** (2.0 g, 2.86 mmol) and (5-decylthiophen-2-yl)trimethylstannane (2.32 g, 6.0 mmol) in 10 mL dry DMF was added $\text{Pd}(\text{PPh}_3)_4$ (150 mg, 0.13 mmol) in a glove box filled with argon. The reaction was heated to 110 °C for 12 hours in

a pressure flask. The reaction mixture was extracted with hexanes twice. The organic phase was combined, washed with saturated brine and dried with anhydrous Na₂SO₄. After removal of solvent, the crude product was recrystallized in hexane and ethanol to afford compound **1c** as a light yellow solid (2.20 g, 78.0 %).

¹H NMR (300.13 MHz, CDCl₃), δ (ppm) = 0.89 (t, 6H, J³_{HH} = 6.9 Hz), 1.04 (m, 42H), 1.29 (m, 28H), 1.73 (m, 4H), 2.84 (t, 4H, J³_{HH} = 7.5 Hz), 6.77 (d, 2H, J³_{HH} = 2.4 Hz), 7.17 (d, 2H, J³_{HH} = 3.0 Hz), 7.53 (d, 4H, J³_{HH} = 8.1 Hz), 7.93 (d, 4H, J³_{HH} = 8.1 Hz).

¹³C NMR (75.48 MHz, CDCl₃), δ (ppm) = 11.3, 14.1, 18.6, 22.7, 29.1, 29.3, 29.4, 29.6, 30.3, 31.7, 31.9, 102.7, 107.0, 122.8, 124.6, 125.1, 128.6, 129.8, 134.4, 137.7, 141.5, 146.0.

EDY-PT: To a solution of **1c** (2.2 g, 2.23 mmol) in THF was added tetrabutylammonium fluoride (8.9 ml, 1M in THF). The mixture was stirred overnight at room temperature. The reaction mixture was then extracted with hexane twice, washed with saturated brine and dried over anhydrous Na₂SO₄. After removal of solvent, the crude product was recrystallized in hexane and ethanol to afford **EDY-PT** as a light yellow solid (1.32 g, 86.5 %).

¹H NMR (300.13 MHz, CDCl₃), δ (ppm) = 0.90 (t, 6H, J³_{HH} = 6.6 Hz), 1.29 (m, 28H), 1.72 (m, 4H), 2.84 (t, 4H, J³_{HH} = 7.5 Hz), 3.46 (s, 2H), 6.77 (d, 2H, J³_{HH} = 3.3 Hz), 7.19 (d, 2H, J³_{HH} = 3.3 Hz), 7.60 (d, 4H, J³_{HH} = 8.4 Hz), 7.86 (d, 4H, J³_{HH} = 8.4 Hz).

¹³C NMR (75.48 MHz, CDCl₃), δ (ppm) = 14.1, 22.7, 29.1, 29.3, 29.4, 30.3, 31.6, 31.9, 83.6, 87.2, 123.1, 124.8, 125.1, 128.4, 129.5, 134.9, 136.8, 141.1, 146.3.

BPA-CH: To the solution of the lithium triptylborate (32.7 mg, 0.146 mmol) in 5 mL dry THF was added 0.2 mL methyl iodide in an argon glovebox, and the resulting solution was stirred for 15 min at room temperature in a loosely capped vial to generate triptylborane. To the solution of in-situ generated borane was added a solution of **EDY-CH** (50.0 mg, 0.130 mmol) in 5 mL dry THF. The reaction was stirred for 20 hours at room temperature, and then it was concentrated under vacuum to 0.5 mL and precipitated in acetone. **BPA-CH** was obtained as a viscous light brown solid after filtration and thorough dry under high vacuum (60.0 mg, 76.6 %).

^1H NMR (300.13 MHz, CDCl_3), δ (ppm) = 0.90-1.27 (60 H, $-(\text{CH}_2)_9\text{CH}_3$ and CH_3 (tripyl)), 2.26-2.36 ($\text{C}=\text{C}-\text{CH}_2$, CH (tripyl)), 2.73 (CH (tripyl)), 2.89 (1H, CH (tripyl)), 5.30-6.29 ($\text{B}-\text{CH}=\text{CH}$), 6.93-6.99 (2H, Ar-H (tripyl)), 7.34-7.45 (Ar-H (tripyl)). ^{13}C NMR (75.48 MHz, CDCl_3), δ (ppm) = 14.1, 22.7, 24.0, 24.1, 24.2, 24.4, 24.7, 29.4, 29.5, 29.7, 32.0, 34.4, 34.7, 119.5, 120.1, 122.1, 129.6, 135.9, 141.1, 149.2, 150.3, 151.2. ^{11}B NMR (160.4 MHz, CDCl_3), δ (ppm) = 49.0 ppm.

BPA-Ph: To the solution of the lithium triptylborate (36.7 mg, 0.164 mmol) in 5 mL dry THF was added 0.2 mL methyl iodide in an argon glovebox, and the resulting solution was stirred for 15 min at room temperature in a loosely capped vial to generate triptylborane. To the solution of in-situ generated borane was added a solution of **EDY-Ph** (50.0 mg, 0.147 mmol) in 5 mL dry THF. The reaction was stirred for 20 hours at room temperature, and then it was concentrated under

vacuum to 0.5 mL and precipitated in acetone. **BPA-Ph** was obtained as a yellow solid after filtration and thorough dry under high vacuum (56.1 mg, 68.6 %).

^1H NMR (300.13 MHz, CDCl_3), δ (ppm) = 0.55-1.23 (36H, ^tBu and CH_3 (tripyl)), 1.99-2.17 (2H, CH (tripyl)), 2.70 (1H, CH (tripyl)), 5.31-6.01 (B-CH=CH), 6.59-7.08 (10H, Ar-H (^tBu -phenyl and tripyl)). ^{13}C NMR (75.48 MHz, CDCl_3), δ (ppm) = 24.1, 31.3, 33.8, 34.4, 34.8, 119.0, 124.5, 129.9, 135.0, 142.2, 145.9, 146.8, 148.5, 149.6, 153.8. ^{11}B NMR (160.4 MHz, CDCl_3), δ (ppm) = 52.0 ppm.

BPA-PT: To the solution of the lithium tripylborate (20.0 mg, 0.089 mmol) in 5 mL dry THF was added 0.2 mL methyl iodide in an argon glovebox, and the resulting solution was stirred for 15 min at room temperature in a loosely capped vial to generate tripylborane. To the solution of in-situ generated borane was added a solution of **EDY-PT** (50.0 mg, 0.074 mmol) in 5 mL dry THF. The reaction was stirred for 20 hours at room temperature, and then it was concentrated under vacuum to 0.5 mL and precipitated in acetone. **BPA-PT** was obtained as a red solid after filtration and thorough dry under high vacuum (45.3 mg, 68.5 %).

^1H NMR (300.13 MHz, CDCl_3), δ (ppm) = 0.80-1.31 (52H, $(\text{CH}_2)_7\text{CH}_3$ and CH_3 (tripyl)), 1.72 (4H, $(\text{C}=\text{CCH}_2\text{CH}_2)$), 1.93 (1H, CH (tripyl)), 2.46 (1H, CH (tripyl)), 2.82 (5H, $(\text{C}=\text{CCH}_2\text{CH}_2$ and CH (tripyl)), 5.60-6.10 (B-CH=CH), 6.50 (2H, Ar-H (tripyl)), 6.70-7.28 (12H, Ar-H (-PhTh)). ^{13}C NMR (75.48 MHz, CDCl_3), δ (ppm) = 14.1, 22.7, 23.6, 23.7, 24.0, 24.5, 29.2, 29.4, 29.7, 30.3, 31.7, 31.9, 33.8, 34.8, 119.0, 122.6, 124.8, 130.5, 133.5, 136.3, 141.4, 145.3, 145.7, 147.3, 148.1, 153.9. ^{11}B NMR (160.4 MHz, CDCl_3), δ (ppm) = 54.6 ppm.

5.3 Results and Discussion

EDY-CH and **EDY-Ph** were prepared by the previously reported method,²⁴⁸ and synthesis of **EDY-PT** is outlined in scheme 5.2 and detailed in the experimental section. BPAs were obtained by treating **EDYs** with the in-situ generated tripylborane to yield **BPA-CH**, **BPA-Ph** and **BPA-PT**, respectively (Scheme 5.1 C). These polymers are stable in air and have good solubility in common nonpolar solvents such as dichloromethane, chloroform, THF, toluene and chlorobenzene. The molecular weights of the polymers were estimated by size exclusion chromatography (SEC) against polystyrene standards to be $M_n = 6.5$ kDa, PDI = 1.41 and DP (degree of polymerization) = 11 for **BPA-CH**; $M_n = 12.2$ kDa, PDI = 1.59 and DP = 22 for **BPA-Ph**; and $M_n = 11.6$ kDa, PDI = 1.59 and DP = 13 for **BPA-PT** (Figure 5.1, data summarized in Table 5.1).

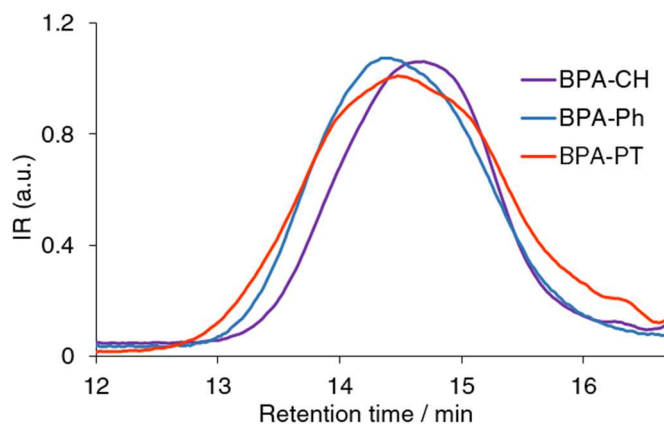


Figure 5.1. Size exclusion chromatograms of **BPA-CH**, **BPA-Ph** and **BPA-PT** (CHCl_3 w/ 0.5% NEt_3 , 1 mL/min, RI detector).

The ^{11}B NMR displays broad peaks at 49.0 ppm, 52.0 ppm and 54.6 ppm for **BPA-CH**, **BPA-Ph** and **BPA-PT**, respectively (Figure 5.2) and these values are comparable with reported tricoordinate boron CPs.^{244,249} The high molecular weights

	M_n/kDa^a	PDI ^b	λ_{max} (nm) ^c	λ_{em} (nm) ^d	Bandgap ^e (eV)	LUMO ^f (eV)	HOMO ^g (eV)	Bandgap ^h (eV)
BPA-CH	65.40	1.41	442 (398)	503 (506)	2.40 (2.39)	-3.08	-5.83	2.75
BPA-Ph	12.20	1.59	452 (386)	528 (522)	2.35 (2.50)	-3.13	-5.63	2.50
BPA-PT	11.60	1.43	464 (461,492)	567 (561)	2.31 (2.30)	-3.19	-5.50	2.31

Table 5.1. Summary of the molecular weights, optical and electrochemical properties of BPAs

^a Number average molecular weight. ^b Polydispersity. ^c THF solution (ca. 10^{-5} M), thin film data in parentheses. ^d Excited at λ_{max} THF solution (ca. 10^{-5} M), thin film data in parentheses. ^e Optical bandgap estimated from absorption edge, thin film data in parentheses. ^f Estimated from electrochemical reduction onset in CH_2Cl_2 solution. ^g Estimated from electrochemical oxidation onset in CH_2Cl_2 solution. ^h Calculated from HOMO and LUMO levels.

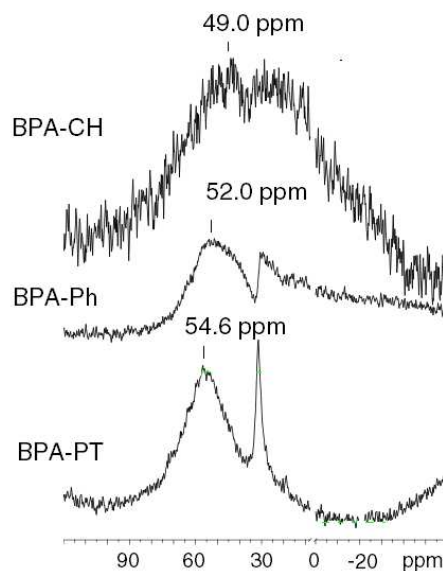


Figure 5.2. ^{11}B NMR of BPAs.

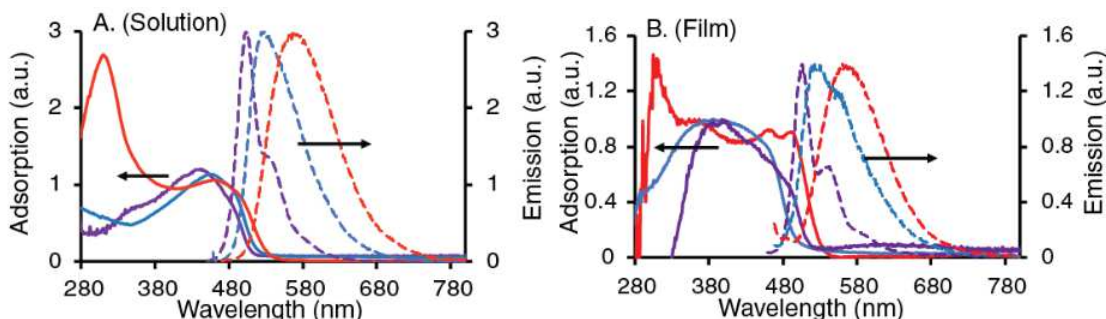


Figure 5.3. Absorption and emission spectra of in THF solution (ca. 10^{-5} M) (A) and as thin film drop casted from chlorobenzene solution (B). Purple, blue and red colors are assigned to **BPA-CH**, **BPA-Ph** and **BPA-PT**, respectively.

of BPAs as well as their ^{11}B NMR values indicate successful hydroboration and well defined polymer structures.

These unique BPAs showed interesting photophysical properties as recorded by UV-Vis and fluorescence spectra (Figure 5.3, data summarized in Table 5.1). The absorption maxima of BPAs in solution are centered between 440 nm and 465 nm, red-shifted comparing with those of poly(vinylenearylenevinylene borane)s prepared by Chujo and his coworkers²³², indicating successful incorporation of boron in the polymer backbones and enhanced conjugation of BPAs. The λ_{max} of the polymers experienced a bathochromic shift from 442 nm for **BPA-CH** to 452 nm for **BPA-Ph** and to 464 nm for **BPA-PT** as the side-groups of the polymers changed from alkyl to phenyl and to phenylthiophene. This observation is attributed to the enhanced electronic delocalization of side-groups to the backbone of polymers which is consistent with the previous findings in the EDY derived polymers.⁹²⁻⁹⁴ The solutions of the polymers are strongly luminescent, green for **BPA-CH**, yellow for **BPA-Ph** and orange for **BPA-PT**. Besides a strong emission

peak at 503 nm, a weak peak at 538 nm were observed for **BPA-CH** in solution, while **BPA-Ph** and **BPA-PT** only displayed one strong peak at 528 nm and 567 nm, respectively. Quantum yields of the polymers in THF solution were determined against coumarin 153²⁵⁰ to be 24.6 % for **BPA-CH**, 5.9 % for **BPA-Ph** and 4.5% for **BPA-PT**, these values are much higher comparing with those of PDAs and PTAs⁹²⁻⁹⁴ derived from the same set of EDYs, indicating strong effect of boron atoms on the electronic property of the polymers.

The thin film absorption spectra of **BPA-CH** and **BPA-Ph** became broad and the λ_{max} blue-shifted to 398 nm and 452 nm, respectively. The blue shift is likely due to the distortion of the main chain and lack of chain packing that caused by the bulky triply groups on the boron unit. Interestingly, opposite trend was observed for the absorption of **BPA-PT** which showed two vibronic bands (461 nm, 492 nm) with similar intensity, indicating certain degree of chain packing in the solid state. The shoulder emission peak at 538 nm for **BPA-CH** thin film became more pronounced comparing with that in solution, while the emission of **BPA-Ph** and **BPA-PT** only showed negligible shifts comparing with those in solution. LUMO and HOMO levels of BPAs were estimated by CV (cyclic voltammetry) to gain insight about the effect of side-groups on the CPs (Figure 5.4, data summarized in Table 5.1). Nonreversible two stepwise reduction waves were evident for **BPA-CH** (onsets at -1.72 V and -2.15 V vs. Fc/Fc⁺ couple) and **BPA-Ph** (onsets at -1.67 V and -2.24 V vs. Fc/Fc⁺ couple), indicative of the sequential reception of two electrons by boron atoms. In contrast, one reduction wave was observed for **BPA-**

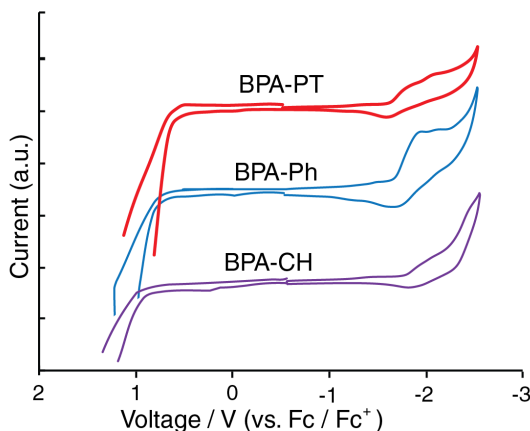


Figure 5.4. Cyclic Voltammograms of **BPA-CH**, **BPA -Ph** and **BPA -PT** (10 mM in CH_2Cl_2) externally referenced to ferrocene redox couple (0.1 M Bu_4NPF_6 as supporting electrolytes, 100 mV/s scan rate).

PT (onsets at -1.61 V vs. Fc/Fc^+ couple), suggesting its less Lewis acidity of boron atoms results from enhanced electron delocalization in **BPA-PT**. The HOMO levels of the polymers increased by 0.33 eV from -5.83 eV to -5.63 eV and to -5.50 eV as the electron richness of the side-groups increase from **BPA-CH** to **BPA-PT** while only 0.11 eV decrease was associated in LUMO levels. This indicates the HOMO levels are mainly determined by the electron rich triene moieties while LUMO levels by the electron deficient boron unit, which is a typical feature often seen in donor-acceptor CPs.^{4,251,252}

Conjugated organoboron polymers generally display excellent anion recognition ability towards toxic anions such as F^- and CN^- . In order to explore the potential application of BPAs as a F^- sensor, F^- titration experiment was performed in THF. During the initial addition of the F^- from 0.02 eq. to 0.30 eq. to the solution of **BPA-CH**, the λ_{max} at 443 nm lost intensity and blue shifted to 400 nm, with further addition

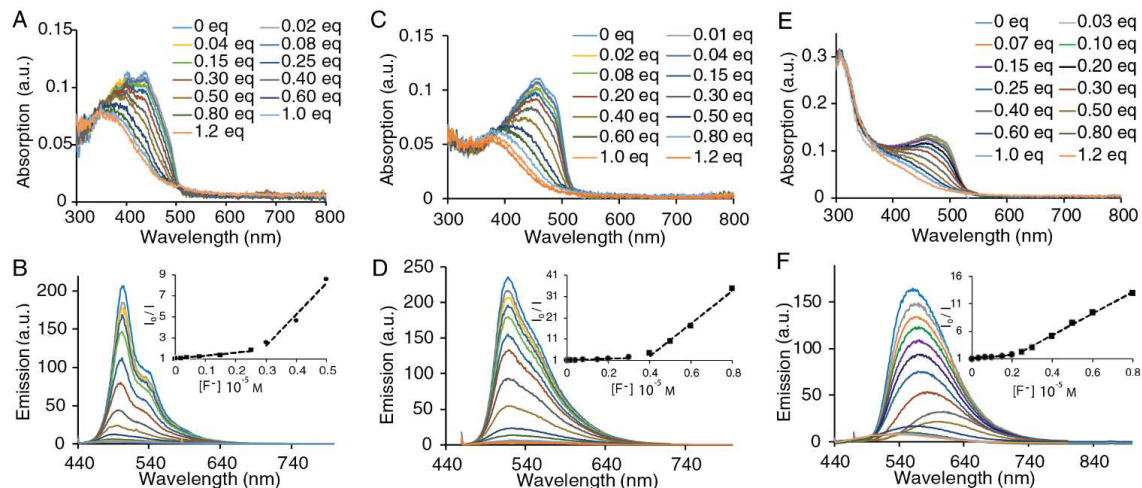


Figure 5.5. Absorption spectra of **BPA-CH** (A), **BPA-Ph** (E) and **BPA-PT** (E) in response to F^- titration. Emission spectra of **BPA-CH** (B), **BPA-Ph** (E) and **BPA-PT** (F) in response to F^- titration. Insets are the Stern-Volmer plots.

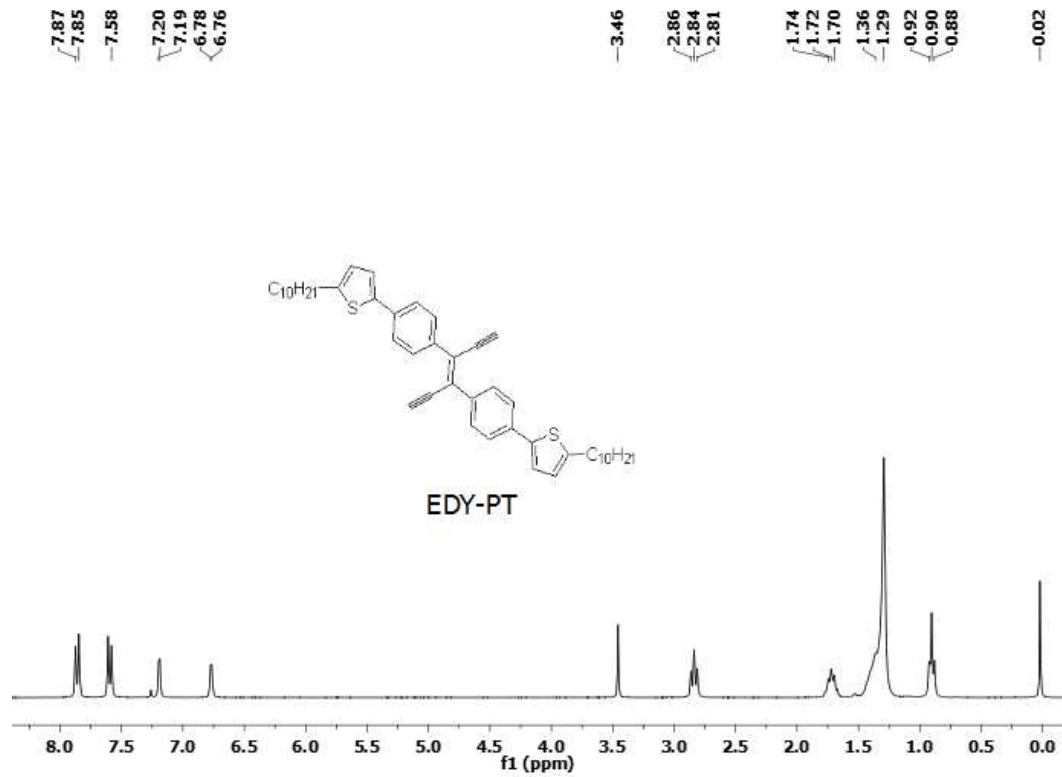
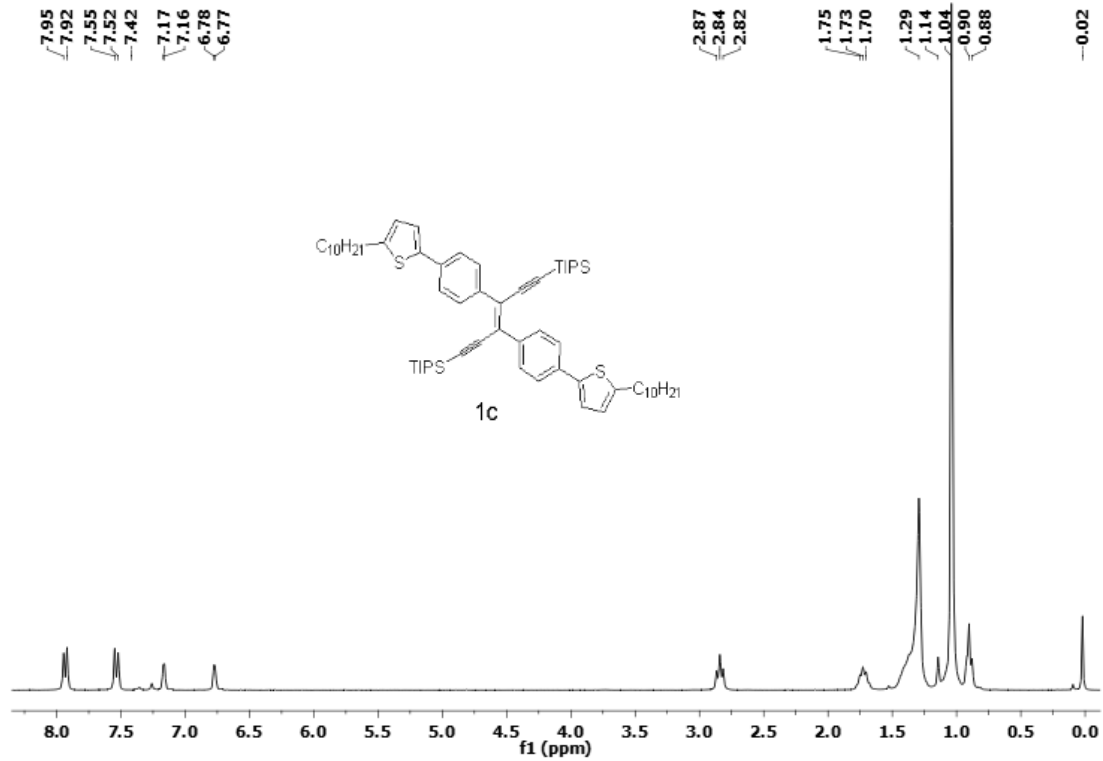
of F^- to 0.8 eq. the λ_{\max} gradually blue-shifted from 400 nm to 346 nm and remained unchanged with addition of another 0.4 eq. of F^- (Figure 5.5 A). At the same time, the intensity of λ_{em} (excited at 442 nm) at 503 nm decreased with slight blue-shift to 492 nm as the F^- increased to 0.5 eq., and then the fluorescence of was almost quenched completely at 0.6 eq. of F^- (Figure 5.5 B). These observations could be explained by interruption of conjugation in **BPA-CH** when F^- binds to boron atoms and gradually convert tricoordinate boron atoms to tetracoordinate boron. The λ_{\max} of **BPA-Ph** blue-shifted from 452 nm to 376 nm as 0.8 eq. of F^- was added, and then the peak remained at 376 nm with further addition of F^- (Figure 5.5 C). The emission (excited at 452 nm) of **BPA-Ph** only slightly blue shifted from 528 nm to 522 nm and it was quenched completely when 0.6 eq. of F^- was added (Figure 5.5 D). In case of **BPA-PT**, as expected the λ_{\max} at 464 nm disappeared completely as

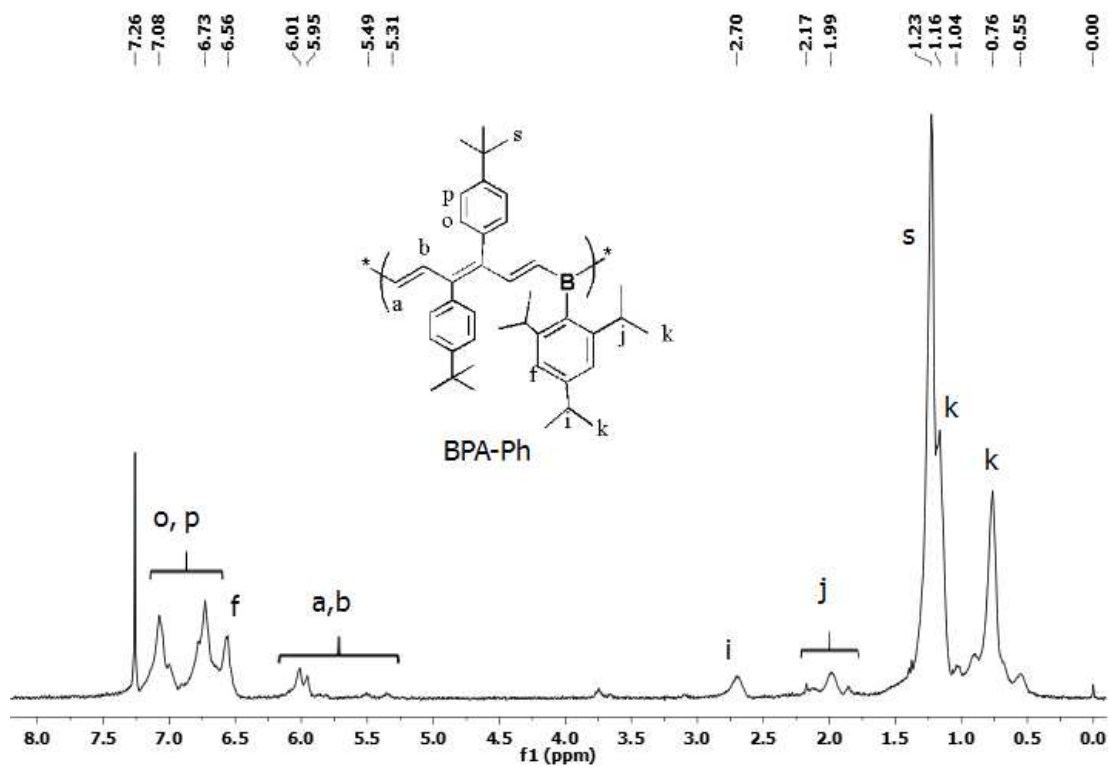
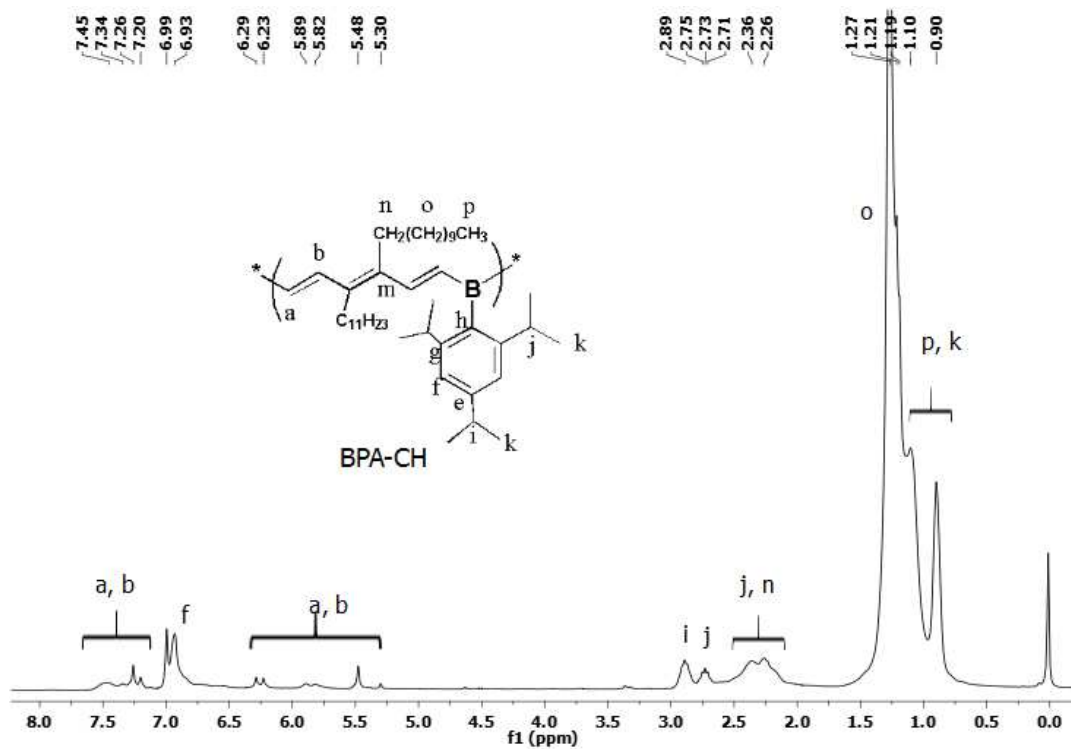
1.2 eq. of F^- was added (Figure 5.5 E). It is noteworthy that the λ_{em} (excited at 464 nm) of **BPA-PT** experienced a bathochromic shift from 567 nm to 600 nm during the first addition of 0.4 eq. of F^- , and later the λ_{em} blue shifted to 531 nm as F^- increased from 0.5 eq. to 1.2 eq. (Figure 5.5 F). Such red shift could be ascribed to the enhances the charge transfer from the electron rich tetracoordinate boron units to electron deficient tricoordinate boron centers.^{244,253,254} The fluorescence quenching constants of F^- towards BPAs were determined by the Stern-Volmer plots and in all cases two quenching constants were observed. For **BPA-CH**, the quenching constants was $3.0 \times 10^5 M^{-1}$ when up to 0.25 eq. of F^- was added, and followed by a 10-fold increase of the quenching constants to $30.0 \times 10^5 M^{-1}$ when more F^- was treated. Similar observation was also revealed before and after the first addition of 0.3 eq. of F^- for **BPA-Ph** and **BPA-PT**. In the case of **BPA-Ph**, its quenching constant experienced a 17-fold increase from $4.53 \times 10^5 M^{-1}$ to $76.3 \times 10^5 M^{-1}$, and in the case of **BPA-PT** the quenching constant showed a 5.4 folds increase from $3.7 \times 10^5 M^{-1}$ to $19.9 \times 10^5 M^{-1}$. These results indicate two different stages might be involved in the fluorescence quenching process. In the first stage, effective conjugation length, the conjugation needed to resemble the optical properties of a given polymer, is maintained in the BPAs as the F^- tends to bind first with tricoordinate borons of high Lewis acidity, those are not in conjugation with neighboring chromophores or on the ends of a conjugated block, leading to unshifted emission profile with reduced peak intensity. In the second stage, the conjugation length was further reduced to a degree that it is shorter than the effective conjugation length with addition of F^- , and it lead to blue-shifted emission

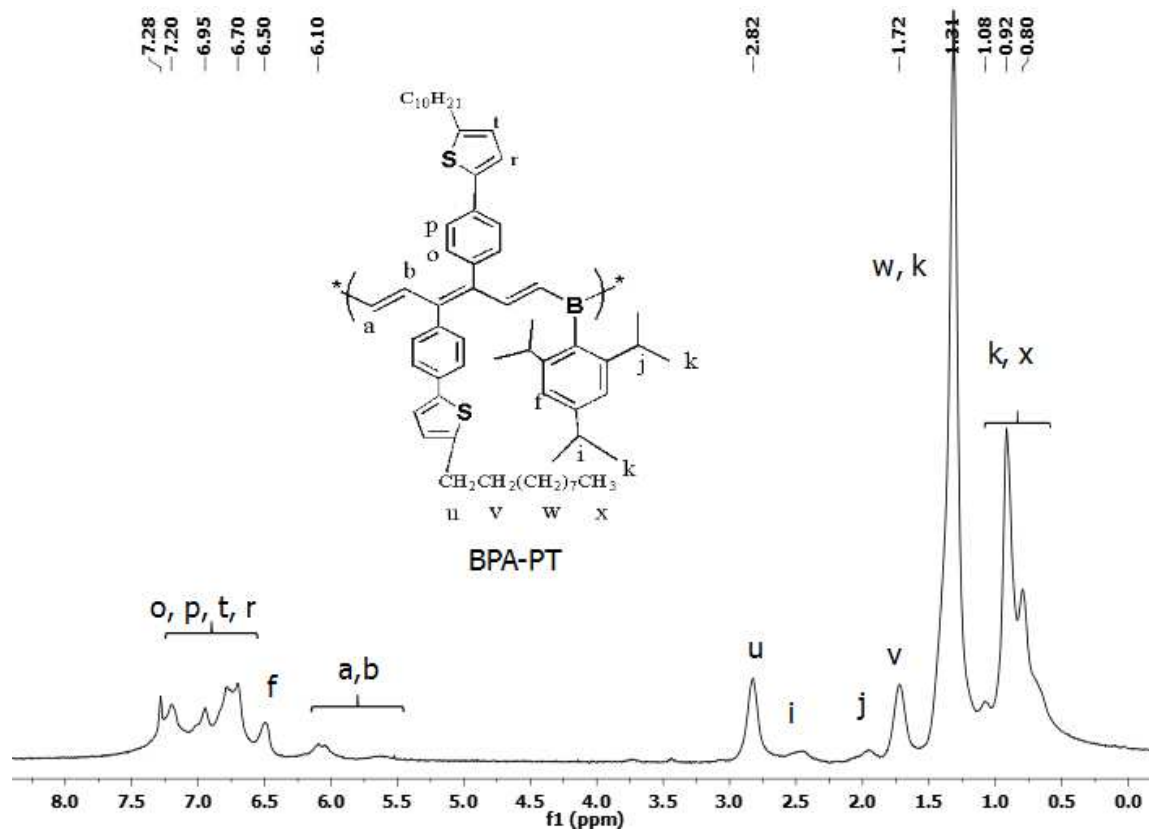
spectra with dramatic reduced intensity as the nonradiative decay was enhanced significantly when the conjugation was short. Based on this proposed mechanism and changing points of fluorescence quenching constants, we could roughly estimate the effective conjugation length of the polymers to be 4, 3, and 5 for **BPA-CH**, **BPA-Ph** and **BPA-PT**, respectively.

5.4 Conclusion

A series of BPAs bearing only double bonds as π conjugation were synthesized for the first time and they have shown enhanced conjugation and red shifted absorption due to its enhanced electron delocalization along the main chain. Their optical and electrochemical properties such as HOMO levels and bandgaps can be systematically tuned by varying the side chains of the polymers. These polymers have displayed high fluorescence quenching constants up to $76.3 \times 10^5 \text{ M}^{-1}$ when F^- was used as a quencher, which makes them good candidates for F^- sensors.







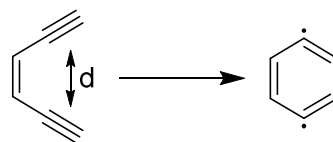
6 Chapter 6

Projects in Progress

6.1 Controlled Bergman Cyclization from Trans Eneidyne

6.1.1 Introduction

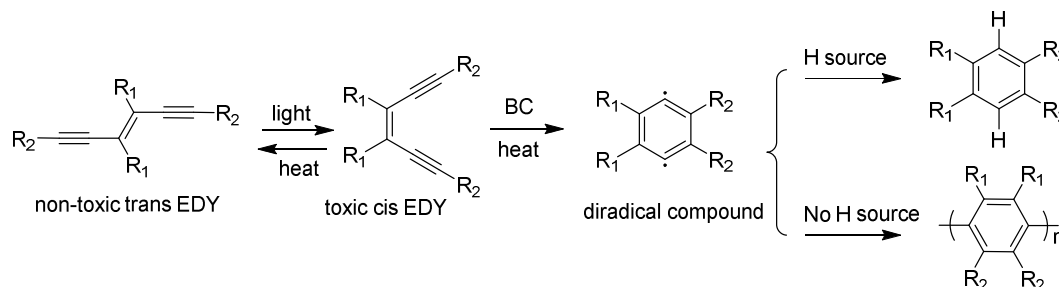
Cis EDYs have been extensively studied as an antitumor agent which can undergo Bergman cyclization (BC) with formation of DNA cleavage species, 1,4-aromatic diradical.^{80,255-259} Many approaches have been applied to trigger BC of these intriguing cis EDYs, including metal-ion-induced BC²⁶⁰⁻²⁶² and organometallic reagents mediated BC²⁶³⁻²⁶⁶. Both theoretical calculation and experimental data have pointed out that the distance between the two triple bonds in the cis EDYs is one of the major factors control the reactivity of BC (Scheme 6.1).^{267,268} Besides the distance theory, molecular strain between the ground state and the transition state as well as electronic effect of substituents are the other two important factors that govern the BC reactivity²⁵⁹. It has been shown that BC could indeed occur at mild conditions when the distance of the triple bonds were closer with aid of metal and ligand interaction.^{88,89} In order to apply there EDYs as the antitumor reagents, one should consider the potential toxicity of the cis EDY since the diradical produced through BC could also kill the normal cells. Ideally, nontoxic precursors should be used and delivered to the desired spots for curing first, and then trigger the BC of the precursors and turn them to toxic reagents by certain stimuli. Guided by this



cyclization, $d < 3.4 \text{ \AA}$

no cyclization, $d > 3.4 \text{ \AA}$

Scheme 6.1. Bergman cyclization controlled by the distance.



Scheme 6.2. Transformation between nontoxic and toxic EDYs

principle, we proposed a simple approach where we could control the transformation of non-toxic trans EDYs to toxic cis EDYs via isomerization by light, a well-studied behavior in EDYs and their derivatives^{269–272} (Scheme 6.2). With hydrogen sources such as cyclohexadiene (CHD) small molecules will be obtained as the BC product, while polymeric materials will form without presence of hydrogen sources (Scheme 6.2).²⁵⁹

6.1.2 Experimental

Materials and General Methods: All reagents and solvents were used as received from Sigma-Aldrich or VWR unless otherwise noted. Triisopropyl((trimethylsilyl)ethynyl)silane¹⁴⁵ was synthesized as described previously. THF was distilled from Na/benzophenone prior to use. Anhydrous

dichloromethane was obtained by distillation over CaH_2 and degassed through several freeze-pump-thaw cycles. The 300.13 MHz ^1H and 75.48 MHz ^{13}C NMR spectra were recorded on a Bruker Avance III Solution 300 spectrometer. All solution ^1H and ^{13}C NMR spectra were referenced internally to the solvent peaks. Ultraviolet-Visible (UV-Vis) absorption spectra were recorded on a Shimadzu UV-2401 PC spectrometer over a wavelength range of 250-800 nm. Fluorescence emission spectra were obtained using a Varian Cary Eclipse Fluorometer.

EDY-Sn: To a solution of 1.0 mg (1.8 mmol) (E)-(3,4-di(thiophen-2-yl)hexa-3-en-1,5-diyne-1,6-diyl)bis(triisopropylsilane) and 0.6 mL (4.3 mmol) dry TMEDA in 30 mL dry hexane was added dropwise 2.9 mL BuLi (7.25 mmol) at 0 °C under N_2 . The mixture was then refluxed for 2 hours, followed by addition of 7.5 mL (7.5 mmol) Me_3SnCl at 0 °C. The reaction was stirred at r.t. overnight, and then quenched with water and extracted with ether twice. The organic layers were combined, washed with saturated NaHCO_3 solution and brine, and dried over anhydrous Na_2SO_4 . Compound EDY-Sn was purified by recrystallization in hexane and ethanol as a yellow solid (1.21 g, 76.1%).

^1H NMR (300.13 MHz, CDCl_3): δ (ppm) = 0.36 (s, 18H), 1.16–1.26 (m, 42H), 7.11 (d, 2H, $J_{\text{HH}}^3 = 3.3$ Hz), 8.01 (d, 2H, $J_{\text{HH}}^3 = 3.3$ Hz)

BTD-Br: A mixture of 530.75 mg (0.18 mmol) 4,7-dibromobenzo[c][1,2,5]thiadiazole, 800 mg (0.18 mmol) tributyl(5-(tridecan-5-yl)thiophen-2-yl)stannane and 80 mg (0.069 mmol) $\text{Pd}(\text{PPh}_3)_4$ in 8 mL dry DMF

was heated at 110 °C overnight. To the reaction mixture was add water and it was extracted with chloroform twice. The organic layers were combined, washed with saturated NaHCO₃ solution and brine, and dried over anhydrous Na₂SO₄. Compound **BTD-Br** was purified by column chromatography (hexanes as eluent) to afford 520 mg (56.2%) product as a red liquid.

¹HNMR (300.13 MHz, CDCl₃): δ (ppm) = 0.88-0.90 (m, 6H), 1.28–1.32 (m, 20H), 1.70 (m, 2H), 2.81 (d, 4H, J³_{HH} = 6.9 Hz), 6.85 (d, 2H, J³_{HH} = 3.6 Hz), 7.64 (d, 2H, J³_{HF} = 7.8 Hz), 7.82 (d, 2H, J³_{HH} = 7.8Hz), 7.95 (d, 2H, J³_{HH} = 3.9 Hz). ¹³C NMR (75.48 MHz, CDCl₃), δ (ppm) =14.1, 22.7, 23.0, 26.6, 28.9, 29.7, 31.9, 33.0, 33.2, 34.7, 40.0, 111.4, 125.0, 126.4, 127.4, 128.1, 132.2, 136.0, 147.1, 151.8, 153.9.

EDY-BTD

A mixture of 134 mg (0.15 mmol) **EDY-Sn**, 162 mg (0.33 mmol) **BTD-Br** and 11 mg (0.01 mmol) Pd(PPh₃)₄ in 5 mL dry DMF was heated at 110 °C overnight. To the reaction mixture was add water and it was extracted with chloroform twice. The organic layers were combined, washed with saturated NaHCO₃ solution and brine, and dried over anhydrous Na₂SO₄. After removal of solvent, crude product was washed by acetone, and filtrated to afford 165 mg (78.5%) product as a dark solid.

¹HNMR (300.13 MHz, CDCl₃): δ (ppm) = 0.87-0.91 (m, 12H), 1.13-1.26 (m, 42H), 1.29 1.55(m, 40H), 1.72 (m, 2H), 2.83 (d, 4H, J³_{HH} = 6.6 Hz), 6.87 (d, 2H, J³_{HF} = 3.3 Hz), 7.79 (d, 2H, J³_{HH} = 7.8Hz), 7.85 (d, 2H, J³_{HH} = 7.5 Hz), 8.00 (d, 2H, J³_{HH} = 3.6 Hz), 8.11 (d, 2H, J³_{HH} = 4.2 Hz), 8.60(d, 2H, J³_{HH} = 4.2 Hz).

EDY-BTD T1

The procedures were protected by aluminum foil to avoid light induced isomerization of the product. To a solution of 35 mg (0.025 mmol) **EDY-BTD** in THF at 0 °C was added TBAF solution (26.5 mg, 0.1 mmol, in 3 mL THF) dropwise. After stirring the reaction at r.t. overnight, water was added to the reaction mixture and it was extracted with chloroform twice. The organic layers were combined, washed with saturated NaHCO₃ solution and brine, and dried over anhydrous Na₂SO₄. After removal of solvent, the solid was washed by methanol, and filtrated to afford **EDY-BTD T1** as a black solid (20.0 mg, 74.1%).

¹HNMR (300.13 MHz, CDCl₃): δ (ppm) = 0.87-0.91 (m, 12H), 1.13-1.26 (m, 42H), 1.29 1.55(m, 40H), 1.72 (m, 2H), 2.83 (d, 4H, J³_{HH} = 6.6 Hz), 6.87 (d, 2H, J³_{HF} = 3.3 Hz), 7.79 (d, 2H, J³_{HH} = 7.8Hz), 7.85 (d, 2H, J³_{HH} = 7.5 Hz), 8.00 (d, 2H, J³_{HH} = 3.6 Hz), 8.11 (d, 2H, J³_{HH} = 4.2 Hz), 8.60(d, 2H, J³_{HH} = 4.2 Hz).

EDY-Ph-OH

A mixture of 100 mg **EDY-Ph**, 142.3 mg of 2-iodo phenol, 17.0 mg of Pd(PPh₃)₄, 5.6 mg CuI and 0.15 mL NH₃H₂O was stirred at room temperature overnight under argon atmosphere. The solvent of the reaction was removed and the residue was subjected to column chromatography (ethyl acetate / hexanes = 4/1). 40 mg of **EDY-Ph-OH** (33.2 %) as a yellow solid was obtained.

¹HNMR (300.13 MHz, DMSO-d₆): δ (ppm) = 1.34 (s, 18H), 6.76 ((t, 2H, J³_{HH} = 8.4 Hz), 6.88 (dd, 2H, J³_{HH1} = 8.1 Hz, J³_{HH2} = 8.1 Hz), 7.09 (dd, 2H, J³_{HH1} = 7.2 Hz, J³_{HH2} = 7.2 Hz), 7.19 (t, 2H, J³_{HH} = 7.5 Hz), 7.48(d, 4H, J³_{HH} = 8.4 Hz), 8.01 (d, 4H, J³_{HH} = 8.1 Hz), 10.10 (s, 2H)

cis **EDY-OH**

A mixture of 52 mg (0.27 mmol) (Z)-5,6-diethynyldec-5-ene, 130 mg (0.59 mmol) of 3-iodophenol, 15.0 mg (0.013 mmol) of Pd(PPh₃)₄, 8 mg (0.042 mmol) CuI and 0.20 mL (3.0 mmol) NH₃H₂O in 15 mL dry THF was stirred at room temperature overnight. The solvent of the reaction was removed and the residue was subjected to column chromatography (hexanes/ethyl acetate = 5/2). 80 mg of cis **EDY-OH** (77.8 %) as a brown liquid was obtained.

¹HNMR (300.13 MHz, CDCl₃): δ (ppm) = 0.95 (t, 6H, J³_{HH} = 7.2 Hz), 1.40 (m, 4H), 1.58 (m, 4H), 2.33 (t, 4H, J³_{HH} = 7.8 Hz), 4.92 (s, 2H), 6.79 (d, 2H, J³_{HH} = 6.3 Hz), 7.00 (s, 2H), 7.06 (d, 2H, J³_{HH} = 7.8 Hz), 7.21 (t, 2H, J³_{HH} = 8.1 Hz).

cis **EDY-crown ether**

To solution of 100.0 mg (0.27 mmol) of cis **EDY-OH** in 10 mL dry THF was added 26 mg (1.08 mmol) of NaH suspended in 15 mL THF at 0 °C. After 15 min stirring of the mixture at 0 °C, 100.5 mg (0.29 mmol) of ethylene glycol derivative (S1) in 10 mL dry THF was charged into the reaction flask. Then the reaction was warmed up to room temperature and refluxed for 3 days. After removal of the solvent under vacuum, the residue was subjected to column chromatography (hexanes/ethyl acetate = 10/3). 50 mg (35.1 %) viscous brown liquid was obtained as product which solidifies after sitting.

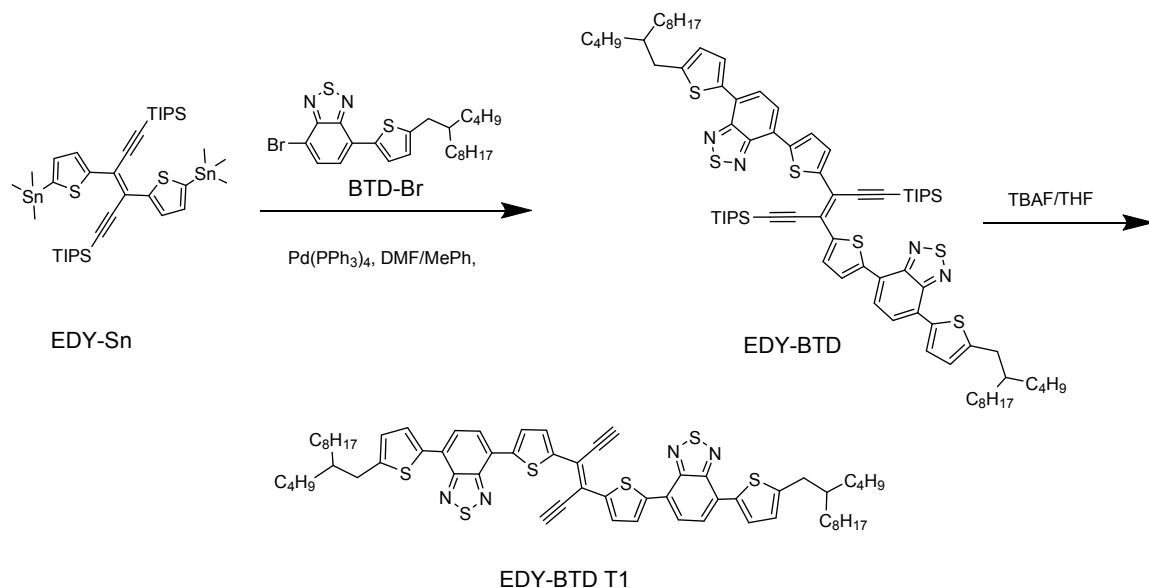
¹HNMR (300.13 MHz, CDCl₃): δ (ppm) = 0.96 (t, 6H, J³_{HH} = 7.2 Hz), 1.38-1.45 (m, 4H), 1.59-1.64 (m, 4H), 2.34 (m, 4H, J³_{HH} = 7.8 Hz), 3.70 (s, 8H), 3.81-3.85 (m,

4H), 3.92-3.95 (m, 4H), 6.89-6.91 (m, 2H), 6.98 (s, 2H), 7.06 (d, 2H, $J_{\text{HH}}^3 = 7.5$ Hz), 7.19 (t, 2H, $J_{\text{HH}}^3 = 7.8$ Hz).

6.1.3 Results and Discussion

Part 1

Long wavelength light, having low energy and little damage to our body, is capable to reach deep tissues and thus make it an attractive trigger for isomerization of EDYs. We designed a trans EDY, **EDY-BTD T1**, bearing extended conjugation on the double bonds, which is expected to undergo isomerization with explosion to visible light (Scheme 6.3). Synthesis of the targeted molecule **EDY-BTD T1** is detailed in the experimental section.



Scheme 6.3. Synthesis of **EDY-BTD T1**

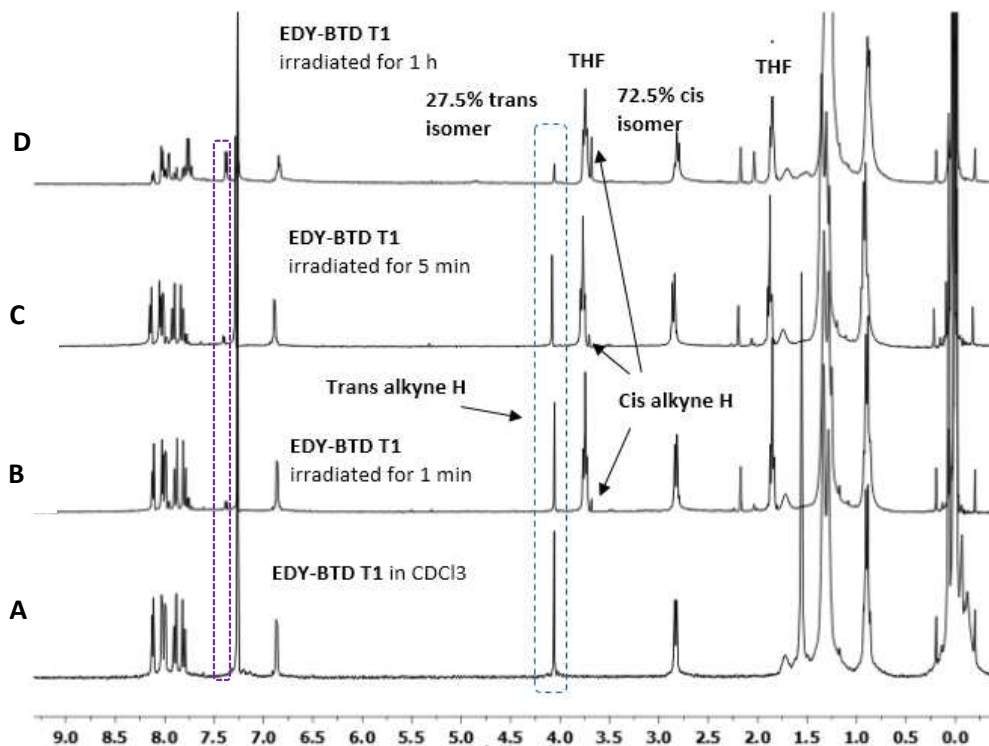


Figure 6.1. ^1H NMR spectra of **EDY-BTD T1** with increased irradiation duration, (A) trans **EDY-BTD T1**, (B) **EDY-BTD T1** irradiated for 1 min, (C) **EDY-BTD T1** irradiated for 5 min, (D) **EDY-BTD T1** irradiated for 1 hour.

The isomerization of **EDY-BTD T1** was monitored by ^1H NMR first (Figure 6.1) with irradiation of 20 W white light. All the solutions mentioned are made from anhydrous and degassed solvents in the glovebox filled with argon unless otherwise specified. As shown in the figure 6.1 as the irradiation time increases (Figure 6.1 B and C) the terminal alkyne proton peak for **EDY-BTD T1** at 4.06 ppm decreases, and a new peak at 3.68 ppm assigned to the alkyne proton of cis form of **EDY-BTD T1** as well as a peak at 7.45 ppm gradually appears and its intensity grows, indicating isomerization of **EDY-BTD T1**. After 1 hour of irradiation the isomerization reached to an equilibrium with 72.5% of cis isomer and 27.5% of

EDY-BTD T1 based on the integrations of two different protons of terminal alkynes (Figure 6.1 D).

Then the BC reaction was attempted by heating the isomers with 72.5% of *cis* **EDY-BTD T1** in presence of 100 eq. cyclohexadiene (CHD) in degassed toluene at 100 °C for 20 hours with irradiation of 20 W white light. Heat and light drive the

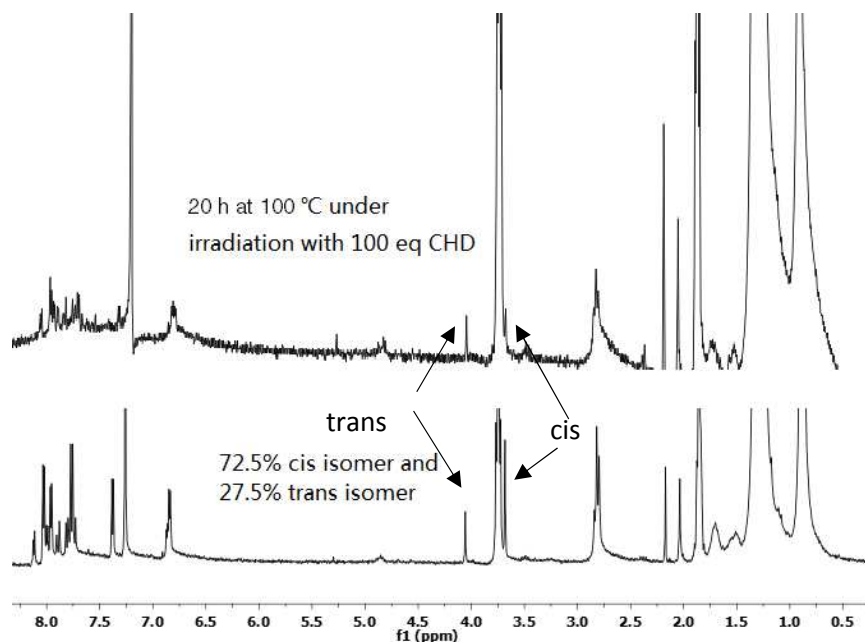


Figure 6.2. ¹H NMR spectra of isomers of **EDY-BTD T1** before (bottom spectrum) and after heating (top spectrum)

isomerization reaction in opposite directions, and thus keeping the irradiation on helps the system to maintain certain concentration of *cis* **EDY-BTD T1** in the mixture for possible BC. The resulting mixture was then pumped under vacuum to remove toluene after heating for 20 hours and its ¹H NMR was obtained and compared with that of isomers with 72.5% of *cis* **EDY-BTD T1** before heating (Figure 6.2). The intensity of the ¹H NMR of the isomer mixture was low due to the loss of the compound during processing. As shown in figure 6.2 a mixture of

isomers, having 1/1 ratio of trans and cis, was obtained based on the alkyne protons from trans and cis **EDY-BTD T1**, which is not consistent with the expected result of the occurrence of BC, where all the trans isomer should be isomerized to the cis isomer because consumption of the cis isomer by BC would drive the isomerization reaction towards formation of cis isomer. And therefore, based on the ^1H NMR result no BC was occurred.

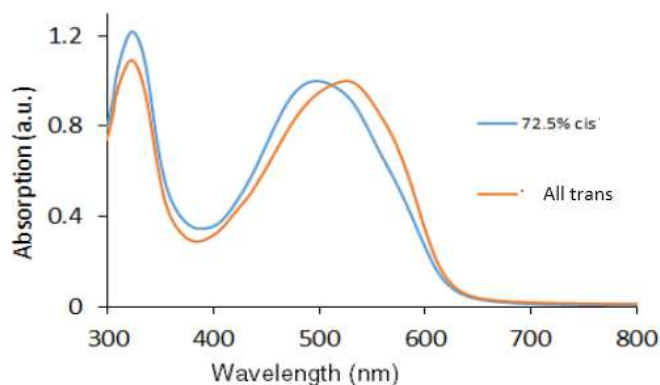


Figure 6.3. Absorption of **EDY-BTD T1** and the mixture of trans and cis isomers in chloroformm (2×10^{-5} M).

UV-vis absorption is a simple method that could allow us to monitor the BC process as formation of BC product would shift the spectra. The absorption profiles of the solution from NMR tube was recorded before and after one hour of irradiation (Figure 6.3). Compound **EDY-BTD T1** has a λ_{max} at ca. 536 nm which is attributed to the conjugation of the main chain, while the mixture of isomers with 72.5% of cis **EDY-BTD T1** shows a blue shifted λ_{max} at ca. 501 nm which could be explained by the less effective electron delocalization in cis **EDY-BTD T1**.

EDY-BTD T1 was dissolved in degassed chlorobenzene in presence of 100 eq. CHD (Figure 6.4, orange trace), and it was irradiated with 20 W white light for 1

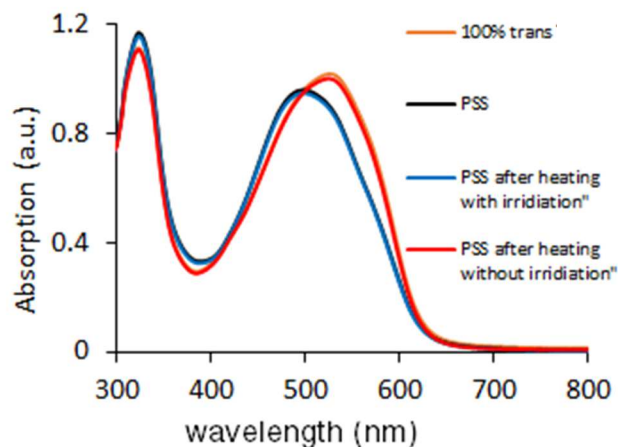


Figure 6.4. Absorption of **EDY-BTD T1** and isomer mixture after heating and irradiation.

hour to reach the photostationary state (PSS) (Figure 6.4, black trace). The λ_{\max} of the PSS solution was blue shifted from 536 nm to 501 nm that is the same value for λ_{\max} of the isomer mixture with 72.5% of cis **EDY-BTD T1**, indicating formation of cis **EDY-BTD T1**. The PSS solution was heated at 130 °C for 10 min with irradiation of white light to induce BC, and the resulting spectrum (figure 6.4, blue trace) is almost the same as that of the solution of PSS, which may suggest the absence of BC. If this speculation is correct, then heating the solution corresponding to the blue curve should convert cis isomer to **EDY-BTD T1** and result in a spectrum the same as that of **EDY-BTD T1**. After heating the solution responsible for blue curve at 130 °C for 10 min without irradiation indeed resulted in a spectrum (Figure 6.4, red curve) almost identical to that of the original solution of **EDY-BTD T1**, indicating the recovery of **EDY-BTD T1**. This result confirms that heating does not induce BC of the cis **EDY-BTD T1**.

The absence of the BC in EDY-BTD T1 might be explained by the large distance between two triple bonds. Copper (I) salts are capable of forming π complexes with triple bonds and catalyzing Glaser coupling reaction^{273,274}, making them promising candidates to bridge two triple bonds in the cis EDY and bring them to closer distance to encourage BC at lower temperature.

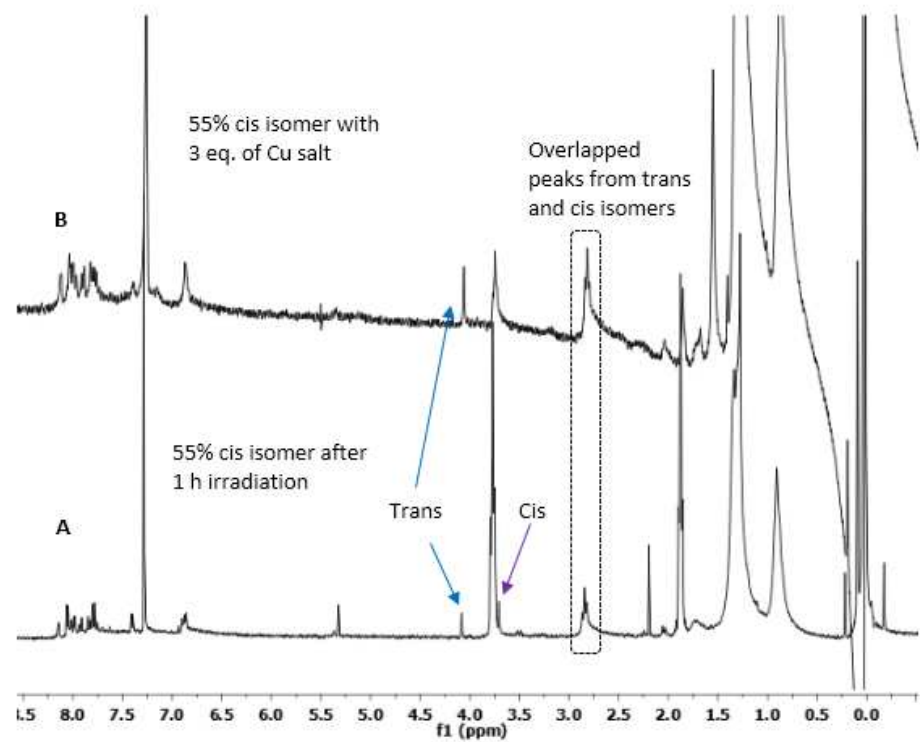


Figure 6.5. ¹H NMR spectra of **EDY-BTD T1** isomers before and after Cu salt addition (A) Isomers of **EDY-BTD T1** with 55% cis isomer, (B) Isomers treated with 3 eq. moles of Cu⁺.

The interaction between cis **EDY-BTD T1** and Cu⁺ was tested by addition of 3 eq. moles of stoichiometric solution of Tetrakis(acetonitrile)copper(I) tetrafluoroborate (dissolved in dry and degassed THF) relative to cis EDY to the THF solution of EDY isomers with 55% of cis content. The resulting solution was protected from light and stirred for 5 min in the glovebox, then THF was removed

under high vacuum and the residue was dissolved in CDCl_3 . As shown in figure 6.5B, after addition of Cu^+ to the isomer mixture, the terminal alkyne proton belongs to cis isomer disappears while the multiple peaks around 3.8 ppm that resulted from the overlapped signals of isomer mixtures remains, indicating coexistence of two isomers and interaction of Cu^+ with the triple bonds of cis isomer.

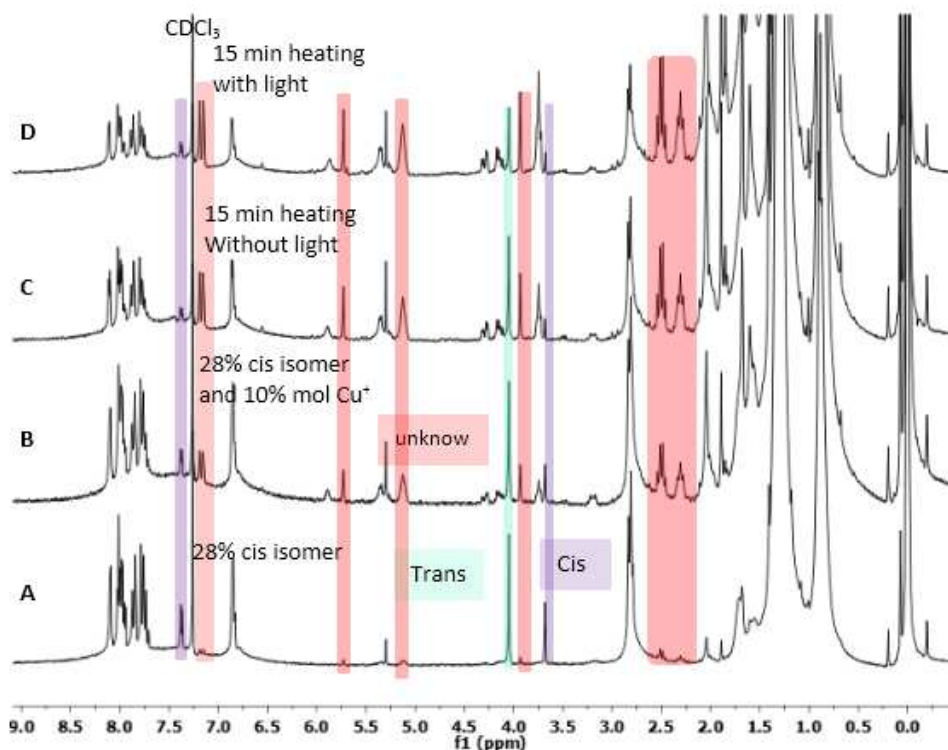


Figure 6.6. ^1H NMR spectra of **EDY-BTD T1** in presence of Cu salt with heating and / or light treatment (A) Isomers of **EDY-BTD T1** with 28% cis isomer, (B) Isomers treated with 10%. mole of Cu^+ , (C) Mixture of isomers and Cu^+ treated with heat only, (D) Mixture of isomers and Cu^+ treated with heat and light.

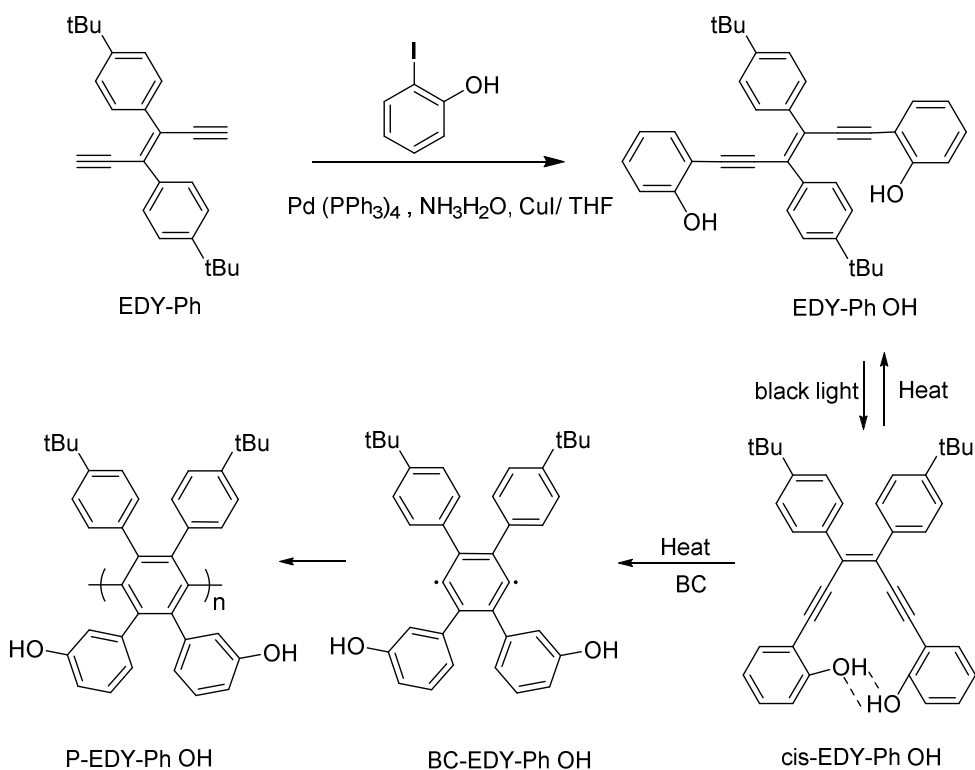
In order to have reasonable signal in ^1H NMR spectra, 10 mg of **EDY-BTD T1** was used for the BC study with presence of Cu^+ . Due to the higher concentration of the EDY in NMR tube, only 28% of cis isomer (Figure 6.6A, indicated by the purple shade) was formed after 1 h irradiation of 20 W white light. The following

steps were taken sequentially to study the BC and the respective ^1H NMR spectrum was collected after each step. (1) 10 % mol of Cu^+ was added to the THF solution of isomers with 28% cis; (2) 100 eq. of CHD was added to the mixture of isomers and Cu^+ from Step (1), which was protected from light and then heated in THF at 85 °C for 15 min under argon; (3) the mixture from Step (2) which was then heated in THF at 85 °C for 15 min in presence of 100 eq. of CHD under argon with irradiation of 20 W white light. It's interesting to see that presence of Cu^+ in the isomer mixture induce the growth of the peaks of an unknown compound at 2.3, 2.5, 3.93, 5.1, 5.7 and 7.1 ppm that are not belonging to either cis or trans EDYs (Figure 6.6B, red shades), and decrease of the peaks at 3.7 and 7.3 ppm belongs to the cis isomer (Figure 6.6B, purple shades). When the mixture of isomers and Cu^+ was treated with heat only, the peaks for the unknown compound continued to increase accompanied with decreased peaks of cis isomer (Figure 6.6C). These observations suggest that Cu^+ can speed up the conversion of cis isomer to the unknown compound and heat can promote such transition with presence of Cu^+ . When treated with both heating and irradiation at the same time, more unknown compound formed and less trans EDY was remained (Figure 6.6D), which could be explained by the conversion of trans isomer to cis isomer under light and the formation of the unknown compound derived from cis isomer. Nevertheless, expected BC product was not observed as the formation of BC product would consume the cis isomer without producing the new alkyne protons. The structure of the unknown compound associated with the new peaks in the red shades of

Figure 6.6 needs to be explored to better understand the chemistry of the EDY in presence of Cu^+ .

Part 2

The distance of the triple bonds in the cis **EDY-BTD T1** could be too far to undergo BC at the condition we tried, and therefore we tried to functionalize its triple bonds with hydrogen bonding moieties that could potentially bring triple bonds closer to



Scheme 6.4. Synthesis of tran **EDY-Ph-OH** and its BC process.

facilitate BC, however, no attempts were successful. We then functionalized **EDY-Ph** with hydrogen bonding moieties to obtain **EDY-Ph-OH** as shown in scheme 6.4 and detailed synthesis was included in the experimental section.

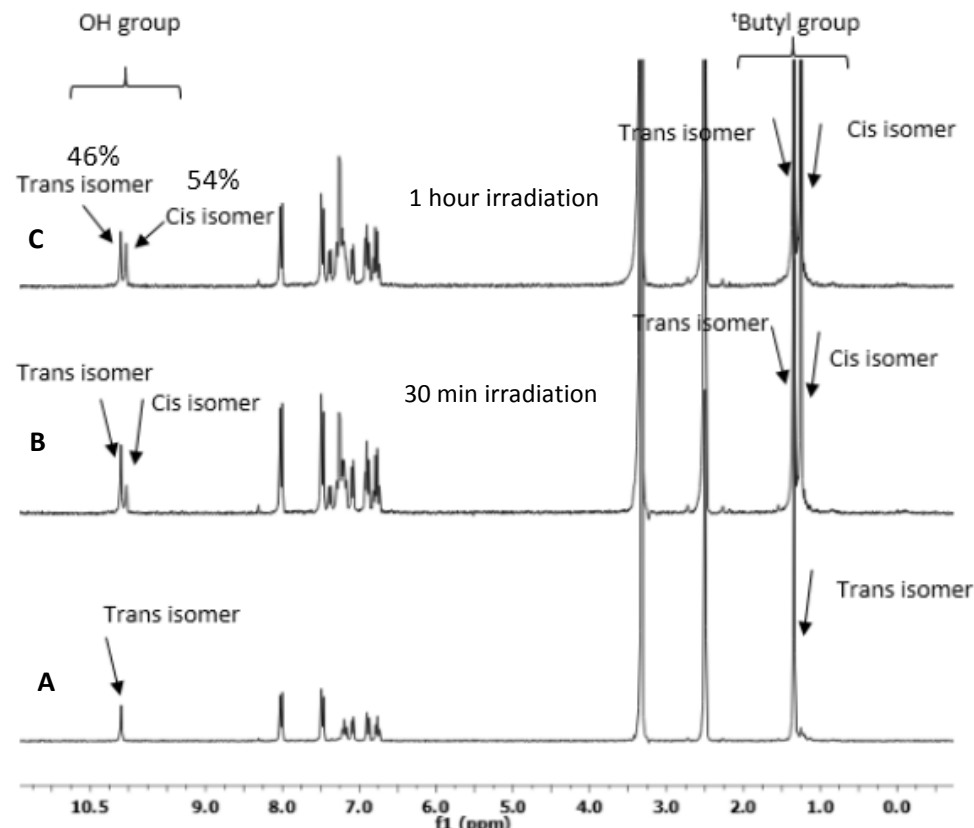


Figure 6.7. ^1H NMR for trans **EDY-Ph-OH** isomerization. (A) trans **EDY-Ph-OH**, (B) trans **EDY-Ph-OH** after 30 min irradiation, (C) trans **EDY-Ph-OH** after 1 hour irradiation.

Cis-trans isomerization of **EDY-Ph-OH** was first studied under the irradiation of a black light at room temperature by monitoring the ^1H NMR spectra of **EDY-Ph-OH** solution in degassed DMSO-d_6 under argon (Figure 6.7). As the irradiation time increased from 30 min to 1 hour (Figure 6.7 B and C), the intensity of the peak at 10.10 ppm assigned to the OH group and the peak at 1.34 for $^1\text{butyl}$ group in the **EDY-Ph-OH** gradually decreases accompanied with increase of two new peaks at 10.03 ppm and 1.25 ppm assigned to the OH group and $^1\text{butyl}$ group in the cis isomer, respectively. Also, appearance of new peaks belongs to the aromatic protons in cis isomer were observed. The isomerization reached to an equilibrium

after one hour of irradiation ending with 54 % cis and 46 % trans **EDY-Ph-OH** according to the integration ratio of the corresponding OH peaks in the ^1H NMR spectra (Figure 6.7C).

The isomer mixture obtained in the DMSO- d_6 solution with 54% cis isomer was heated at various temperature from 40 °C to 150 °C with the irradiation of black

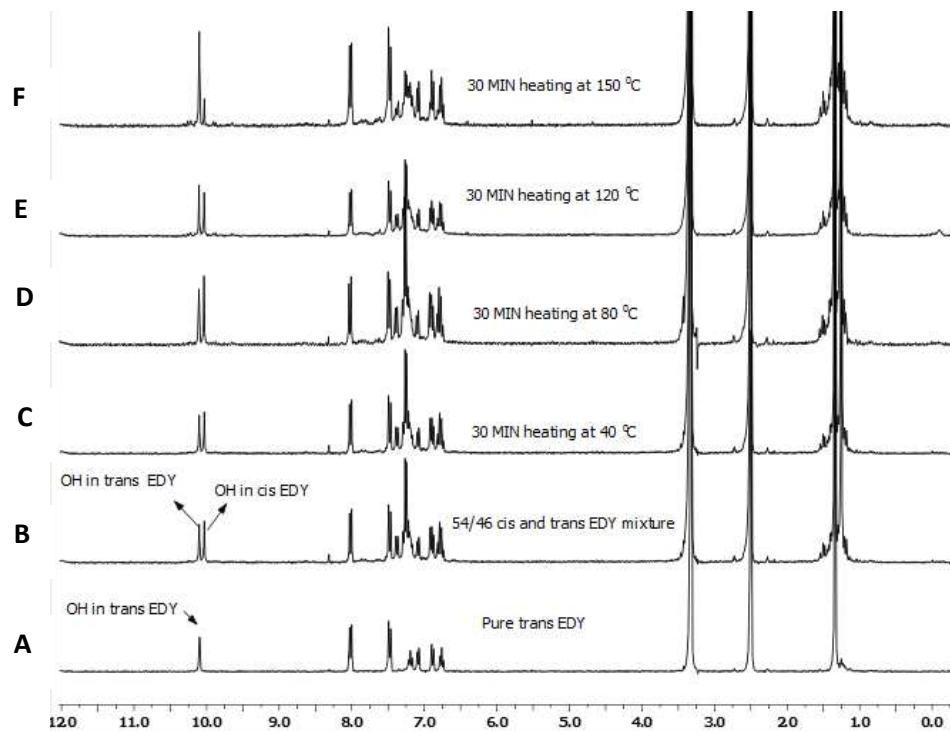


Figure 6.8. ^1H NMR of isomers of **EDY-Ph-OH1** after heating at various temperature, (A) trans **EDY-Ph-OH**, (B) trans **EDY-Ph-OH** after 1 hour irradiation, (C) isomer mixture heated at 40 °C for 30 min, (D) isomer mixture heated at 80 °C for 30 min, (E) isomer mixture heated at 120 °C for 30 min, (F) isomer mixture heated at 150 °C for 30 min.

light and the ^1H NMR spectrum was obtained after 30 min of heating at each temperature. The ratio of cis and trans isomers remained the same after heating the isomers at 40 °C and 80 °C for 30 min, indicated by the relative intensity of the OH peaks at 10.10 ppm and 10.03 ppm (Figure 6.8 C and D). After heating the

isomers at 120 °C, the OH peak and 'butyl group for cis **EDY-Ph-OH** become smaller, and those peaks for trans isomer increase (Figure 6.8E), suggesting part of cis isomer converts back to the trans isomer at higher temperature. When the isomer mixture was further treated at 150 °C for 30 min with irradiation, the content of the trans isomer in the mixture increased significantly accompanied with obvious decrease of cis isomer (Figure 6.8F). These observations indicate that at lower temperature the isomerization direction is dominated by the light, favoring formation of cis **EDY-Ph-OH**, while at higher temperature the formation of **EDY-Ph-OH** is favored. Thus, heating in fact did not trigger BC, firstly because the proton peaks of the heat-treated isomers did not become broad, indicative of absence of polymeric material, and secondly because in the event of BC all the trans isomer should be isomerized to the cis isomer as consumption of the cis isomer by BC would drive the isomerization reaction towards formation of cis isomer.

Part 3

Coordination interaction between K^+ and Na^+ crown ethers were applied to bring triple bonds closer to facilitate the BC in cis EDYs that bears one crown ether unit on each of the triple bonds, however, the effect on BC by this method was marginal²⁷⁵⁻²⁷⁷ presumably due to the fact that two crown ether units were too far away in space for the a metal cation to bind both of them at the same time. Thus, an EDY bearing one crown ether unit that bridges two triple bonds would be a good candidate for BC study as coordination of the crown ether with metal ions could

The BC was monitored by ^1H NMR after heating the cis **EDY-crown ether** in presence of NaAsF_6 and 100 eq. CHD in degassed DMSO-d_6 under argon (Figure 6.9). In the event of BC, a new proton peak from the newly formed benzene unit in the **BC P2** (Scheme 6.5) as well as change of chemical shifts for the two original benzene units would be expected. The mixture was first heated at $60\text{ }^\circ\text{C}$ for 24 hours, and the obtained ^1H NMR was almost the same as the pristine mixture, indicating no occurrence of BC (Figure 6.9B). Then the temperature was increased to $150\text{ }^\circ\text{C}$, and the mixture was further heated for 24 hours; however, the spectrum of the resulting mixture did not show any new peaks or shift of the aromatic peaks (Figure 6.9C).

Then KPF_6 with a larger K^+ cation was used to binds with the crown ether unit of the EDY, considering the size of Na^+ might be too small for the cavity of the crown ether. The cis **EDY-crown ether** in presence of KPF_6 and 100 eq. CHD in degassed DMSO-d_6 under argon was directly heated at $150\text{ }^\circ\text{C}$ for 24 hours, as shown in Figure 6.10, no new peaks or shift of the aromatic peaks belonging to the cis **EDY-crown ether** were observed, suggesting absence of the expected product **BC P2**.

The successful binding of medal cation with crown ether could be reflected by the chemical shift changes of the benzene units bridged by the crown ether ring.

²⁷⁸ Then we tested the binding interaction of Na^+ and K^+ with the cis **EDY-crown**

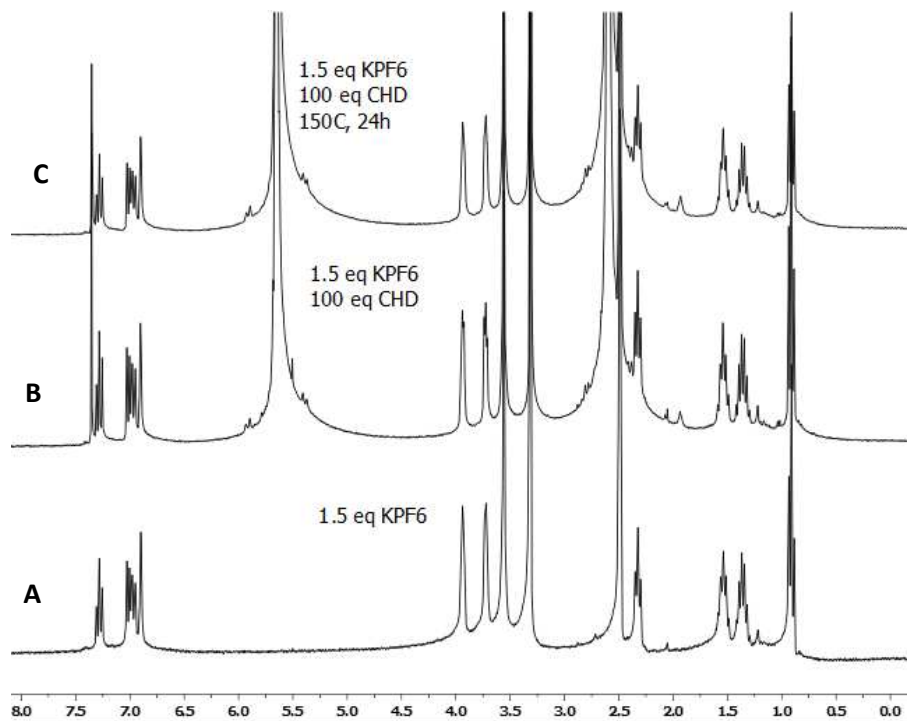


Figure 6.10. ^1H NMR spectra of **EDY-crown ether** in presence of KPF_6 with heating treatment (A) **EDY-crown ether** in DMSO-d_6 solution (B) mixture of **EDY-crown ether** and 1.5 eq. of KPF_6 (C) mixture of **EDY-crown ether**, 1.5 eq. of KPF_6 and 100 eq. of CHD heated for 24 hours at 150 °C

ether in DMSO-d_6 with various loading of the cations to confirm whether there was such interaction. NaAsF_6 was added gradually to the **EDY-crown ether** solution of DMSO-d_6 and after each addition a ^1H NMR spectrum was obtained. As shown in figure 6.11 the proton peaks belonging to the benzene units on the *cis* **EDY-crown ether** did not experience any shifts as the NaAsF_6 loading increased from 0 eq. to 1.5 eq., suggesting negligible interaction between Na^+ and crown ether. KPF_6 was then used to exam the binding interaction with *cis* **EDY-crow ether** in DMSO-d_6 , and as shown in figure 6.12 the proton peaks belonging to the benzene units on the *cis* **EDY-crown ether** did not display any shifts either when 1.5 eq. of KPF_6 was added, indicative of no presence of K^+ and crow ether binding interaction. The

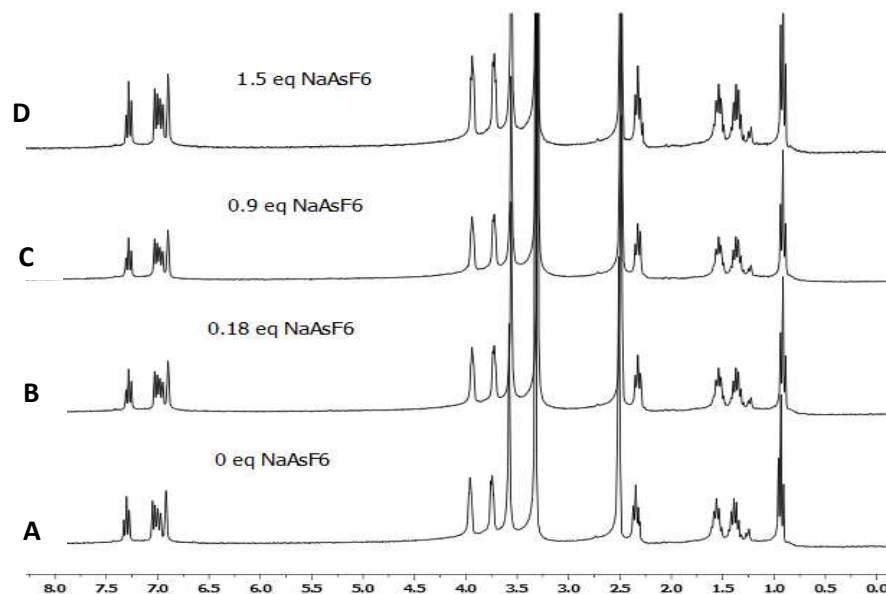


Figure 6.11. ^1H NMR spectra of **EDY-crown ether** in presence of various equivalents of NaAsF_6 (A) **EDY-crown ether** in DMSO-d_6 solution, (B) mixture of **EDY-crown ether** and 0.18 eq. of NaAsF_6 , (C) mixture of **EDY-crown ether** and 0.9 eq. of NaAsF_6 , (D) mixture of **EDY-crown ether** and 1.5 eq. of NaAsF_6 .

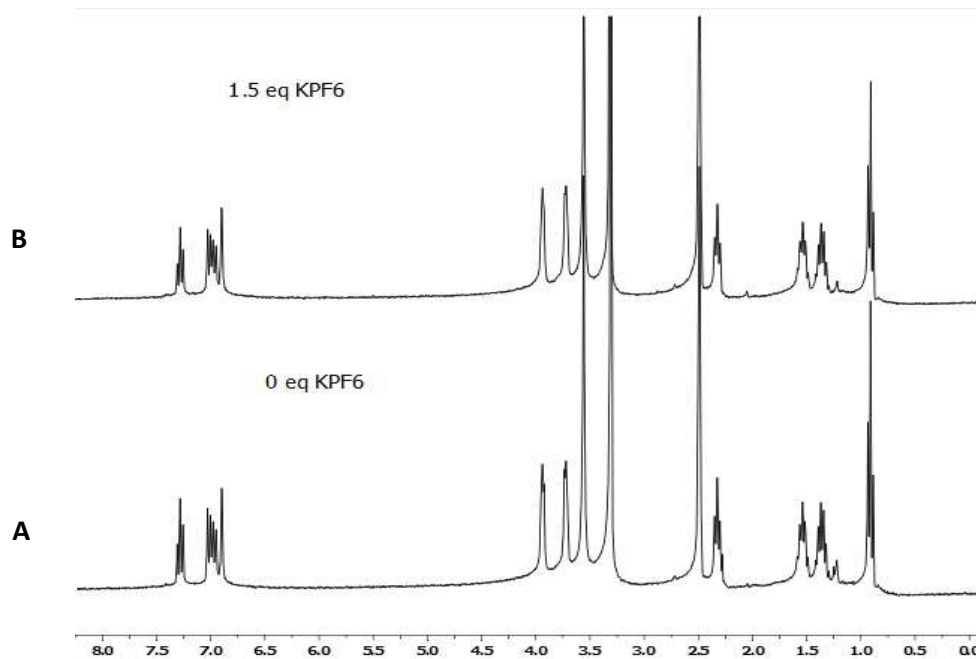


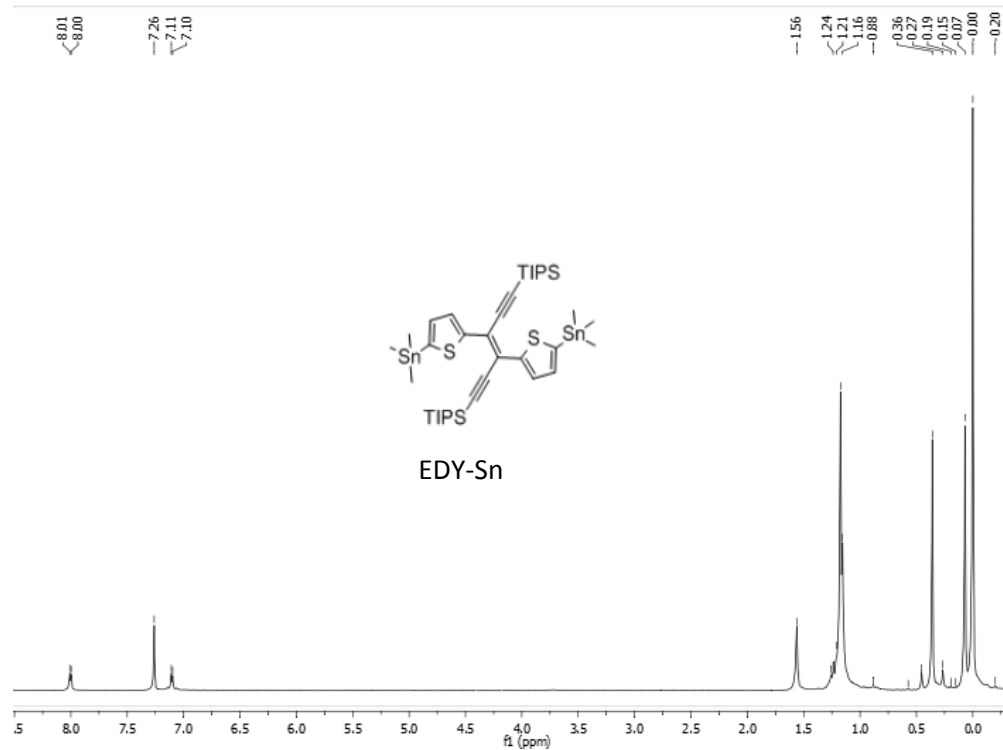
Figure 6.12. ^1H NMR spectra of **EDY-crown ether** in presence of various equivalents of KPF_6 (A) **EDY-crown ether** in DMSO-d_6 solution, (B) mixture of **EDY-crown ether** and 1.5 eq. of KPF_6 .

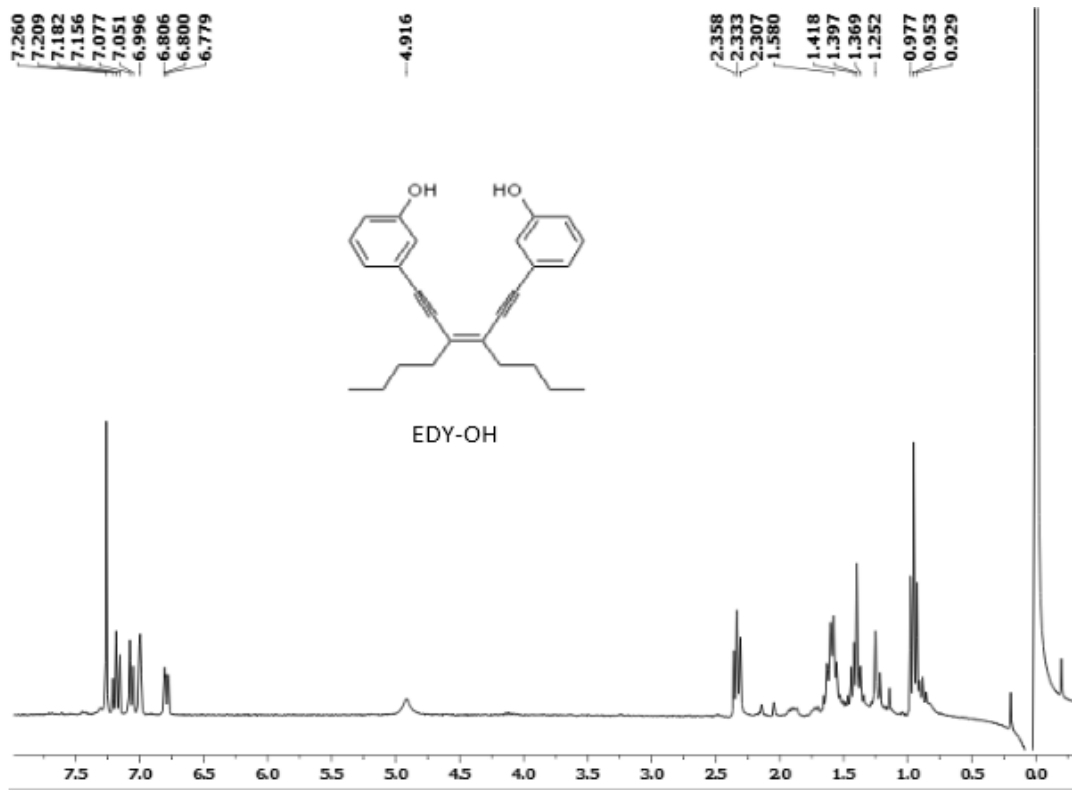
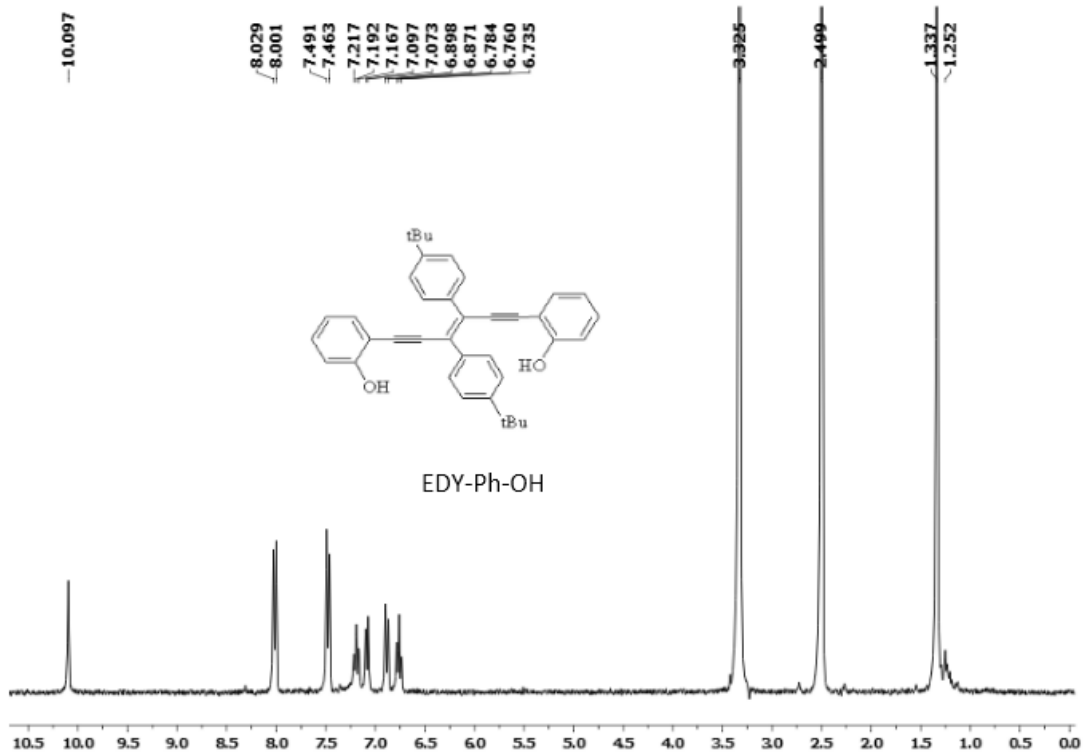
absence of the cation and crown ether binding is likely the reason that BC did not take place at elevated temperature with prolonged heating since the distance of the triple bonds is still too far.

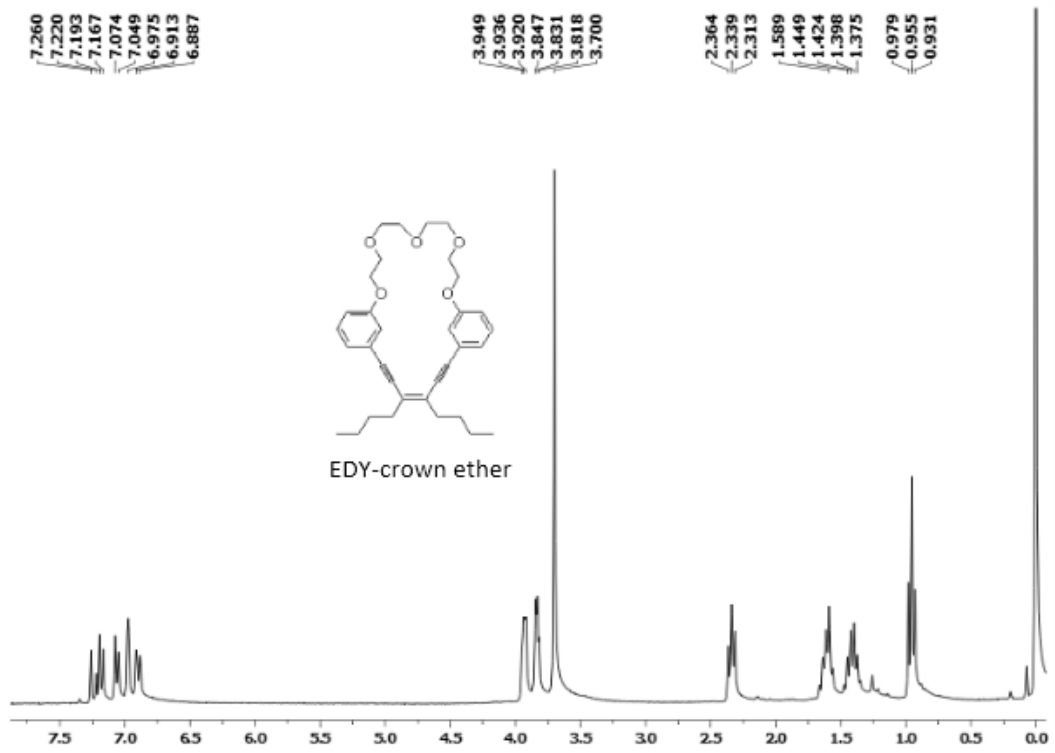
6.1.4 Conclusion

Our proposal for convenient transformation of nontoxic trans EDYs to toxic cis EDYs with light was successfully studied on **EDY-BTD T1** and **EDY-Ph-OH**, particularly, high content of cis EDYs up to 72.5% and 54% were achieved for **EDY-BTD T1** and **EDY-Ph-OH**, respectively. BC reaction, however, was not observed in the cis form of EDYs with triple bonds either bearing protons, hydrogen bonding moiety or crown ether unit.

6.1.5 NMR spectra of key compounds





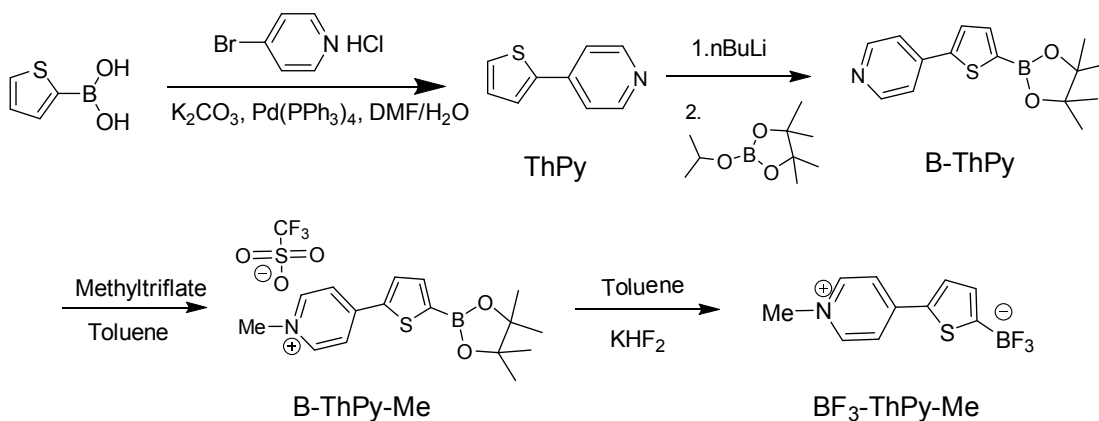


6.2 Conjugated Zwitterion

6.2.1 Introduction

A conjugated zwitterion is a neutral conjugated molecule that bears positive and negative charges and has a high dipole moment within the molecule. When they are perfectly lined up from the negative heads to the positive tails within a small distance, huge electric field would build up which could be applied to separated excitons in OPV devices for example.

A conjugated zwitterion, $\text{BF}_3\text{-ThPy-Me}$, containing a positively charged pyridinium and a negatively charged trifluoroborate was prepared as shown in scheme 6.6. The detailed synthetic procedures were included in the experimental part.



Scheme 6.6. Synthesis of the conjugated zwitterion, $\text{BF}_3\text{-ThPy-Me}$.

6.2.2 Experimental

ThPy:

The suspension of thiophen-2-ylboronic acid (5 g, 39.07 mmol) and 4-bromopyridine hydrochloride (6.9 g, 35.48 mmol) in DMF as well as K_2CO_3 (21.6 g,

156.3 mmol, 3M) aqueous solution were bubbled with nitrogen for 30 min respectively. K_2CO_3 solution was transferred to the DMF suspension slowly over 10 min, and then $Pd(PPh_3)_4$ (400 mg, 0.35 mmol) in toluene was injected to the reaction mixture with a degassed syringe. The reaction was refluxed overnight and then it was added water. The reaction mixture was extracted twice with hexanes. The organic layers were combined, washed with saturated $NaHCO_3$ solution and brine, and dried over anhydrous Na_2SO_4 . 5.7 g of crude product **ThPy** was obtained after removal of solvent. It was used without further purification for the next step. 1H NMR (300.13 MHz, $CDCl_3$): δ (ppm) = 7.13 (dd, 1H, $J^3_{HH} = 5.1$ and 3.6 Hz), 7.42 (dd, 2H, $J^3_{HH} = 5.1$ and 1.2 Hz), 7.48 (dd, 1H, $J^3_{HH} = 4.5$ and 1.8 Hz), 7.51 (dd, 2H, $J^3_{HH} = 3.6$ and 1.2 Hz), 8.59 (dd, 1H, $J^3_{HH} = 4.8$ and 1.5 Hz).

B-ThPy:

To a solution of **ThPy** (688 mg, 4.27 mmol) in 50 mL dry THF was added 1.9 mL nBuLi (2.5 M in hexanes, 4.75 mmol) dropwise at -78 °C under nitrogen atmosphere. The mixture was stirred for 15 min at -78 °C and 1.4 mL 2-isopropoxy-4,4,5,5-tetramethyl-1,3,2-dioxaborolane (6.86 mmol) was added through a syringe. The solution was warmed up to room temperature and stirred overnight. The reaction mixture was quenched with water, extracted with hexanes twice. The combined organic phase was washed with brine solution and dried over Na_2SO_4 . After removal of solvent the crude product was purified by recrystallized from acetone and THF to give **B-ThPy** (410 mg, 33.5%). 1H NMR (300.13 MHz, $CDCl_3$): δ (ppm) = 1.35 (s, 12H), 7.49 (d, 2H, $J^3_{HH} = 6.0$ Hz), 7.54 (d, 1H, $J^3_{HH} = 3.6$

Hz.), 7.61 (d, 1H $J_{\text{HH}}^3 = 3.6$ Hz), 8.59 (d, 2H, $J_{\text{HH}}^3 = 6.0$ Hz). ^{13}C NMR (75.48 MHz, CDCl_3), δ (ppm) = 24.7, 84.4, 120.1, 126.4, 138.1, 141.1, 147.5, 150.4. ^{11}B NMR (96.30 MHz, CDCl_3), δ (ppm) = 28.9.

B-ThPy-Me:

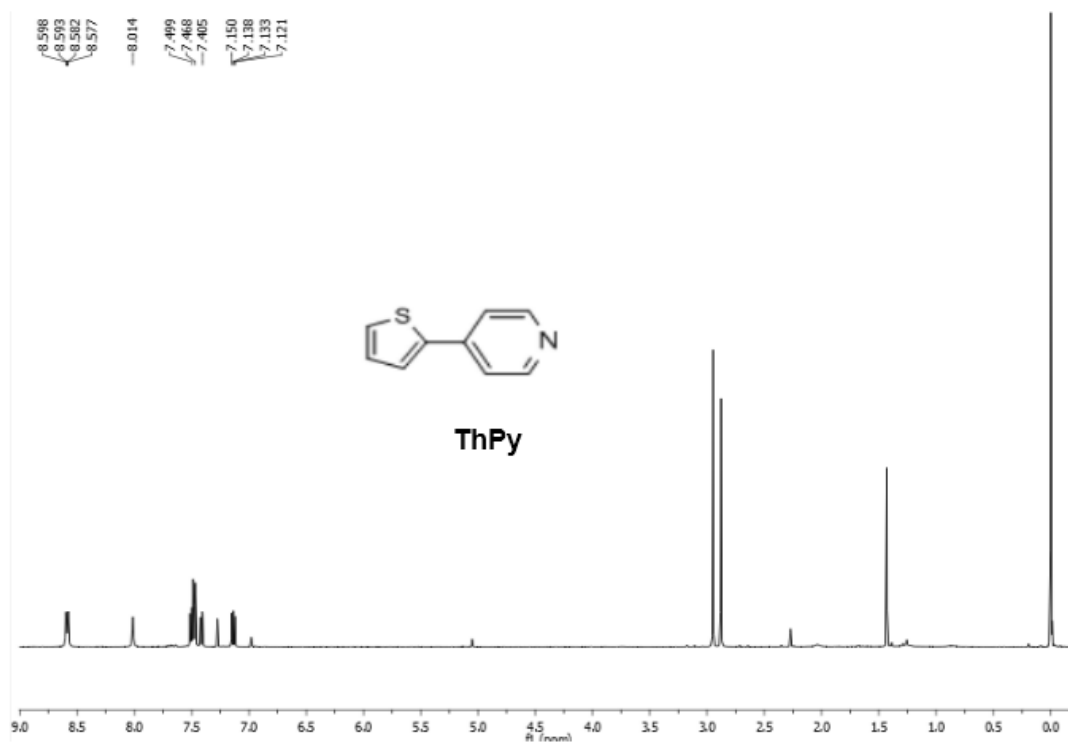
To the solution of 160 mg **B-ThPy** (0.56 mmol) in 20 mL toluene was added 0.13 mL (1.14 mmol) methyl triflate. The solid precipitate formed in toluene was collected by filtration, washed with diethyl ether and dried under high vacuum to afford 213 mg (84.7 %) **B-ThPy-Me** as a light green powder. ^1H NMR (300.13 MHz, CDCl_3): δ (ppm) = 1.37 (s, 12H), 4.40 (s, 3H), 7.68 (d, 1H, $J_{\text{HH}}^3 = 3.6$ Hz), 7.88 (d, 1H, $J_{\text{HH}}^3 = 3.6$ Hz), 8.04 (d, 2H $J_{\text{HH}}^3 = 6.3$ Hz), 8.78 (d, 2H, $J_{\text{HH}}^3 = 6.3$ Hz). ^{13}C NMR (75.48 MHz, CDCl_3), δ (ppm) = 24.7, 47.6, 84.9, 122.8, 131.8, 138.9, 142.3, 145.4, 148.8. ^{19}F NMR (111.9 MHz, CDCl_3), δ (ppm) = -77.1.

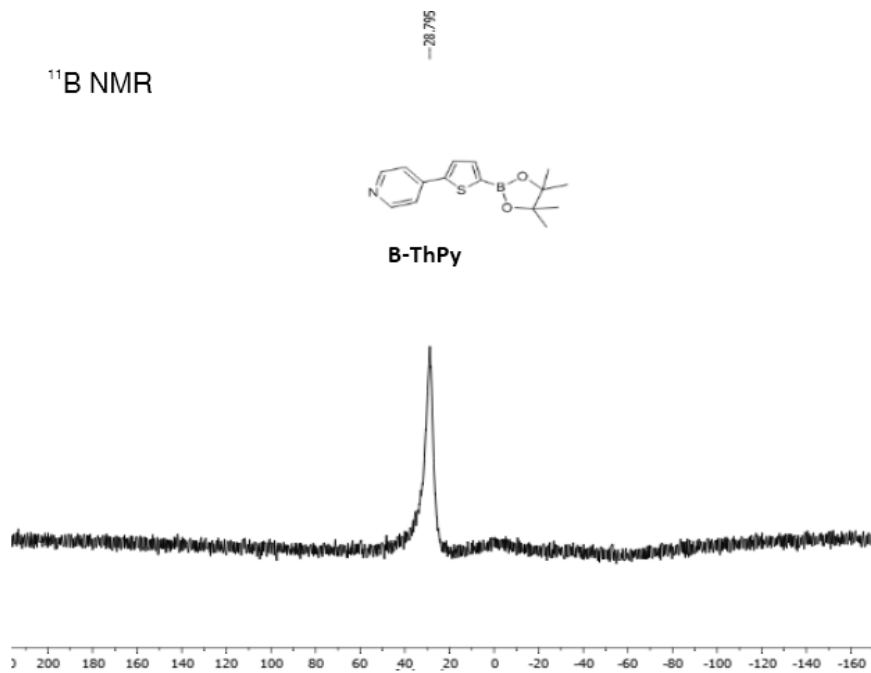
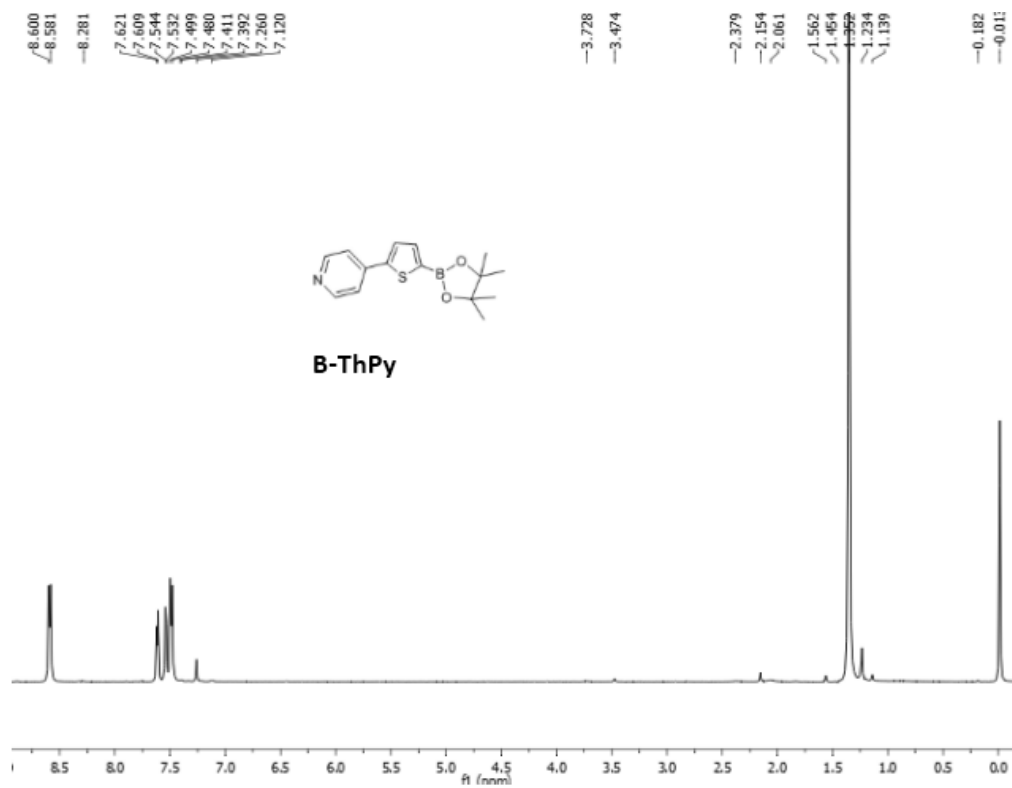
BF₃-ThPy-Me:

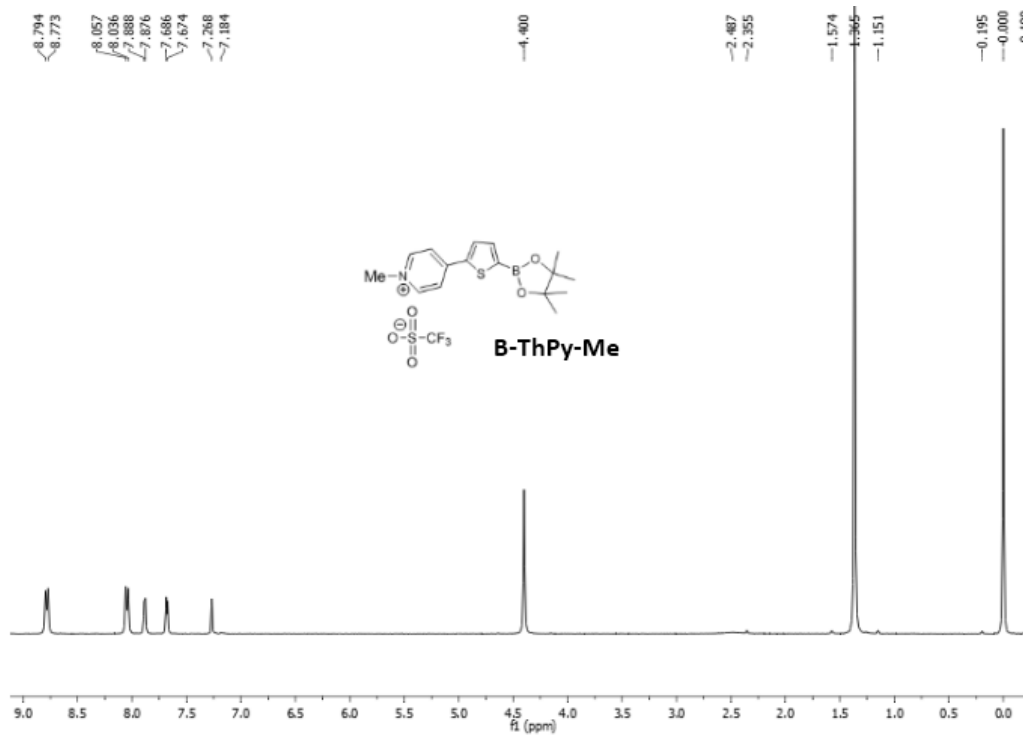
To the solution of 157 mg of **B-ThPy-Me** (0.35 mmol) in 20 ml toluene was added dropwise KHF_2 (108.8 mg, 1.39 mmol) solution in water and THF. The precipitate formed in toluene was filtered, then re-dissolved in minimum amount of DMSO. The DMSO solution was then added dropwise to 20 mL of acetone. The precipitate formed in acetone was filtered, washed with THF and dried under vacuum to afford 42 mg **BF₃-ThPy-Me** (51.4%) as a pale yellow solid. ^1H NMR (300.13 MHz, DMSO): δ (ppm) = 4.16 (s, 3H), 7.06 (d, 1H, $J_{\text{HH}}^3 = 3.0$ Hz), 7.80 (d, 1H, $J_{\text{HH}}^3 = 3.0$ Hz), 8.12 (d, 2H $J_{\text{HH}}^3 = 6.3$ Hz), 8.66 (d, 2H, $J_{\text{HH}}^3 = 6.3$ Hz). ^{13}C NMR (75.48 MHz, DMSO), δ

(ppm) = 46.4, 120.9, 130.7, 132.3, 135.8, 144.9, 148.5. ^{11}B NMR (96.30 MHz, CDCl_3), δ (ppm) = 2.3. ^{19}F NMR (111.9 MHz, CDCl_3), δ (ppm) = -130.6.

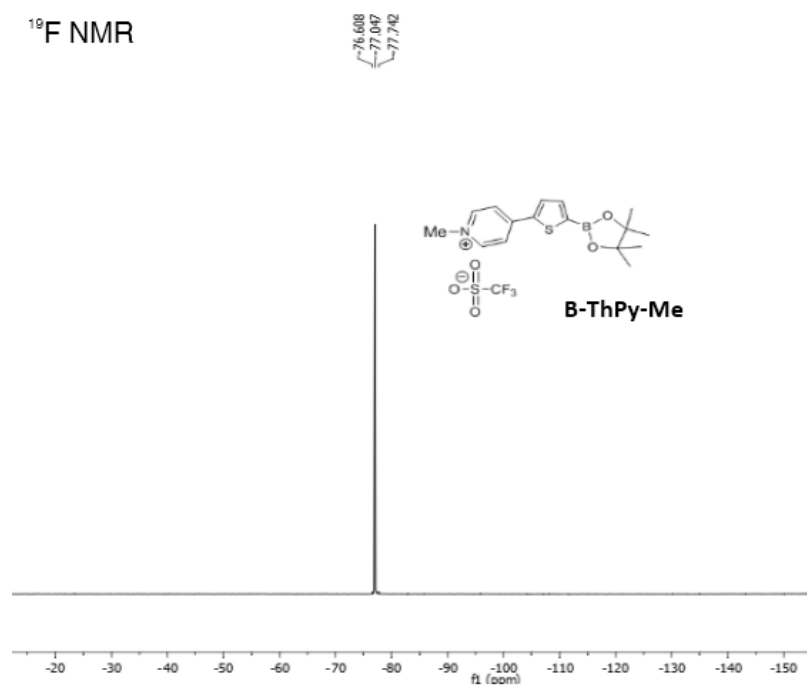
6.2.3 NMR spectra of key compounds

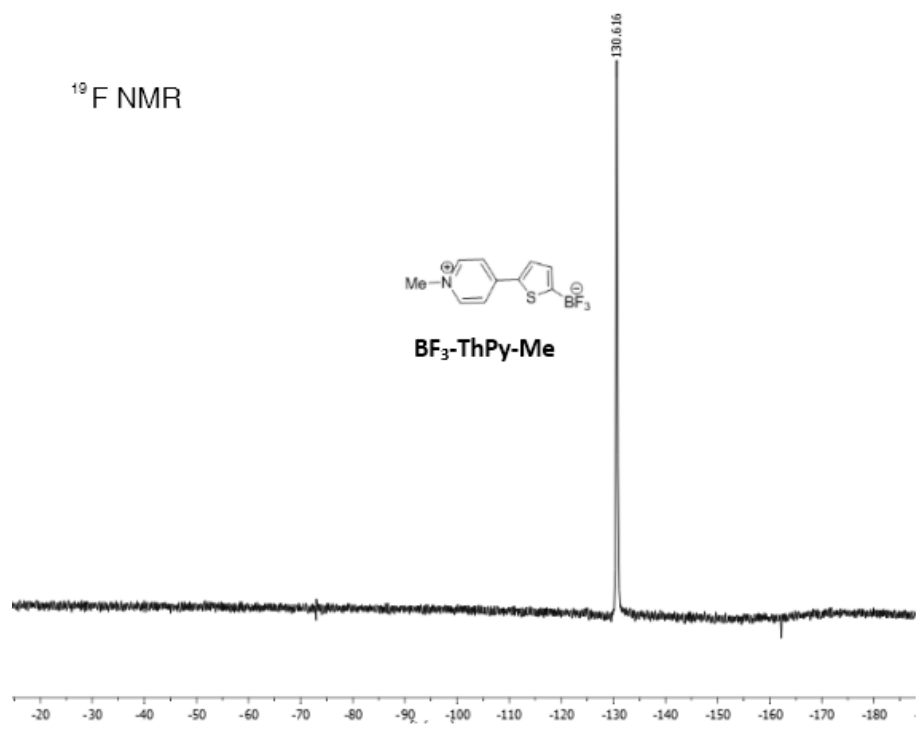
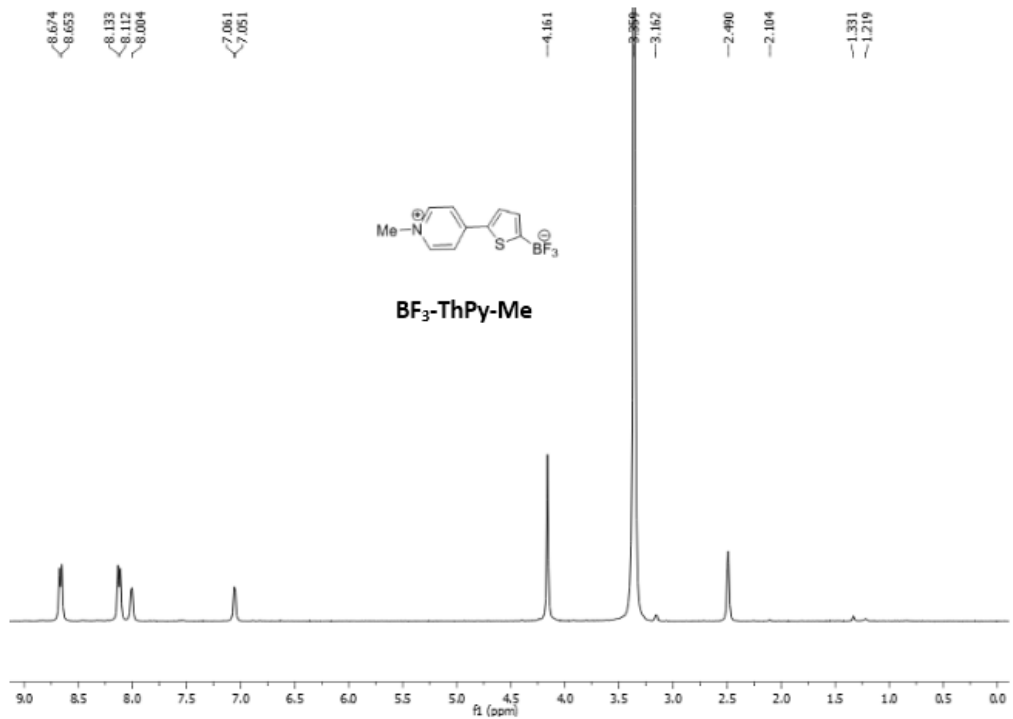




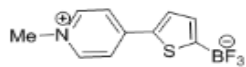


¹⁹F NMR

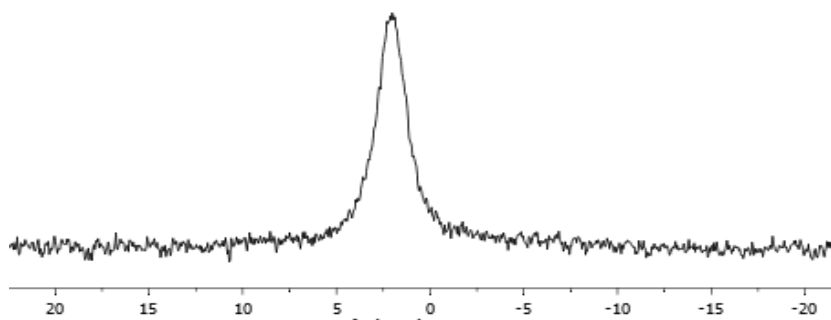




^{11}B NMR



$\text{BF}_3\text{-ThPy-Me}$



References:

- (1) Inzelt, G. *Conducting Polymers*; Monographs in Electrochemistry; Springer Berlin Heidelberg: Berlin, Heidelberg, **2008**.
- (2) Chiang, C. K.; Fincher, C. R.; Park, Y. W.; Heeger, A. J.; Shirakawa, H.; Louis, E. J.; Gau, S. C.; MacDiarmid, A. G. *Phys. Rev. Lett.* **1977**, *39*, 1098.
- (3) Chiang, C. K.; Fincher, C. R.; Park, Y. W.; Heeger, A. J.; Shirakawa, H.; Louis, E. J.; Gau, S. C.; MacDiarmid, A. G. *Phys. Rev. Lett.* **1977**, *39*, 1098.
- (4) Cheng, Y. J.; Yang, S. H.; Hsu, C. S. *Chem. Rev.* **2009**, *109*, 5868.
- (5) Wessling, R. A. *J. Polym. Sci. Polym. Symp.* **1985**, *72*, 55.
- (6) Burroughes, J. H.; Bradley, D. D. C.; Brown, A. R.; Marks, R. N.; Mackay, K.; Friend, R. H.; Burns, P. L.; Holmes, A. B. *Nature* **1990**, *347*, 539.
- (7) Neef, C. J.; Ferraris, J. P. *Macromolecules* **2000**, *33*, 2311.
- (8) Roncali, J. *Chem. Rev.* **1992**, *92*, 711.
- (9) Chen, T. A.; Rieke, R. D. *J. Am. Chem. Soc.* **1992**, *114*, 10087.
- (10) McCullough, R. D.; Lowe, R. D.; Jayaraman, M.; Anderson, D. L. *J. Org. Chem.* **1993**, *58*, 904.
- (11) Loewe, R. S.; Khersonsky, S. M.; McCullough, R. D. *Adv. Mater.* **1999**, *11*, 250.
- (12) Scherf, U.; List, E. J. W. *Adv. Mater.* **2002**, *14*, 477.
- (13) Anthony, J. E. *Chem. Rev.* **2006**, *106*, 5028.

- (14) Tang, W.; Ke, L.; Tan, L.; Lin, T.; Kietzke, T.; Chen, Z.-K. *Macromolecules* **2007**, *40*, 6164.
- (15) Alam, M. M.; Jenekhe, S. A. *Chem. Mater.* **2002**, *14*, 4775.
- (16) Colladet, K.; Fourier, S.; Cleij, T. J.; Lutsen, L.; Gelan, J.; Vanderzande, D.; Huong Nguyen, L.; Neugebauer, H.; Sariciftci, S.; Aguirre, A.; Janssen, G.; Goovaerts, E. *Macromolecules* **2007**, *40*, 65.
- (17) Herguth, P.; Jiang, X.; Liu, M. S.; Jen, A. K. Y. *Macromolecules* **2002**, *35*, 6094.
- (18) Li, J.; Dierschke, F.; Wu, J.; Grimsdale, A. C.; Müllen, K. *J. Mater. Chem.* **2006**, *16*, 96.
- (19) Blouin, N.; Michaud, A.; Leclerc, M. *Adv. Mater.* **2007**, *19*, 2295.
- (20) Hou, J.; Tan, Z.; Yan, Y.; He, Y.; Yang, C.; Li, Y. *J. Am. Chem. Soc.* **2006**, *128*, 4911.
- (21) Li, Y.; Zou, Y. *Adv. Mater.* **2008**, *20*, 2952.
- (22) Zhou, H.; Yang, L.; You, W. *Macromolecules* **2012**, *45*, 607.
- (23) Price, S. C.; Stuart, A. C.; Yang, L.; Zhou, H.; You, W. *J. Am. Chem. Soc.* **2011**, *133*, 4625.
- (24) Günes, S.; Neugebauer, H.; Sariciftci, N. S. *Chem. Rev.* **2007**, *107*, 1324.
- (25) Swager, T. M. *Acc. Chem. Res.* **1998**, *31*, 201.
- (26) McQuade, D. T.; Pullen, A. E.; Swager, T. M. *Chem. Rev.* **2000**, *100*, 2537.
- (27) Thomas III, S. W.; Guy, D. J.; Swager, T. M. *Chem. Rev.* **2007**, *107*, 1339.
- (28) Braun, D.; Heeger, A. J. *Appl. Phys. Lett.* **1991**, *58*, 1982.

- (29) Noda, T.; Ogawa, H.; Shirota, Y. *Adv. Mater.* **1999**, *11*, 283.
- (30) Sekine, C.; Tsubata, Y.; Yamada, T.; Kitano, M.; Doi, S. *Sci. Technol. Adv. Mater.* **2014**, *15*, 34203.
- (31) Noda, T.; Shirota, Y. *J. Am. Chem. Soc.* **1998**, *120*, 9714.
- (32) Wöhrle, D.; Meissner, D. *Adv. Mater.* **1991**, *3*, 129.
- (33) Bin, H.; Gao, L.; Zhang, Z.-G.; Yang, Y.; Zhang, Y.; Zhang, C.; Chen, S.; Xue, L.; Yang, C.; Xiao, M.; Li, Y.; Yu, G.; Gao, J.; Hummelen, J. C.; Wudl, F.; Heeger, A. J.; Thompson, B. C.; Fréchet, J. M. J.; Li, G.; Zhu, R.; Yang, Y.; He, Y.; Li, Y.; Zhan, X.; Zhou, E.; Facchetti, A.; Kim, T.; Jung, J. W.; Hwang, Y.-J.; Courtright, B. A. E.; Ferreira, A. S.; Tolbert, S. H.; Jenekhe, S. A.; Gao, L.; Benten, H.; Mori, D.; Ohkita, H.; Ito, S.; Holliday, S.; Nielsen, C. B.; Holliday, S.; Chen, H.-Y.; Cryer, S. J.; McCulloch, I.; Hwang, Y.-J.; Li, H.; Courtright, B. A. E.; Subramaniyan, S.; Jenekhe, S. A.; Zhong, Y.; Zhang, X.; Hartnett, P. E.; Lin, Y.; Lin, Y.; Li, Y.; Lin, Y.; Meng, D.; Liu, J.; Bin, H.; Zhao, W.; Ran, N. A.; Janssen, R. A. J.; Nelson, J.; Coakley, K. M.; McGehee, M. D.; Li, Y.; Dennler, G.; Scharber, M. C.; Brabec, C. J.; Scharber, M. C.; Sariciftci, N. S.; Veldman, D.; Meskers, S. C. J.; Janssen, R. A. J.; Faist, M. A.; Kawashima, K.; Tamai, Y.; Ohkita, H.; Osaka, I.; Takimiya, K.; Scharber, M. C.; Burke, T. M.; Sweetnam, S.; Vandewal, K.; McGehee, M. D.; Lin, H.; Min, J.; Zhang, Z.-G.; Zhang, S.; Li, Y.; Chen, J.; Cao, Y.; Zhou, H.; Yang, L.; You, W.; Zhang, Z.-G.; Li, Y. F.; Wang, J.-Y.; Ashraf, R. S.; Love, J. A.; Wu, J.-S.; Cheng, S.-W.; Cheng, Y.-J.; Hsu, C.-S.; Ohshita, J.; Price, S. C.; Stuart, A. C.; Yang, L.; Zhou, H.; You, W.; Eckhardt, H.; Shacklette, L. W.; Jen, K. Y.; Elsenbaumer, R. L.; Sun, Q.; Wang, H.; Yang, C.; Li, Y.; Zhang, Z.-G.; Wang, C.; Li, W.; Hendriks, K. H.; Furlan, A.; Wienk, M. M.; Janssen, R. A. J.; Liu, F.; Tumbleston, J. R.; Rivnay, J.; Mannsfeld, S. C. B.; Miller, C. E.; Salleo, A.; Toney, M. F.; Blom, P. W. M.; Jong, M. J. M. de; Munster, M. G. van; Malliaras, G. G.; Salem, J. R.; Brock, P. J.; Scott, C. *Nat. Commun.* **2016**, *7*, 13651.
- (34) Zhao, W.; Qian, D.; Zhang, S.; Li, S.; Inganäs, O.; Gao, F.; Hou, J. *Adv. Mater.* **2016**, *28*, 4734.
- (35) Liu, J.; Chen, S.; Qian, D.; Gautam, B.; Yang, G.; Zhao, J.; Bergqvist, J.; Zhang, F.; Ma, W.; Ade, H.; Inganäs, O.; Gundogdu, K.; Gao, F.; Yan, H. *Nat. Energy* **2016**, *1*, 16089.

- (36) Natta, G. *Angew. Chemie* **1964**, 76, 553.
- (37) Ziegler, K. *Angew. Chemie* **1964**, 76, 545.
- (38) Kern, R. J. *J. Polym. Sci. Part A-1 Polym. Chem.* **1969**, 7, 621.
- (39) Ciardelli, F.; Lanzillo, S.; Pieroni, O. *Macromolecules* **1974**, 7, 174.
- (40) Lam, J. W. Y.; Dong, Y.; Cheuk, K. K. L.; Luo, J.; Xie, Z.; Kwok, H. S.; Mo, Z.; Tang, B. Z. *Macromolecules* **2002**, 35, 1229.
- (41) Kong, X.; Lam, J. W. Y.; Tang, B. Z. *Macromolecules* **1999**, 32, 1722.
- (42) Hua, J.; Li, Z.; Lam, J. W. Y.; Xu, H.; Sun, J.; Dong; Dong; Qin, A.; Yuan, W.; Chen, H.; Wang, M.; Tang, B. Z. *Macromolecules* **2005**, 38, 8127.
- (43) Masuda, T.; Hasegawa, K.; Higashimura, T. *Macromolecules* **1974**, 7, 728.
- (44) Masuda, T.; Sasaki, N. *Macromolecules* **1975**, 8, 717.
- (45) Sasaki, N.; Masuda, T.; Higashimura, T. *Macromolecules* **1976**, 9, 664.
- (46) Masuda, T.; Kawasaki, M.; Okano, Y.; Higashimura, T. *Polym. J.* **1982**, 14, 371.
- (47) Masuda, T.; Higashimura, T. *Acc. Chem. Res.* **1984**, 17, 51.
- (48) Eleuterio, H. S. *US Pat.* **1957**, 3,074,913,.
- (49) Natta, G.; Dall'Asta, G.; Mazzanti, G. *Angew. Chemie Int. Ed.* **1964**, 3, 723.
- (50) Grubbs, R. H. *Angew. Chemie Int. Ed.* **2005**, 45, 3760.
- (51) Schrock, R. R. *Angew. Chemie Int. Ed.* **2006**, 45, 3748.

- (52) Chauvin, Y. *Angew. Chemie Int. Ed.* **2006**, *45*, 3741.
- (53) Bielawski, C. W.; Grubbs, R. H. *Prog. Polym. Sci.* **2007**, *32*, 1.
- (54) Korshak, Y. V.; Korshak, V. V.; Kanischka, G.; Höcker, H. *Die Makromol. Chemie, Rapid Commun.* **1985**, *6*, 685
- (55) Klavetter, F. L.; Grubbs, R. H. *J. Am. Chem. Soc.* **1988**, *110*, 7807.
- (56) Ginsburg, E. J.; Gorman, C. B.; Marder, S. R.; Grubbs, R. H. *J. Am. Chem. Soc.* **1989**, *111*, 7621.
- (57) Gorman, C. B.; Ginsburg, E. J.; Grubbs, R. H. *J. Am. Chem. Soc.* **1993**, *115*, 1397.
- (58) Wagener, K. B.; Boncella, J. M.; Nel, J. G. *Macromolecules* **1991**, *24*, 2649.
- (59) Konzelman, J.; Wagener, K. B. *Macromolecules* **1995**, *28*, 4686.
- (60) Schwendeman, J. E.; Church, A. C.; Wagener, K. B. *Advanced Synthesis and Catalysis* **2002**, *344*, 597.
- (61) Mutlu, H.; Montero de Espinosa, L.; Meier, M. a R. *Chem. Soc. Rev.* **2011**, *40*, 1404.
- (62) Banks, R. L.; Bailey, G. C. *Ind. Eng. Chem. Prod. Res. Dev.* **1964**, *3*, 170.
- (63) Jean-Louis Hérisson, P.; Chauvin, Y. *Die Makromol. Chemie* **1971**, *141*, 161.
- (64) K. B. Wagener ; T. W. Baughman. *Adv Polym Sci* **2005**, *176*, 1.
- (65) Qin, Y.; Hillmyer, M. A. *Macromolecules* **2009**, *42*, 6429.
- (66) Yamamoto, N.; Ito, R.; Geerts, Y.; Nomura, K. *Macromolecules* **2009**, *42*, 5104.

- (67) Nomura, K.; Miyamoto, Y.; Morimoto, H.; Geerts, Y. *J. Polym. Sci. Part A Polym. Chem.* **2005**, *43*, 6166.
- (68) Weskamp, T.; Schattenmann, W. C.; Spiegler, M.; Herrmann, W. a. *Angew. Chemie Int. Ed.* **1998**, *37*, 2490.
- (69) Huang, J.; Stevens, E. D.; Nolan, S. P.; Petersen, J. L. *J. Am. Chem. Soc.* **1999**, *121*, 2674.
- (70) Scholl, M.; Ding, S.; Lee, C. W.; Grubbs, R. H. *Org. Lett.* **1999**, *1*, 953.
- (71) Trnka, T. M.; Grubbs, R. H. *Acc. Chem. Res.* **2001**, *34*, 18.
- (72) Kingsbury, J. S.; Harrity, J. P. A.; Bonitatebus, P. J.; Hoveyda, A. H. *J. Am. Chem. Soc.* **1999**, *121*, 791.
- (73) Reif, L.; Höcker, H. *Die Makromol. Chemie, Rapid Commun.* **1983**, *4*, 693.
- (74) Grissom, J. W.; Gunawardena, G. U.; Klingberg, D.; Huang, D. *Tetrahedron* **1996**, *52*, 6453.
- (75) Nicolaou, K. C.; Dai, W.-M. *Angew. Chemie Int. Ed.* **1991**, *30*, 1387.
- (76) Maier, M. E. *Synlett* **1995**, 13.
- (77) Wenk, H. H.; Winkler, M.; Sander, W. *Angew. Chemie Int. Ed.* **2003**, *42*, 502.
- (78) Kar, M.; Basak, A. *Chem. Rev.* **2007**, *107*, 2861.
- (79) Lockhart, T. P.; Bergman, R. G. *J. Am. Chem. Soc.* **1981**, *103*, 4091.
- (80) Bergman, R. G. *Acc. Chem. Res.* **1973**, *6*, 25.
- (81) Jones, R. R.; Bergman, R. G. *J. Am. Chem. Soc.* **1972**, *94*, 660.

- (82) Basak, A.; Mandal, S.; Bag, S. S. *Chem. Rev.* **2003**, *103*, 4077.
- (83) Lee, M. D.; Dunne, T. S.; Siegel, M. M.; Chang, C. C.; Morton, G. O.; Borders, D. B. *J. Am. Chem. Soc.* **1987**, *109*, 3464.
- (84) Zein, N.; McGahren, W. J.; Morton, G. O.; Ashcroft, J.; Ellestad, G. A. *J. Am. Chem. Soc.* **1989**, *111*, 6888.
- (85) De Voss, J. J.; Townsend, C. A.; Ding, W. D.; Morton, G. O.; Ellestad, G. A.; Zein, N.; Tabor, A. B.; Schreiber, S. L. *J. Am. Chem. Soc.* **1990**, *112*, 9669.
- (86) McPhee, M. M.; Kerwin, S. M. *J. Org. Chem.* **1996**, *61*, 9385.
- (87) O'Connor, J. M.; Friese, S. J.; Rodgers, B. L. *J. Am. Chem. Soc.* **2005**, *127*, 16342.
- (88) Rawat, D. S.; Zaleski, J. M. *J. Am. Chem. Soc.* **2001**, *123*, 9675.
- (89) Warner, B. P.; Millar, S. P.; Broene, R. D.; Buchwald, S. L. *Science* **1995**, *269*, 814.
- (90) Sud, D.; Wigglesworth, T. J.; Branda, N. R. *Angew. Chemie Int. Ed.* **2007**, *46*, 8017.
- (91) Bhattacharyya, S.; Clark, A. E.; Pink, M.; Zaleski, J. M. *Chem. Commun.* **2003**, *10*, 1156.
- (92) Hu, K.; Yang, H.; Zhang, W.; Qin, Y. *Chem. Sci.* **2013**, *4*, 3649.
- (93) Hu, K.; Pandres, E.; Qin, Y. *J. Polym. Sci. Part A Polym. Chem.* **2014**, *52*, 2662.
- (94) Hu, K.; Qin, Y. *J. Polym. Sci. Part A Polym. Chem.* **2016**, *54*, 1391.
- (95) Wegner, G. Z. *Naturforsch* **1969**, *B24*, 824.

- (96) Zuilhof, H.; Barentsen, H. M.; van Dijk, M.; Sudhölter, E. J. R.; Hoofman, J. O. M.; Siebbeles, L. D. A.; de Haas, M. P.; Warman, J. M. *In Supramolecular Photosensitive and Electroactive Materials; Nalwa, H. S., Ed.; Academic Press: San Diego. 2001*, p.339.
- (97) Schott, M. *Photophysics Mol. Mater. Lanzani, G., Ed.; Wiley-VCH Weinheim 2006*, p.49.
- (98) Dubin, F.; Melet, R.; Barisien, T.; Grousson, R.; Legrand, L.; Schott, M.; Voliotis, V. *Nat. Phys.* **2005**, 2, 12.
- (99) Legrand, L.; Choueiry, A. Al; Holcman, J.; Enderlin, A.; Melet, R.; Barisien, T.; Voliotis, V.; Grousson, R.; Schott, M. *Phys. status solidi (b)* **2008**, 245, 2702.
- (100) Chance, R. R.; Baughman, R. H.; Müller, H.; Eckhardt, C. J. *J. Chem. Phys.* **1977**, 67, 3616.
- (101) Dei, S.; Matsumoto, A.; Matsumoto, A. *Macromolecules* **2008**, 41, 2467.
- (102) Tanioku, C.; Matsukawa, K.; Matsumoto, A. *ACS Appl. Mater. Interfaces* **2013**, 5, 940.
- (103) Patel, G. N.; Chance, R. R.; Witt, J. D. *J. Polym. Sci. Polym. Lett. Ed.* **1978**, 16, 607.
- (104) Müller, H.; Eckhardt, C. J. *Mol. Cryst. Liq. Cryst.* **1978**, 45, 313.
- (105) Carpick, R. W.; Sasaki, D. Y.; Burns, A. R. *Langmuir* **2000**, 16, 1270.
- (106) Tieke, B.; Lieser, G.; Wegner, G. *J. Polym. Sci. Polym. Chem. Ed.* **1979**, 17, 1631.
- (107) Charych, D.; Nagy, J.; Spevak, W.; Bednarski, M. *Science (80-.)*. **1993**, 261, 585.

- (108) Reichert, A.; Nagy, J. O.; Spevak, W.; Charych, D. *J. Am. Chem. Soc.* **1995**, *117*, 829.
- (109) T. Kanetake, K. Ishikawa, T. Hasegawa, T. K.; K. Takeda, M. Hasegawa, K. K. and H. K. *Appl. Phys. Lett.* **1989**, No. 54, 2287.
- (110) Sarkar, A.; Okada, S.; Matsuzawa, H.; Matsuda, H.; Nakanishi, H. *J. Mater. Chem.* **2000**, *10*, 819.
- (111) Nakanishi, H.; Matsuda, H.; Kato, M. *Mol. Cryst. Liq. Cryst.* **1984**, *105*, 77.
- (112) Se, K.; Ohnuma, H.; Kotaka, T. *Macromolecules* **1984**, *17*, 2126.
- (113) Peng, H.; Lu, Y. *Langmuir* **2006**, *22*, 5525.
- (114) Peng, H. *J. Phys. Chem. B* **2007**, *111*, 8885.
- (115) Sun, X.; Chen, T.; Huang, S.; Li, L.; Peng, H. *Chem. Soc. Rev.* **2010**, *39*, 4244.
- (116) Kim, T.; Ye, Q.; Sun, L.; Chan, K. C.; Crooks, R. M. *Langmuir* **1996**, *12*, 6065.
- (117) Barentsen, H. M.; van Dijk, M.; Kimkes, P.; Zuilhof, H.; Sudhölter, E. J. R. *Macromolecules* **1999**, *32*, 1753.
- (118) Talwar, S.; M. Kamath, K. D. and U. S. *Polym. Commun.* **1990**, *31*, 198.
- (119) Kamath, M.; Kim, W. H.; Li, L.; Kumar, J.; Tripathy, S.; Babu, K. N.; Talwar, S. S. *Macromolecules* **1993**, *26*, 5954.
- (120) Sarkar, A.; Kodali, N. B.; Kamath, M. B.; Bhagwat, L. P.; Talwar, S. S. *J. Macromol. Sci. Part A* **1999**, *36*, 211.
- (121) Wudl, F.; Bitler, S. P. *J. Am. Chem. Soc.* **1986**, *108*, 4685.
- (122) Schilke, B. E. K. and D. E. *J. Chem. Phys.* **1987**, No. 86, 5214.

- (123) Lindsell, W. E.; Preston, P. N.; Tomb, P. J. *J. Organomet. Chem.* **1992**, *439*, 201.
- (124) Giesa, R.; Schulz, R. C. *Polym. Int.* **1994**, *33*, 43.
- (125) Kosinski, C.; Hirsch, A.; Heinemann, F. W.; Hampel, F. *European J. Org. Chem.* **2001**, *2001*, 3879.
- (126) Takayama, Y.; Delas, C.; Muraoka, K.; Uemura, M.; Sato, F. *J. Am. Chem. Soc.* **2003**, *125*, 14163.
- (127) Takayama, Y.; Delas, C.; Muraoka, K.; Sato, F. *Org. Lett.* **2003**, *5*, 365.
- (128) Polhuis, M.; Hendrikx, C. C. J.; Zuilhof, H.; Sudhölter, E. J. R. *Tetrahedron Lett.* **2003**, *44*, 899.
- (129) Hendrikx, C. C. J.; Polhuis, M.; Pul-Hootsen, A.; Koehorst, R. B. M.; van Hoek, A.; Zuilhof, H.; Sudhölter, E. J. R. *Phys. Chem. Chem. Phys.* **2005**, *7*, 548.
- (130) Balkowski, G. M.; Groeneveld, M.; Zhang, H.; Hendrikx, C. C. J.; Polhuis, M.; Zuilhof, H.; Buma, W. J. *J. Phys. Chem. A* **2006**, *110*, 11435.
- (131) Pilzak, G. S.; van Lagen, B.; Hendrikx, C. C. J.; Sudhölter, E. J. R.; Zuilhof, H. *Chem. - A Eur. J.* **2008**, *14*, 7939.
- (132) Pilzak, G. S.; van Lagen, B.; Sudhölter, E. J. R.; Zuilhof, H. *Tetrahedron Lett.* **2008**, *49*, 4949.
- (133) Weiss, K.; Michel, A.; Auth, E.-M.; Bunz, U. H. F.; Mangel, T.; Müllen, K. *Angew. Chemie Int. Ed. English* **1997**, *36*, 506.
- (134) Bunz, U. H. F. *Acc. Chem. Res.* **2001**, *34*, 998.
- (135) A. D. Finke and J. S. Moore, in *Synthesis of Polymers*, E.; D. A. Schluter, C. H. and J. S. *Wiley-VCH, Weinheim, Ger.* **2012**, p.135.

- (136) Fürstner, A.; Davies, P. W. *Chem. Commun.* **2005**, 50, 2307.
- (137) Fürstner, A. *Angew. Chemie Int. Ed.* **2013**, 52, 2794.
- (138) Carnes, M.; Buccella, D.; Siegrist, T.; Steigerwald, M. L.; Nuckolls, C. *J. Am. Chem. Soc.* **2008**, 130, 14078.
- (139) Fischer, F. R.; Nuckolls, C. *Angew. Chemie Int. Ed.* **2010**, 49, 7257.
- (140) Sedbrook, D. F.; Paley, D. W.; Steigerwald, M. L.; Nuckolls, C.; Fischer, F. R. *Macromolecules* **2012**, 45, 5040.
- (141) F. Diederich, in *Modular Chemistry*, ed. J. Michl, K.; Publishers, A. Netherlands, **1997**, p. 17.
- (142) Gubler, U.; Bosshard, C.; Günter, P.; Balakina, M. Y.; Cornil, J.; Brédas, J. L.; Martin, R. E.; Diederich, F. *Opt. Lett.* **1999**, 24, 1599.
- (143) Martin, R. E.; Gubler, U.; Boudon, C.; Bosshard, C.; Gisselbrecht, J.-P.; Günter, P.; Gross, M.; Diederich, F. *Chemistry (Easton)*. **2000**, 6, 4400.
- (144) Martin, R. E.; Gubler, U.; Cornil, J.; Balakina, M.; Boudon, C.; Bosshard, C.; Gisselbrecht, J.-P.; Diederich, F.; Günter, P.; Gross, M.; Brédas, J.-L. *Chem. - A Eur. J.* **2000**, 6, 3622.
- (145) Helal, C. J.; Magriotis, P. A.; Corey, E. J. *J. Am. Chem. Soc.* **1996**, 118, 10938.
- (146) O. Klein, H. H. and J. G. *J. Org. Chem.* **2009**, 2009, 2141.
- (147) Kloppenburg, L.; Song, D.; Bunz, U. H. F. *J. Am. Chem. Soc.* **1998**, 120, 7973.
- (148) G. Brizius, N. G. P.; W. Steffen, K. Stitzer, H.-C. zur L. and U. H. F. B. *J. Am. Chem. Soc.* **2000**, 122, 12435.
- (149) Sashuk, V.; J. Ignatowska and K. Grela. *J. Org. Chem.* **2004**, 69, 7748.

- (150) V. Maraval, C. Lepetit, A.-M. Caminade, J.-P. M.; Chauvin, and R. *Tetrahedron Lett.* **2006**, 47, 2155.
- (151) Schrock, R. R. *Polyhedron* **1995**, 14, 3177.
- (152) Lacombe, F.; Radkowski, K.; Seidel, G.; Fürstner, A. *Tetrahedron* **2004**, 60, 7315.
- (153) Yang, H.; Liu, Z.; Zhang, W. *Adv. Synth. Catal.* **2013**, 355, 885.
- (154) Jyothish, K.; Zhang, W. *Angew. Chemie Int. Ed.* **2011**, 50, 3435.
- (155) Jyothish, K.; Zhang, W. *Angew. Chemie Int. Ed.* **2011**, 50, 8478.
- (156) K. Jyothish, Q. W. and W. Z. *Adv. Synth. Catal.* **2012**, 354, 2073.
- (157) Paley, D. W.; Sedbrook, D. F.; Decatur, J.; Fischer, F. R.; Steigerwald, M. L.; Nuckolls, C. *Angew. Chemie Int. Ed.* **2013**, 52, 4591.
- (158) Heppekausen, J.; Stade, R.; Goddard, R.; Fürstner, A. *J. Am. Chem. Soc.* **2010**, 132, 11045.
- (159) Babbitt, G. E.; Patel, G. N. *Macromolecules* **1981**, 14, 554.
- (160) Nava, A. D.; Thakur, M.; Tonelli, A. E. *Macromolecules* **1990**, 23, 3055.
- (161) Wenz, G.; Mueller, M. A.; Schmidt, M.; Wegner, G. *Macromolecules* **1984**, 17, 837.
- (162) J. P. Aime, F. B.; J. L. Fave, M. R. and M. S. *J. Chem. Phys.* **1988**, 89, 6477.
- (163) S. D. D. V. Rughooputh, D. Phillips, D. B. and D. J. A. *Chem. Phys. Lett.* **1984**, 106, 247.
- (164) Gaussian 03, Revision C.01, M. J. Frisch, G. W. Trucks, H. B. Schlegel, G. E. S.; M. A. Robb, J. R. Cheeseman, J. A. Montgomery, Jr., T. Vreven, K. N.

Kudin, J. C.; Burant, J. M. Millam, S. S. Iyengar, J. Tomasi, V. Barone, B. Mennucci, M. Cossi, G.; Scalmani, N. Rega, G. A. Petersson, H. Nakatsuji, M. Hada, M. Ehara, K. Toyota, R.; Fukuda, J. Hasegawa, M. Ishida, T. Nakajima, Y. Honda, O. Kitao, H. Nakai, M. K.; X. Li, J. E. Knox, H. P. Hratchian, J. B. Cross, V. Bakken, C. Adamo, J. Jaramillo, R.; Gomperts, R. E. Stratmann, O. Yazyev, A. J. Austin, R. Cammi, C. Pomelli, J. W.; Ochterski, P. Y. Ayala, K. Morokuma, G. A. Voth, P. Salvador, J. J. Dannenberg, V. G.; Zakrzewski, S. Dapprich, A. D. Daniels, M. C. Strain, O. Farkas, D. K. Malick, A. D.; Rabuck, K. Raghavachari, J. B. Foresman, J. V. Ortiz, Q. Cui, A. G. Baboul, S. C.; J. Cioslowski, B. B. Stefanov, G. Liu, A. Liashenko, P. Piskorz, I. Komaromi, R. L.; Martin, D. J. Fox, T. Keith, M. A. Al-Laham, C. Y. Peng, A. Nanayakkara, M.; Challacombe, P. M. W. Gill, B. Johnson, W. Chen, M. W. Wong, C. Gonzalez, and J. A.; Pople, Gaussian, Inc., Wallingford CT, **2004**.

(165) Campbell, A. J.; Davies, C. K. L.; Batchelder, D. N. *Macromol. Chem. Phys.* **1998**, *199*, 109.

(166) Schott, M. *J. Phys. Chem. B* **2006**, *110*, 15864.

(167) Filhol, J.-S.; Deschamps, J.; Dutremez, S. G.; Boury, B.; Barisien, T.; Legrand, L.; Schott, M. *J. Am. Chem. Soc.* **2009**, *131*, 6976.

(168) Al Choueiry, A.; Barisien, T.; Holcman, J.; Legrand, L.; Schott, M.; Weiser, G.; Balog, M.; Deschamps, J.; Dutremez, S. G.; Filhol, J.-S. *Phys. Rev. B* **2010**, *81*, 125208.

(169) Brabec, C. J.; Sariciftci, N. S.; Hummelen, J. C. *Adv. Funct. Mater.* **2001**, *11*, 15.

(170) Coakley, K. M.; McGehee, M. D. *Chem. Mater.* **2004**, *16*, 4533.

(171) Winder, C.; Sariciftci, N. S. *J. Mater. Chem.* **2004**, *14*, 1077.

(172) Muthitamongkol, P.; Thanachayanont, C.; Sukwattanasinitt, M. *Curr. Appl. Phys.* **2011**, *11*, S163.

(173) Handbook of Conducting Polymers, 3rd ed.; T. A. Skotheim;; J. R. Reynolds, E. . C. P. B. R. **2007**.

- (174) Schreiber, M.; Anthony, J.; Diederich, F.; Spahr, M. E.; Nesper, R.; Hubrich, M.; Bommeli, F.; Degiorgi, L.; Wachter, P.; Kaatz, P.; Bosshard, C.; Günter, P.; Colussi, M.; Suter, U. W.; Boudon, C.; Gisselbrecht, J.-P.; Gross, M. *Adv. Mater.* **1994**, *6*, 786.
- (175) Anthony, J.; Boudon, C.; Diederich, F.; Gisselbrecht, J.-P.; Gramlich, V.; Gross, M.; Hobi, M.; Seiler, P. *Angew. Chemie Int. Ed. English* **1994**, *33*, 763.
- (176) Fowler, F. W.; Lauher, J. W. *J. Phys. Org. Chem.* **2000**, *13*, 850.
- (177) M. J. Edelmann, S. Ordermatt, F. D. *Chimia (Aarau)*. **2001**, *55*, 132.
- (178) Schenning, A. P. H. J.; Arndt, J.-D.; Ito, M.; Stoddart, A.; Schreiber, M.; Siemsen, P.; Martin, R. E.; Boudon, C.; Gisselbrecht, J.-P.; Gross, M.; Gramlich, V.; Diederich, F. *Helv. Chim. Acta* **2001**, *84*, 296.
- (179) Schenning, A. P. H. J.; Martin, R. E.; Ito, M.; Diederich, F.; Schenning, A. P. H. J.; Martin, R. E.; Boudon, C.; Gisselbrecht, J.-P.; Gross, M. *Chem. Commun.* **1998**, *35*, 1013.
- (180) Martin, R. E.; Günter, P.; Bosshard, C.; Gubler, U.; Gramlich, V.; Gross, M.; Boudon, C.; Gisselbrecht, J.-P.; Diederich, F. *Chem. - A Eur. J.* **1997**, *3*, 1505.
- (181) Martin, R. E.; Gubler, U.; Cornil, J.; Balakina, M.; Boudon, C.; Bosshard, C.; Gisselbrecht, J.-P.; Diederich, F.; Günter, P.; Gross, M.; Brédas, J.-L. *Chem. - A Eur. J.* **2000**, *6*, 3622.
- (182) Martin, R. E.; Gubler, U.; Boudon, C.; Bosshard, C.; Gisselbrecht, J.-P.; Günter, P.; Gross, M.; Diederich, F. *Chemistry (Easton)*. **2000**, *6*, 4400.
- (183) Xiao, J.; Yang, M.; Lauher, J. W.; Fowler, F. W. *Angew. Chemie Int. Ed.* **2000**, *39*, 2132.
- (184) Lauher, J. W.; Fowler, F. W.; Goroff, N. S. *Acc. Chem. Res.* **2008**, *41*, 1215.
- (185) Q. Liu, D. J. B. *Tetrahedron Lett.* **1997**, *38*, 4371.

- (186) T. D. Nielsen, C. Cruickshank, S. Forged, J. Thorsen, F. C.; Krebs. *Sol. Energy Mater. Sol. Cells* **2010**, *94*, 1553.
- (187) Krebs, F. C.; Espinosa, N.; Hösel, M.; Søndergaard, R. R.; Jørgensen, M. *Adv. Mater.* **2014**, *26*, 29.
- (188) Thompson, B. C.; Fréchet, J. M. J. *Angew. Chemie Int. Ed.* **2008**, *47*, 58.
- (189) Sonar, P.; Fong Lim, J. P.; Chan, K. L. *Energy Environ. Sci.* **2011**, *4*, 1558.
- (190) Zhou, G.-J.; Wong, W.-Y. *Chem. Soc. Rev.* **2011**, *40*, 2541.
- (191) Zhou, G.-J.; Wong, W.-Y.; Lin, Z.; Ye, C. *Angew. Chemie Int. Ed.* **2006**, *45*, 6189.
- (192) Zhou, G.-J.; Wong, W.-Y.; Ye, C.; Lin, Z. *Adv. Funct. Mater.* **2007**, *17*, 963.
- (193) Manners, I. *Science.* **2001**, *294*, 1664.
- (194) P., R.; Kingsborough, T. M. Swager, I. P. in I. C.; K. D. Karlin, Ed.; Wiley: Hoboken, N. **1999**, 48.
- (195) Hirao, T. *Coord. Chem. Rev.* **2002**, 226, 81.
- (196) Liu, Y.; Li, Y.; Schanze, K. S. *J. Photochem. Photobiol. C Photochem. Rev.* **2002**, *3*, 1.
- (197) Moorlag, C.; Sih, B. C.; Stott, T. L.; Wolf, M. O. *J. Mater. Chem.* **2005**, *15*, 2433.
- (198) Wolf, M. O. *J. Inorg. Organomet. Polym. Mater.* **2006**, *16*, 189.
- (199) Wong, W.-Y.; Ho, C.-L. *Coord. Chem. Rev.* **2006**, *250*, 2627.
- (200) Ho, C.-L.; Wong, W.-Y. *Coord. Chem. Rev.* **2011**, *255*, 2469.

- (201) Wong, W.-Y.; Chan, S.-M.; Choi, K.-H.; Cheah, K.-W.; Chan, W.-K. *Macromol. Rapid Commun.* **2000**, *21*, 453.
- (202) Guo, F.; Kim, Y.-G.; Reynolds, J. R.; Schanze, K. S. *Chem. Commun.* **2006**, 353, 1887.
- (203) Wong, W.-Y.; Wang, X.-Z.; He, Z.; Chan, K.-K.; Djurišić, A. B.; Cheung, K.-Y.; Yip, C.-T.; Ng, A. M.-C.; Xi, Y. Y.; Mak, C. S. K.; Chan, W.-K. *J. Am. Chem. Soc.* **2007**, *129*, 14372.
- (204) Wong, W.-Y.; Wang, X.; Zhang, H.-L.; Cheung, K.-Y.; Fung, M.-K.; Djurišić, A. B.; Chan, W.-K. *J. Organomet. Chem.* **2008**, *693*, 3603.
- (205) Mei, J.; Ogawa, K.; Kim, Y.-G.; Heston, N. C.; Arenas, D. J.; Nasrollahi, Z.; McCarley, T. D.; Tanner, D. B.; Reynolds, J. R.; Schanze, K. S. *ACS Appl. Mater. Interfaces* **2009**, *1*, 150.
- (206) Wu, P.-T.; Bull, T.; Kim, F. S.; Luscombe, C. K.; Jenekhe, S. A. *Macromolecules* **2009**, *42*, 671.
- (207) Zhan, H.; Lamare, S.; Ng, A.; Kenny, T.; Guernon, H.; Chan, W.-K.; Djurišić, A. B.; Harvey, P. D.; Wong, W.-Y. *Macromolecules* **2011**, *44*, 5155
- (208) Wong, W.-Y. *Macromol. Chem. Phys.* **2008**, *209*, 14.
- (209) Wong, W.-Y.; Ho, C.-L. *Acc. Chem. Res.* **2010**, *43*, 1246.
- (210) Wong, W.-Y.; Harvey, P. D. *Macromol. Rapid Commun.* **2010**, *31*, 671.
- (211) Ho, C.-L.; Wong, W.-Y. *Coord. Chem. Rev.* **2013**, *257*, 1614.
- (212) Wong, W.-Y. *Dalt. Trans.* **2007**, *5*, 4495.
- (213) Wong, W.-Y. *J. Inorg. Organomet. Polym. Mater.* **2005**, *15*, 197.
- (214) Liu, L.; Ho, C.-L.; Wong, W.-Y.; Cheung, K.-Y.; Fung, M.-K.; Lam, W.-T.; Djurišić, A. B.; Chan, W.-K. *Adv. Funct. Mater.* **2008**, *18*, 2824.

- (215) Wong, W.-Y.; Wang, X.-Z.; He, Z.; Djurišić, A. B.; Yip, C.-T.; Cheung, K.-Y.; Wang, H.; Mak, C. S. K.; Chan, W.-K. *Nat. Mater.* **2007**, *6*, 521.
- (216) Baek, N. S.; Hau, S. K.; Yip, H.-L.; Acton, O.; Chen, K.-S.; Jen, A. K.-Y. *Chem. Mater.* **2008**, *20*, 5734.
- (217) Wang, X.-Z.; Wong, W.-Y.; Cheung, K.-Y.; Fung, M.-K.; Djurišić, A. B.; Chan, W.-K. *Dalt. Trans.* **2008**, *18*, 5484.
- (218) Wang, X.-Z.; Wang, Q.; Yan, L.; Wong, W.-Y.; Cheung, K.-Y.; Ng, A.; Djurišić, A. B.; Chan, W.-K. *Macromol. Rapid Commun.* **2010**, *31*, 861.
- (219) Wang, Q.; Wong, W.-Y. *Polym. Chem.* **2011**, *2*, 432.
- (220) Qin, C.; Fu, Y.; Chui, C.-H.; Kan, C.-W.; Xie, Z.; Wang, L.; Wong, W.-Y. *Macromol. Rapid Commun.* **2011**, *32*, 1472.
- (221) Yan, L.; Zhao, Y.; Wang, X.; Wang, X.-Z.; Wong, W.-Y.; Liu, Y.; Wu, W.; Xiao, Q.; Wang, G.; Zhou, X.; Zeng, W.; Li, C.; Wang, X.; Wu, H. *Macromol. Rapid Commun.* **2012**, *33*, 603.
- (222) Köhler, A.; Wittmann, H. F.; Friend, R. H.; Khan, M. S.; Lewis, J. *Synth. Met.* **1996**, *77*, 147.
- (223) Beljonne, D.; Wittmann, H. F.; Köhler, A.; Graham, S.; Younus, M.; Lewis, J.; Raithby, P. R.; Khan, M. S.; Friend, R. H.; Brédas, J. L. *J. Chem. Phys.* **1996**, *105*, 3868.
- (224) N. Chawdhury, Köhler, A., R. H.; Friend, W.-Y. Wong, J. Lewis, M. Younus, P. R. Raithby, T. C.; Corcoran, M. R. A. Al-Mandhary, M. S. K. *J. Chem. Phys.* **1999**, *110*, 4963.
- (225) J. S. Wilson, Köhler, A., R. H. F.; M. K. Al-Suti, M. R. A. Al-Mandhary, M. S. Khan, P. R. R. *J. Chem. Phys.* **2000**, *113*, 7627.
- (226) Liu, Y.; Jiang, S.; Glusac, K.; Powell, D. H.; Anderson, D. F.; Schanze, K. S. *J. Am. Chem. Soc.* **2002**, *124*, 12412.

- (227) Ramakrishna, G.; Goodson, T.; Rogers-Haley, J. E.; Cooper, T. M.; McLean, D. G.; Urbas, A. *J. Phys. Chem. C* **2009**, *113*, 1060.
- (228) He, W.; Jiang, Y.; Qin, Y. *Polym. Chem.* **2014**, *5*, 1298.
- (229) Younus, M.; Köhler, A.; Cron, S.; Chawdhury, N.; Al-Mandhary, M. R. A.; Khan, M. S.; Lewis, J.; Long, N. J.; Friend, R. H.; Raithby, P. R. *Angew. Chemie Int. Ed.* **1998**, *37*, 3036.
- (230) Corriu, R. J.-P.; Deforth, T.; Douglas, W. E.; Guerrero, G.; Deforth, T.; Siebert, W. S. *Chem. Commun.* **1998**, No. 9, 963
- (231) Jäkle, F. *Chem. Rev.* **2010**, *110*, 3985.
- (232) Matsumi, N.; Naka, K.; Chujo, Y. *J. Am. Chem. Soc.* **1998**, *120*, 5112.
- (233) Entwistle, C. D.; Marder, T. B. *Chemistry of Materials.* **2004**, *16*, 4574.
- (234) Matsumi, N.; Chujo, Y. *Polym. J.* **2008**, *40*, 77.
- (235) Miyata, M.; Chujo, Y. *Polym. J.* **2002**, *34*, 967.
- (236) Bonifácio, V. D. B.; Morgado, J.; Scherf, U. *J. Polym. Sci. Part A Polym. Chem.* **2008**, *46*, 2878.
- (237) Matsumi, N.; Umeyama, T.; Chujo, Y. *Polym. Bull.* **2000**, *44*, 431.
- (238) Jäkle, F. *Coord. Chem. Rev.* **2006**, *250*, 1107.
- (239) Smith, K.; Pelter, A.; Jin, Z. *Angew. Chem. Int. Ed.* **1994**, *33*, 851.
- (240) Pelter, A.; Smith, K.; Elgandy, S.; Rowlands, M. *Tetrahedron Lett.* **1989**, *30*, 5643.
- (241) Pelter, A.; Smith, K.; Buss, D.; Jin, Z. *Heteroat. Chem.* **1992**, *3*, 275.

- (242) Matsumi, N.; Naka, K.; Chujo, Y. *J. Am. Chem. Soc.* **1998**, *120*, 10776.
- (243) Sundararaman, A.; Victor, M.; Varughese, R.; Jäkle, F. *J. Am. Chem. Soc.* **2005**, *127*, 13748.
- (244) Li, H.; Jäkle, F. *Angew. Chem. Int. Ed.* **2009**, *48*, 2313.
- (245) Li, H.; Jäkle, F. *Macromol. Rapid Commun.* **2010**, *31*, 915.
- (246) Yin, X.; Chen, J.; Lalancette, R. A.; Marder, T. B.; Jäkle, F. *Angew. Chemie Int. Ed.* **2014**, *53*, 9761.
- (247) Tanaka, K.; Ueda, K.; Koike, T.; Ando, M.; Tamabe, T. *Phys. Rev. B* **1985**, *32*, 4279.
- (248) Hu, K.; Yang, H.; Zhang, W.; Qin, Y. *Chem. Sci.* **2013**, *4*, 3649.
- (249) Miyata, M.; Matsumi, N.; Chujo, Y. *Polym. Bull.* **1999**, *42*, 505.
- (250) Jones, G.; Jackson, W. *J. Phys. Chem* **1985**, *89*, 294.
- (251) Yu, G.; Heeger, A. J. *J. Appl. Phys.* **1995**, *78*, 4510.
- (252) Peumans, P.; Uchida, S.; Forrest, S. R. *Nature* **2003**, *425*, 158.
- (253) Zhou, G.; Baumgarten, M.; Müllen, K. *J. Am. Chem. Soc.* **2008**, *130*, 12477.
- (254) Zhao, S.-B.; Wucher, P.; Hudson, Z. M.; McCormick, T. M.; Liu, X.-Y.; Wang, S.; Feng, X.-D.; Lu, Z.-H. *Organometallics* **2008**, *27*, 6446.
- (255) Inoue, M.; Usuki, T.; Lee, N.; Hiram, M.; Tanaka, T.; Hosoi, F.; Ohie, S.; Otani, T. *J. Am. Chem. Soc.* **2006**, *128*, 7896.
- (256) Semmelhack, M. F.; Wu, L.; Pascal, R. A.; Ho, D. M. *J. Am. Chem. Soc.* **2003**, *125*, 10496.

- (257) Schreiner, P. R.; Navarro-Vazquez, A.; Prall, M. *Acc. Chem. Res.* **2005**, *38*, 29.
- (258) Zeidan, T. A.; Manoharan, M.; Alabugin, I. V. *J. Org. Chem.* **2006**, *71*, 954.
- (259) Xiao, Y.; Hu, A. *Macromol. Rapid Commun.* **2011**, *32*, 1688.
- (260) Basak, A.; Shain, J. C. *Tetrahedron Lett.* **1998**, No. 19, 3029.
- (261) König, B.; Hollnagel, H.; Ahrens, B.; Jones, P. G. *Angew. Chemie Int. Ed. English* **1995**, *34*, 2538.
- (262) Koenig, B.; Schofield, E.; Bubenitschek, P.; Jones, P. G. *J. Org. Chem.* **1994**, *59*, 7142.
- (263) Semmelhack, M. F.; Neu, T.; Foubelo, F. *J. Org. Chem.* **1994**, *59*, 5038.
- (264) Wang, Y.; Finn, M. G. *J. Am. Chem. Soc.* **1995**, *117*, 8045.
- (265) Schmitt, E. W.; Huffman, J. C.; Zaleski, J. M. *Chem. Commun.* **2001**, 57, 167.
- (266) Merlic, C. A.; Pauly, M. E. *J. Am. Chem. Soc.* **1996**, *118*, 11319.
- (267) Nicolaou, K. C.; Smith, a L.; Yue, E. W. *Proc. Natl. Acad. Sci.* **1993**, *90*, 5881.
- (268) Schreiner, P. R. *J. Am. Chem. Soc.* **1998**, *120*, 4184.
- (269) Hilger, A.; Gisselbrecht, J.-P.; Tykwinski, R. R.; Boudon, C.; Schreiber, M.; Martin, R. E.; Lüthi, H. P.; Gross, M.; Diederich, F. *J. Am. Chem. Soc.* **1997**, *119*, 2069.
- (270) Martin, R. E.; Bartek, J.; Diederich, F.; Tykwinski, R. R.; Meister, E. C.; Hilger, A.; Lüthi, H. P. *J. Chem. Soc. Perkin Trans. 2* **1998**, No. 2, 233.
- (271) Gobbi, L.; Seiler, P.; Diederich, F. *Angew. Chemie Int. Ed.* **1999**, *38*, 674.

- (272) Sakamoto, R.; Murata, M.; Nishihara, H. *Angew. Chemie Int. Ed.* **2006**, *45*, 4793.
- (273) Bohlmann, F.; Schönowsky, H.; Inhoffen, E.; Grau, G. *Chem. Ber.* **1964**, *97*, 794.
- (274) Kennedy, J. C.; MacCallum, J. R.; MacKerron, D. H. *Can. J. Chem.* **1995**, *73*, 1914.
- (275) Sonogashira, K.; Tohoda, Y.; Hagihara, N. *Tetrahedron Lett.* **1975**, *16*, 4467.
- (276) Takahashi, S.; Kuroyama, Y.; Sonogashira, K.; Hagihara, N. *Synthesis.* **1980**, 627.
- (277) Grubbs, R. H.; Kratz, D. *Chem. Ber.* **1993**, p 149.
- (278) Shukla, R.; Lindeman, S. V; Rathore, R. *Chem. Commun.* **2009**, *6*, 5600.